DIFFUSION AND NONCATALYTIC REACTION IN A PORE

A Thesis Submitted
In Partial Fulfilment of the Requirements
for the Degree of
DOCTOR OF PHILOSOPHY

BY
ARUN BHAURAO KULKARNI

to the

DEPARTMENT OF CHEMICAL ENGINEERING
INDIAN INSTITUTE OF TECHNOLOGY KANPUR
OCTOBER 1972

TO

MY GURUS

CERTIFICATE

It is certified that this work has been carried out under my supervision and that this has not been submitted elsewhere for a degree.

(G. Narsimhan)

16th August 1972

Department of Chemical Engineering
Indian Institute of Science
Bangalore.

ACKNOWLEDGEMENTS

I express my sincere and heartfelt gratitude to Professor G. Narsimhan not only for having initiated the thesis problem but also for having rendered continued assistance and inspiring guidance at various stages. I am grateful to Dr. P.K. Kelkar and Dr. M.S. Muthana for the institutional support and encouragement that I have received throughout. I will fail in my duty if I do not acknowledge the co-operation given by Dr. Gopala Rao, Dr. C.V. Seshadri and Dr. V.V. Rao in the matter of registration and official formalities in supporting my candidature through the department. My thanks are due to Dr. D. Ramkrishna and Dr. D.N. Saraf for their valuable advice and suggestions at critical stages and for their patient efforts in proof correction work. I am also thankful to various faculty members from Mathematics Department for their help in clarifying some of my mathematical doubts and difficulties. Thanks to the Departments of Chemistry and Metallurgy for their cooperation in offering some of the experimental facilities such as T.G.A. and high temperature utilities. Last but not the least, I am grateful to Mr. Pandey, Mr. Angirish, Mr. Panesar, Mr. Seth and other supporting staff for their help in typing, drawing and binding work.

Author

TABLE OF CONTENTS

...

LIST OF TABLES

...

LIST OF FIGURES

...

LIST OF SYMBOLS

A	positive constant defined in equation 4-78
A_e	external curved surface area of the cylinder
A_i	internal curved surface area of the cylinder
A_m	maximum cross-sectional area of a pellet
A_1	constant of integration in equation 4-47, a constant independent of h,k,j in Lees' scheme
A_2	maximum of the derivatives defined in Lees' scheme
A_3, A_4	constants in equations 4-112 and 4-115
a	stoichiometric number in the reaction $C+O_2=CO_2$, constant in equations 4-8 and 4-126
a_i	argument of Bessel function in equation 4-10
a^*, a_*	extremums defined in equations 4-147, 4-148
B', b'	subscripted coefficients in equations 4-204 and 4-179
B_1	constant of integration in equation 4-47
b	radius of convergence, constant in equations 4-8 and 4-127
C	dimensionless oxygen concentration C_A/C_{Ao}
C_A	concentration of oxygen in gas phase
C_{Ao}	initial concentration of oxygen in gas phase
$\bar{C}$	average of C defined in equation 4-53
C', c'	subscripted coefficients in equations 4-204, 4-179
C_{pa}	specific heat of air
C_{ps}	specific heat of solid
C_R	uniform gas concentration throughout porous graphite
C_{so}	initial concentration of solid
D	binary diffusivity of oxygen in air
D_{eff}	effective diffusivity of oxygen in porous graphite
D_-	backward difference

D_+	forward difference
D_o	central difference
E	activation energy for graphite oxygen reaction
E_a	apparent activation energy
E_t	true activation energy
F	Laplace transform function defined in equation 4-23, function defined in Rose's scheme, equation 4-144
F_1, F_2	functions defined in equations 4-161
G	function of $x, t, \bar{R}_i$ and $\bar{C}$, sufficiently large positive quantity defined in equation 4-194
$\bar{G}(h)$	finite set defined in equation 4-77
$G(h)$	intersection of $\bar{G}(h)$ with the open interval $o<x<1$
G_j	difference approximation of $g(x,t)$
(g)	gaseous state of reactants and products
g	function of x and t, or t and z
H	half the length of the cylinder, perpendicular height of the cone
h	dimensionless parameter in equation 4-61, discrete interval defined in Lees' scheme
I_o, I_1	modified Bessel functions of 0th and 1st order
J	largest integer defined in Lees' scheme
J_o, J_1	Bessel functions of 0th and 1st order
j	modified Thiele modulus defined in equation 4-48, subscript denoting discrete time interval
K	function defined in equation 4-72
K_e	effective thermal conductivity of graphite
K_p	equilibrium constant expressed as ratio of partial pressures
K_v, k_v	volumetric rate constants, $(\text{time})^{-1}$

k	first order surface rate constant length/time, discrete interval of t defined in difference schemes
k_a	thermal conductivity of air
k'	rate constant for a pth order reaction
k_o	pre-exponential factor in equation 5-8
L	half the dimensionless length of the cylinder H/R_i
$\mathcal{L}$	Laplace transform defined in equation 4-23
l	length of the stagnant air column
l_o	initial length of the stagnant air column
m	modified Thiele modulus defined in equation 4-12, maximum defined in equation 4-99, discretised variable
N	total number of axial grids, positive integer defined in Lees' scheme
n	true order of reaction, exponent of (V/R), discretised variable for x
p	variable in equation 4-72, order of a general heterogeneous surface reaction
q	derivative of w with respect to x
R	characteristic dimension for plane, cylinder and sphere
R_{av}	average radius in a porous pellet
R'	rate of oxidation of graphite
R_e	external radius of the graphite cylinder
R_i	internal radius of the graphite cylinder
$\bar{R}_i$	average of R_i
R_{im}	pore mouth radius
R_j	residue defined in equations 4-88 to 4-93
r	dimensionless radial distance R/R_i
S	plane surface area of reaction

s	weighting factor in difference scheme 4-145, Laplace transform parameter in equation 4-23
(s)	solid state of reactant
T	temperature, limit of variation of t
t	time of reaction, variable in various difference forms
u	function of x defined in Lees' scheme
u_j	sequence defined in Lees' scheme
V	velocity of oxidant gas
W	weight of the graphite sample
W_t	weight of the sample at time t
W_o	initial weight of the sample
w	function defined in equation 4-72
w_j	sequence defined in Lees' scheme
x	dimensionless axial distance z/H and z/R_i, variable in equations 4-72, 4-144, 4-158 and 4-182
y	vertical distance over the sample
Z	denotes zero in the matrix on page 36
Z_m	supremum defined in equation 4-195
z	variable axial distance, subscripted variable in equation 4-191, error term defined in equation 4-95

GREEK SYMBOLS

α	exponent of T in equation 5-9, constant of proportionality on page 58
$\propto$	proportional to
α_s	thermal diffusivity of graphite
β	crystalline form of graphite, constant of integration in equation 4-47, exponent of T in equation 5-10
ε	activation energy, belonging to, effectiveness factor, voidage in the solid, positive constant in Eqn. 4-109

ε_1	one dimensional effectiveness factor
ε_2	two dimensional effectiveness factor
η	Thiele utilization factor
δ, δ	small positive quantity defined in Lees' scheme
ΔG	free energy of reaction
ΔH	heat of reaction, maximum heat of combustion
Δ	finite differences in R, R_i, $\bar{R}_i$, T, t, or x
ζ	real linear space of all functions u(x)
ζ_o	N dimensional subspace of ζ
θ	fraction of graphite surface covered by oxygen, half the apical angle of the cone, exponent in eqn. 4-185
λ	mesh ratio defined in eqn.4-146, a positive constant defined in Lees' scheme, exponent in eqn. 4-185
μ	positive constant defined in equation 4-76
σ	positive quantity defined by equation 4-100
ρ_a	density of air
ρ_s	density of graphite or solid
τ	error estimate in Lees' scheme
φ, ϕ	dimensionless ratio defined in Table 2-3, specified function in equation 4-73
φ^+, φ^-	specified functions in equations 4-74, 4-75
Ω	rectangular region defined in equations 4-72, 4-146
ψ	predictivity parameter defined in equation 4-71
$\|\| \ \|\|$	norm of
$< >$	a sequence

SYNOPSIS

"DIFFUSION AND NONCATALYTIC REACTION IN A PORE" A Thesis Submitted in Partial Fulfilment of the Requirements for the Degree of Doctor of Philosophy in Chemical Engineering by A.B. Kulkarni to the Department of Chemical Engineering, Indian Institute of Technology, Kanpur, August 1972.

A study on "Diffusion and Noncatalytic Reaction in a Pore" has been undertaken with a view to analyse a chemical reaction in a porous mass in terms of that in a single pore. The shrinking pore approach illustrates the role of physical factors in heterogeneous kinetics with special reference to the possible inverse effect of temperature on the overall rate of a nonsolid forming reaction. The scope and limitations of single pore analysis in relation to the existing methods of investigation are discussed in the introductory note.

The review of literature enumerates some of the important developments in the field of heterogeneous fluid-solid reactions with special regard to micromechanistic, phenomenological and empirical aspects. The subject matter of graphite oxidation is reviewed with the objective of arriving at a suitable experimental procedure and appropriate mathematical approximations. Some of the controversies regarding the mechanism and order of carbon gasification, role of mass transport, catalytic activity of impurities and control regimes are highlighted. Important aerospace and nuclear applications of graphite are also included in the review.

Experimental efforts are confined essentially to weight loss measurements during the course of oxidation of graphite by air or oxygen. A plane surface of graphite is allowed to react in a stagnant air column and the resulting weight loss curves are used to determine the apparent first order rate constant. For studying the reaction in a pore, the external surface of a hollow graphite cylinder is coated with a protective layer and the internal surface is allowed to react. Difficulties encountered therein are discussed. Thermo-Gravimetric Analyser (T.G.A.), Veeco vacuum evaporator and gas chromatograph are used in the experimentation.

One dimensional diffusion equation with the reacting flux boundary condition is solved to obtain a suitable mathematical algorithem for the determination of surface rate constant k. This k is used in building various mathematical models to describe the reaction in a pore. After exhausting the possibility of analytical and seminumerical solutions, implicit and explicit finite difference approximations for the relevant set of simultaneous partial differential equations are tested. Von Neumann's stability criterion for explicit schemes and l_2 error estimates for Milton Lees', Rose's and Modified Backward difference schemes are discussed in detail. The major portion of the thesis work is concerned with the numerical solution of a number of stable finite difference equations and with the minimization of machine time on IBM -7044 and IBM-360. Conclusions are then drawn by critical analysis of the numerical data on pore wall profile and axial concentration distribution.

...

1. INTRODUCTION

Even though the parameters pressure and flow invariably have a telling effect on the rate of a heterogeneous fluid-solid reaction, temperature seems to have occupied a more prominent position in the scientific and technological investigations of a number of industrially important reactions such as reduction of iron ores, roasting and smelting of metal sulphides, combustion of solid fuels and solid propellant, gasification of coal or oil shale, regeneration of catalysts, oxidation of iron by steam, calcination of carbonates, flourination of uranium ores, chlorination of titanium dioxide, and aluminium oxide, sulphation of carbon and carbonization of calcium oxide. Besides the inherent technical difficulties associated with high pressure and high flow systems, the factors responsible for this undue importance of temperature seem to be a lack of qualitative appreciation and quantitative understanding of the role of mass transport in a porous reacting solid system. Traditionally the relative importance of physical and chemical factors have been studied on one or more of the following lines:

(a) Langmuir type of adsorption isotherms and their application to mechanistic and kinetic studies.

(b) Extension of well established method of catalytic kinetics.

(c) Microstudies of reactions involving single crystals.

(d) Phenomenological approach to shrinking core models.

When the rates of diffusion through fluid film and porous solid are both very fast, the overall rate of a fluid-solid reaction is solely controlled by the inherent chemical reactivity of the solid reactant. Based on the Langmuir type of adsorption isotherm, it is possible quantitatively to describe the mechanism of uncatalysed heterogeneous fluid-solid reactions under this condition. However, depending on the mechanism, the resultant rate equation involves more than two arbitrary constants, some times as many as seven. In selecting these constants for each mechanism, the curve representing the rate equation of the favoured mechanism which best fits the experimental data is chosen. Because of the unavoidable intrinsic scatter of the experimental data, it is clear that in many instances little meaning can be attributed to the magnitude of the adsorption equilibrium constants, the frequency factor, and the apparent activation energy. Often, the difference in fit may be so small that it is very difficult to determine whether it is simply due to experimental error or truly due to the difference in mechanism. Furthermore, an alternative mechanism may fit the data equally well necessitating an additional extensive experimental search for the correct mechanism. Although a correct mechanism which is difficult to determine, will allow extrapolation to conditions not actually investigated, there is no reason why simple rate

equations which fit the data satisfactorily should not be used provided no extrapolation is done beyond the range investigated. Based on the adsorption isotherms, the order of fluid-solid reactions can be shown to vary from zero to two depending on whether the gas reactant is strongly, moderately or weakly adsorbed. Experimental studies also indicate many reactions to have a similar range of the order of reaction depending on conditions such as structure of the solid, reactivity, pressure, temperature etc.[1],[2]. The very fact that adsorption is only one of the six steps involved in the rate process of a heterogeneous reaction, any attempt to describe the entire process kinetics by means of just one step is bound to have serious inadequacies. Moreover, the assumptions made in the Langmuir approach are too ideal to be applicable to an engineering fluid-solid system. Thus adsorption isotherms can at best be useful in mechanistic studies.

Although comprehensive theories of catalytic reactions are available, studies on noncatalytic reactions have not been advanced and organized into a distinct and coherent branch of chemical reaction engineering. This slow development stems from little understanding of intrusion of complex physical phenomena on chemical reactivity on one hand and the heterogeneous surface properties and pore size distributions on the other hand. One of the major difficulties involved in the analysis of noncatalytic systems is the time varying moving boundary condition and the resulting "geometric instability"[3]

of the porous structure. Some attempts have been made in recent years to develop the concept of effectiveness factor and Thiele parameter for simple first order irreversible fluid-solid reactions with no change in number of moles during the course of reaction [3 , 4 , 5 , 6]. However, too many simplifying assumptions involved in such analyses restrict the application of these developments to a number of important designs. Unlike catalytic reactions, most of the reactions on the solid surface cannot be truly reversible, since the phenomenon of solid deposition in the reverse reaction does not necessarily provide the solid product with a structure that is exactly the same as that of the original solid reactant. While for the first order reactions it is possible to provide an additional term to account for the "equilibrium hindrance"[3] the same may become very complicated for other orders of reaction. The thermodynamic and transport properties of a noncatalytic system are dependent not only on temperature, pressure, and composition, but also on the time varying pore structure. The limited applicability of Wheeler's single pore model [7] or Smith's macro-micro pore diffusion model [8] is also due to the timevarying pore structure. Thus it is felt that the study of variation of pore structure in general and a single pore in particular, during the course of a fluid-solid reaction, may become a key factor in understanding a heterogeneous reactive system. It is in this background the present work has been undertaken.

In the recent past gas-solid reactions have been studied on microscale by means of a number of new methods such as etchpit expansion [9] , measurement of varying thermo e.m.f. at the reacting junction [10] , microcinographic technique [11], molecular beams, electronmicroscopy, EPR, ESR techniques etc. While these studies yield results directly applicable in the field of solid state chemistry, their utility in obtaining design data for macro-heterogeneous systems appears quite doubtful and remote. Until well developed statistical theories to predict the macrodata from microdata are made available, the results of the above microinvestigations can be considered only of potential future use.

A good number of engineering investigations have made use of a "shrinking core model" to obtain the kinetic data required in the design of heterogeneous reactors [12 , 13 , 14 , 15 , 16 , 17 , 3]. Despite a wide application of the shrinking core model, it is by no means the panacea for complex non-catalytic reactions. One of the most common assumptions made in this model is the "quasi-steady state of shrinkage" which may not be valid for systems with high pressure and low solid reactant concentration. When the solid contains enough voidage or develops enough voidage during the course of reaction, so that the diffusion into the interior of the solid is free and fast, the shrinking core model will no longer be applicable. This model cannot be used uniformly when shifting of the rate controlling regimes takes place. In such cases Wen [3] has

considered the reaction to occur homogeneously throughout the solid. He has developed a generalized model which also has its limitations to the extent that the rate controlling regimes are replaced by "stages of reaction" i.e. using different sets of equations and solutions for initial, intermediate and final stages of reaction. The shrinking core model assumes a sharp demarcation between the reacted and unreacted zones and invariably uses a heterogeneous rate constant defined on the basis of surface reaction only. However, when "geometrical instability" appears, the reaction interface is no longer smooth, and the mathematical model may at best become an approximation of the real process. If the results obtained for a regular shaped pellet are to be generalised and applied for an irregular shaped pellet, the manner in which the timevarying pore geometry changes with the core geometry (spherical, cylindrical or rectangular) poses a problem in the shrinking core model. Thus it appears that some of the limitations of the shrinking core model may be overcome by a quantitative understanding of the variation of pore surface area, porosity, and the poresize distribution during the course of fluid-solid reactions.

After having realized the importance of a "shrinking* pore model" in making the "shrinking core model" more versatile and useful, and after realizing the fact that a single pore forms the most natural fundamental unit of an entire solid core, one may think in terms of two lines of approach for the

*The term hereafter refers to shrinkage of length.

development of a "shrinking pore model".

(a) The deterministic approach which starts with the study of a single pore and then tries to describe the variation of the entire pore structure in terms of its fundamental unit.

(b) The stochastic approach which makes use of time-dependent probability distribution parameters to describe the variation of a pore structure which consists of a large number of pores of various sizes and shapes with a complex interlinkage among them.

In the present work, an investigation on a single pore is undertaken with the objective of making a modest beginning in the deterministic approach so that a basis for a new method is made available for future research investigations. The essence of the present effort is to determine both the axial concentration and the radius of the inner surface of the pore as functions of time and axial distance when a fluid-solid reaction is taking place within a pore. These functional relations in turn are used to predict some of the design data pertaining to heterogeneous kinetics. Attempts are made to substantiate the numerical calculations with the experimental investigations. Some of the areas in which the above single pore analysis may be used are indicated below.

The Kozeny Carman equation for the pressure drop across a packed bed or a porous medium can be derived either from a "grain model" or from a "pore model". It is surprising that

similar exaustive treatment has not been extended to reactive porous media. Only recently Szekley and Evans [18] have reported such developments for the reduction of ironioxide by carbon monoxide. It is interesting to note that the grain and pore models are implicitly synonymous with the volumetric and the surface reaction rate constants respectively. As long as one of the products of reaction is a solid, (i.e. when the porosity during the course of reaction remains more or less constant) it is not of great consequence whether the voidage is represented in terms of interspace between the grains or the volume of pores. However, when a fluid-solid reaction produces only gaseous matter, pore structure undergoes a continuous change, and pore model - at least intuitively - may have an edge over the grain model, because physically it is a pore which forms the fundamental unit of a reacting porous solid. It should hence be logical to follow the changes occurring in a single pore and then extend this knowledge to a multiple pore system by making suitable estimates of the mean pore dimensions, their distributions and their linkage. Alternatively, single pore data may enable us to predict the rate constant in a porous medium from the known rate constant in a nonporous medium.

Except the new experimental technique of Westenberg and Walker [19], there probably exists no accurate method for the determination of gaseous diffusivities at temperatures above 600°K. Frequently, experiments to determine diffusivities are conducted in nonreacting gaseous systems with constant

compositions, and the data is used for the reacting systems. If the first order surface rate constant is known, the method developed in the present investigation can be used to determine the gaseous diffusivities in a multicomponent reacting mixture. This method acquires a special significance when it is desired to consider the dependence of diffusivities on concentration, and on the possible dissociation of gases at high temperatures. Secondly, if the gaseous diffusivity through a porous reactive solid medium is to be determined, one needs to know the change in cross-sectional area available for the diffusion as the reaction progresses. The model presented in this work may serve as a basis for the estimation of changes in cross-sectional area of a reactive porous solid at various stages of reaction. With the advent of high speed computers and newer finite difference schemes for the quasilinear parabolic differential equation, the time-consuming trial and error procedure of numerical calculations should not be too problematic. At the same time, the experimental procedure is simple and can be adapted easily to new systems.

As a corollary, one can utilize the same analysis to determine the first order surface reaction rate constant, if the diffusivity and rest of the parameters are already known. The conventional experimental methods for determining the heterogeneous rate constants employ a system wherein the reacting fluid either flows over the solid or remains stagnant on it. If it is a flow system, the true rate constant is

invariably an extrapolated value at infinite velocities. If the gas is stagnant, it is rather difficult to eliminate the convection currents. To avoid both these difficulties, the present method employs the inner surface of a pore of a smaller diameter where the radial symmetry for temperature and concentration more or less frees the system from the effects of convection; and hence, the bulk diffusion terms do not appear in the mathematical model.

Whenever diffusion and chemical reaction occur simultaneously, the transition zone between the diffusion controlled regime and the chemical reaction controlled regime becomes an important factor in the design of a reactor. If the experiments are carried out at various temperatures, the present method may serve as a starting point in distinguishing the diffusion controlled regime from the reaction controlled regime. As will be seen in the conclusions, steeper profiles of the reacting pore-wall would indicate broadly a diffusion controlled regime and the flat profiles, a reaction rate controlled regime. It will also be seen that the conventional method of deciding the regimes by the criterion of an almost constant reaction rate equalling the diffusion flux at the pore mouth, may at times give misleading conclusion. The present method may serve as an additional check to resolve the controversies if any regarding the nature of the transition zone.

By introducing some extra terms for natural convection, or bulk mass transport with or without flow, the present model

can be modified to predict the rate of chemical corrosion of tube walls, storage tanks, or the metallurgical laddles or any vessel which contains a corrosive fluid. Of course, the mathematical complexity of the problem increases when we try to incorporate the terms for convection or flow. Nevertheless, the model with its numerical solution provides a fundamental system theory approach to corrosion problem. This may also help to isolate the effect of corrosion from that of errosion in metallurgical laddles or runways. So far, the methods for predicting the corrosion of reacting walls are mostly empirical and with the present model, a beginning in the fundamental approach can be made.

Sometimes, the specific reaction rate constants depend on the geometry and the heterogeneity of the sample surface [20, 21]. This may be due to the difference in surface potentials for different geometries, or may be due to the difference in the crystallite orientation on the machined surface of the solids. Quite often, corners act as the points of stress concentration and hence are more susceptible to chemical reactions. If such a phenomenon is anticipated or observed, one can cast or machine a hollow cylinder out of the solid and carry out the reaction in the pore so that variation of rate constant with geometrical configuration can be detected or confirmed. For example, the orientation of carbon atoms on the surface of a machined graphite depends on the relative geometry of the sample. Therefore, the surface rate constants in the initial stages of

oxidation of rectangular, spherical, and cylindrical graphite samples are observed to be slightly different from one another [2].

One of the important considerations for deciding the optimum particle size is the ratio of the overall rate of reaction on the inner surface of the pores to that on the outer surface of the solid. A mathematical model with its analytical solution presented in this work deals with this ratio which also indicates the ratio of mass transfer due to convection on the exterior surface to that due to molecular diffusion inside the pore. Variations in porosity during the course of reaction can also be studied in the present experimental set up.

In view of all the possible interesting applications of the study of noncatalytic reactions in pores, one may think in terms of a solid-liquid system or a solid-gas system for the experimental investigations. The latter is preferred in this work because of the following reasons:

The magnitude of gaseous diffusivities is generally larger than that of liquid diffusivities and this helps to establish appreciable axial concentration gradients during the course of reaction. Besides, the larger magnitude of gaseous diffusivities provide a good spread for temperature as a variable in the numerical calculations. Pressure can be a meaningful variable in case of a gas-solid system while this possibility is almost absent in a liquid-solid system. Heats of wetting for liquids in general are larger than those for

gases and hence the changes resulting exclusively from the variations in the heats of wetting tend to become relatively less significant. The formation of a curvature on the liquid surface inside a pore and the effect of this curvature on the equilibrium vapor pressures are very typical of a solid-liquid system while these are almost absent in case of noncondensable gases in contact with solids. In fact almost all physical phenomena resulting from heterogeneity of the surface of the solid become less significant in case of a gaseous system. In a restricted sense (i.e. confining to a few systems which are under present consideration) it may be noted that the nonideal behaviour with respect to activity coefficients is more severe in case of liquids than in case of gases, For gases one can have better control on the parameters like flow, temperature, pressure and composition. Low viscosity of gases reduces the momentum entry length at the pore mouth so that the end effects due to flow are minimized. All these factors tend to reduce the side effects in the main stream of analysis and experimentation so that the certainty and the validity of the conclusions are enhanced. After having decided upon a gas-solid system, the particular reaction of oxidation of graphite by air has been selected for a number of reasons.

Well defined crystal structure with minimum number of defects is an important criterion for the choice of a solid. Next to diamond, graphite is the most ideal carboniferous material for the study of reactions of carbon with oxygen. The

structure of graphite is well defined and is easily controlled at its formative stages, and therefore one may be confident in building the atomic or molecular models for studying the surface properties. Extensive studies pertaining to the kinetics and mechanism of graphite oxidation are already available and therefore one can be more certain about the validity of the experimentally determined parameters like order of reaction, primary products of oxidation, specific reaction rate constant, and activation energy. This, in turn, will naturally minimize the uncertainty about the main stream of analysis. Also prior knowledge concerning the transition temperature zone between the diffusion controlled regime and reaction rate controlled regime, provides some additional guide lines for simplifying the experimental and numerical procedures. Substantial knowledge about the variation of properties of graphite with respect to porosity is already available [22] and this supports some of the assumptions made in the mathematical modelling. Graphite has a good machinable property and hence samples of the desired shape and size can easily be obtained. Air happens to be a versatile material for which the thermodynamic and transport properties are tabulated over a wide range of temperature and pressure. This again enhances the certainty of the main stream of analysis. Besides, experimental and analytical simplicity, the subject of oxidation of porous graphite in recent days is gaining considerable importance in the field of nuclear power generation and rocket propulsion where graphite is used as a

material of construction. And lastly the analytical techniques used in following the course of chemical kinetics of graphite oxidation are fairly simple irrespective of whether one uses weight loss measurement technique and/or gas composition measurement technique. However the aforementioned considerations should not in any way undermine the contraversy that exists in the field of graphite oxidation[2 , 23].

Before concluding this introductory note, it is felt necessary to mention some of the limitations of the approach introduced in this work. The most important aspect in this respect is the specific meaning of the title "diffusion and noncatalytic reaction in a pore". The term "diffusion" in general would mean mass transfer under concentration gradient which may be resultant of a partial pressure gradient, total pressure gradient, temperature gradient, velocity gradient, surface potential gradient, ionic, molecular and steeric factor gradients. However in the context of the present work, mass transfer due to partial pressure gradient alone will be considered as diffusion. The diffusion controlled regime mentioned in this work refers to this aspect of diffusion only. The reaction is carried out at a constant pressure and it is assumed that the number of moles do not change during the course of reaction and therefore the total pressure gradient cannot possibly exist in the system. Mass transport with unequal absolute pressures at the ends of the transport path, often called permeability, is specifically excluded from consideration.

In fact, the use of a macropore for the experiment should rule out the above possibility. It goes without saying that the Knudsen diffusivity is also out of consideration. It may be noted that this microdiffusivity is proportional to the absolute temperature to the power of half, while the ordinary diffusivity is proportional to a power variously reported as from about 1.5 to 2.0. The assumption of an isothermal condition of reaction, eliminates the possibility of thermal diffusion. In absence of external fields, and negligible dissociation of molecular oxygen below 1500°C, other types of diffusivities are not likely to be significant. According to Nichols [24] inspite of the above limitations, we may still be encountering two types of diffusivities. The first one is ordinary, bulk, or the Poiseulle diffusion and the second one is surface diffusion, a process of mobile adsorption which can occur in parallel with either of the above types of diffusion. It is independent of total pressure but is proportional to a complicated function of temperature. Wicke and Kallenbach [25] claim that their data on diffusion of carbondioxide through charcoal at atmospheric pressure shows a sizeable fraction of such surface diffusion in the total mass transport. Surface diffusion is generally considered to occur mainly at a temperature close to the boiling point of the diffusing gas or in extremely fine pores at other temperatures [24]. In this work, neither of these conditions is prevalent, and therefore surface diffusion is less likely to interfere with the kinetic

data. Before concluding, it may be worth recalling another kind of diffusion which occurs when molecular dimensions are approximately equal to the diameter of the pore. This kind of activated diffusion is exponentially dependent on temperature. This also is a remote possibility on the open surface of the graphite walls. It may be noted that only gas phase axial diffusivity is considered in the present model. For reasons mentioned in the chapter on mathematical modelling, no radial diffusion in the gas or solid phase is considered.

The term "chemical reaction" refers to a simple first order isothermal irreversible surface reaction without any change in the number of moles. No complex or compound reactions due to secondary changes or inhibitive poisoning actions are dealt with. The apparent density of the solid during the course of reaction is assumed constant even though occasionally there is a density variation in the direction of "depth" from the surface of the solid. The "equilibrium hindrance factor"[3] due to the change in the pore structure or in the geometrical stability of the solid does not enter the picture because of the assumption of irreversibility. The term "pore" in the context of this analysis refers to a macropore only. A perfect cylindrical geometry with two open mouths is taken into account at the start of reaction.

Even through reference is made to a number of potential applications of the present study, the actual work is restricted only to the prediction of wall profiles and concentration

profiles in a graphite cylinder, the inner surface of which is continuously reacting with air. The author is well aware of the limitations experienced in representing the surface reaction by a single first order rate constant at all chronological stages of reaction - more so at higher temperatures. Of course, the inherent inadequacies associated with the concept of the order of a heterogeneous reaction and Fick's second law of unsteady state diffusion are common to most of the investigations on heterogeneous systems.

Thus the first chapter of the thesis introduces the single pore method with its scope and limitations. Chapter two gives a brief review of literature on heterogeneous gas-solid systems in general and the specific reaction of graphite oxidation by air in particular. The third chapter describes the experimental methods both for the determination of the first order rate constant and the study of the reaction in a single pore. Chapter four presents various possible mathematical models and the assumptions involved there in. The fifth and the final chapter deals with the results of computation from which some conclusions are drawn.

* * *

2. REVIEW OF LITERATURE

Depending on the extent of stress that is laid on the thermodynamic, mechanistic, kinetic, heat or mass transfer principles, the existing literature on heterogeneous fluid-solid reactions may be classified into three broad categories:

(a) Mechanistic studies dealing essentially with the micro aspects.

(b) Empirical and semiempirical studies with utilitarian objectives.

(c) Phenomenological studies taking a macro approach to the process of simultaneous diffusion and chemical reaction.

While microstudies are quite useful in understanding the mechanisms of reaction, heterogeneity of the solid surface and the inadequacies associated with the micro-experimental techniques are two factors which limit the scope of the micro-mechanistic investigations. Even if accurate microdata is available, its application to macrosystems poses a number of physical and mathematical problems for which no satisfactory solutions exist. The details of the microtechniques and the difficulties involved in their utilization for design purposes are discussed in the later part of the review.

As regards the empirical and semiempirical data, they are too numerous to be comprehended. Every investigation has a limited objective of its own and invariably scientific generalizations are not possible. For example, thin films of

lad and graphite act as bearing lubricants and their oxidation by air or oxygen [26, 27] has some unique features which are not common to heterogeneous fluid-solid reactions in general. The data of Bowden and Young [26] regarding the effect of degasification of graphite surface on its lubricating properties cannot be generalized and used elsewhere. Maberry et.al. [28] have studied the performance of graphite nozzles used in rockets and their data on the corrosion and errosion of internal wall surface are valid only over a restricted range of operating conditions. Most of the investigations pertaining to the reduction of iron ore pellets and the sintering effects involved therein are by and large empirical in nature. The data regarding the change in porous structure of the solids [29] during the course of heterogeneous reactions is still at large empirical. The quantitative effect of irradiation on the oxidation characteristics of a graphite moderator [30] has usually been described by means of empirical formulae. In spite of enormous efforts, the study of the effect of impurities and crystal defects on the course of a heterogeneous reaction has remained an empirical science. Many more instances of empiricism can be cited from the literature, but compilation of such data is not the aim of this review.

"Conceptual modelling" or a "phenomenological formulation" has been an essential theme of a large number of engineering and technological investigations. In fact this has been the most versatile approach to the synthesis of design data. The

necessary mathematical model is built by taking into consideration all possible phenomena or steps that are involved in the chemical reaction. Owing to the close resemblance between catalytic and noncatalytic systems, the scheme suggested by Hougan and Watson [31] for a catalytic reaction has served as the basis for formulating a parallel scheme for noncatalytic reactions. Wen [3] has described a surface reaction to consist of the following steps:

(1) Diffusion of the fluid reactants across the fluid-film surrounding the solid, (2) Diffusion of the fluid reactants through porous solid layer of reactant and/or product, (3) adsorption of the fluid reactants at the solid reactant surface, (4) chemical reaction with the solid surface, (5) desorption of the fluid products from the solid reaction surface, and (6) diffusion of the product away from the reaction surface through the porous solid media and through the fluid film surrounding the solid. Since the above steps take place consecutively if any one of them is much slower than all others, that step becomes rate-determining. In other words, for a given set of reaction conditions, that step which offers the highest resistance controls the overall rate. In phenomenological formulations, it has been a customary practice to combine the steps 3 and 5 with the step 4 so that the surface reaction can be represented by means of a single equation involving only two constants. Thus the reactions may be external mass transfer controlled, inter or intra particle diffusion controlled, chemical reaction

controlled, heat transfer controlled or mixed controlled. However single-step rate determining processes are limiting cases. The majority of fluid-solid reactions are influenced simultaneously by more than one step.

Thus a rigorous treatment seems unattainable even for the solid of the simplest geometry, under isothermal conditions of reaction. Partly this is due to the intricate relationship among the rates of chemical reactions and the rates of mass and energy transfer. Overall rates are influenced not only by the rate of chemical reactions occurring in or at the surface of a solid and by the mass transfer rates of fluids through the solid as well as across the fluid-film surrounding the solid, but also by factors such as solid reactivity of crystallite orientation, crystallite size, surface characteristics, impurities etc. Besides a great number of difficult problems exist in practical systems, such as the changing size and shape of the solid during the reaction and formation of a product around the solid reactant which may crack or ablate or change the porestructure drastically. In addition, the complex velocity profile of the surrounding fluid makes the problems of mass and energy transfers to the solid reactant more difficult to analyse. Often one encounters the problems of adulterating the chemical reaction constants with the structural parameters and other physical factors. If during the course of reaction there is an appreciable change in the solid density or if there is a structural nonuniformity or a thermal stress in the solid, the

solid particles may undergo cracking, ablation, and peeling off, during the course of reaction. Most of the reversible fluid-solid reactions cannot be truely considered as reversible, since the phenomena of solid deposition in the reverse reaction do not necessarily provide the solid product with a structure that is exactly the same as that of the initial solid reactant in the forward reaction. This is seen in a number of fluid-solid reactions which have been known to exceed their normal thermodynamic equilibrium [32,33,34]. If this is the state of affairs for a simple reaction system, one can well imagine the magnitude and complexity of the situation when compound and complex reactions with nonisothermal and nonisobaric conditions are prevailent in the system. Therefore it should not be surprising if there has been a lack of co-ordination from the phenomenological approach resulting in, for the most part, fragmentary and some times obscure nature of theories of non-catalytic reactions which have not been advanced and organized into a distinct and coherent branch of chemical reaction engineering.

Although there are a number of diverse and complex fluid-solid reaction systems, Wen[3] has shown that it is possible to group them phenomenologically in two ways. One grouping is based on the phase combination of the reactants and the products, and the other is based on the manner by which a reaction progresses.

Classification based on the phases of reactants and products:

(A) Solid reactants $\longrightarrow$ fluid products

Some of the examples for type A are pyrolysis of carbonaceous materials, combustion of double-base propellants, and thermal decomposition of some organic or inorganic compound especially explosives such as ammonium nitrate.

$$NH_4NO_3(s) \longrightarrow N_2O(g) + 2H_2O(g)$$

(B) Solid reactants $\longrightarrow$ fluid and solid products

Examples are

$$CaCO_3(s) \longrightarrow CaO(s) + CO_2(g)$$

$$CaSO_4 \cdot 2H_2O(s) \longrightarrow CaSO_4 \cdot \tfrac{1}{2} H_2O(s) + \tfrac{3}{2} H_2O(g),$$

$$CaOCl_2(s) \longrightarrow CaCl_2(s) + \tfrac{1}{2} O_2(g).$$

(C) Fluid and solid reactants $\longrightarrow$ fluid products

Examples are

$$C(s) + S_2(g) \longrightarrow CS_2(g),$$

$$NaNH_2(l) + C(s) \longrightarrow NaCN(l) + H_2(g),$$

$$2Al_2O_3(s) + 6Cl_2(g) \longrightarrow 4AlCl_3(g) + 3O_2(g).$$

(D) Fluid and solid reactants $\longrightarrow$ solid products

e.g. $CaC_2(s) + N_2(g) \longrightarrow CaCN_2(s) + C(s)$

(E) Fluid and solid reactants $\longrightarrow$ fluid and solid products.

Examples are

$$Fe_2O_3(s) + 3CO(g) \longrightarrow 2Fe(s) + 3CO_2(g)$$

$$2ZnS(s) + 3O_2(g) \longrightarrow 2ZnO(s) + 2SO_2(g)$$

$$4FeS_2(s) + 11\ O_2(g) \longrightarrow 2Fe_2O_3(s) + 8\ SO_2(g)$$

Classification based on the control regimes:

(A) Diffusion controlled reactions or heterogeneous surface reactions: When the chemical reaction rate is very rapid and relatively the diffusion is sufficiently slow, the zone of reaction or the chemical reaction propogating front is narrowly confined to the interface between the unreacted solid reactant and the product. Also when the porosity of the unreacted solid is very small so that the solid is practically impervious to the fluid reactants, the reactions will occur at the surface of the solid or at the interface between unreacted solid and the porous product layer. Such a reaction may be considered a heterogeneous surface reaction or the diffusion controlled reaction. Since there exists a sharp demarcation between the reacted and unreacted zones, an unreacted shrinking core model is conveniently used to describe the reaction. Yagi and Kunni's analysis [35] is a classical example of a shrinking core model.

(B) Reactions controlled by the chemical reaction rates or the homogeneous reactions: In many cases, the solid contains enough voidage to permit free passage of the fluid reactant and the fluid product and the solid reactants are distributed homogeneously through out the phase. In other words, the effective diffusivity of each fluid component through the entire solid phase is sufficiently large and also the rate of mass transfer to the periferi of the solid is sufficiently fast. Then under such circumstances it may be reasonable to assume that the reactions between fluid and solid components are occurring

homogeneously through out the solid phase. Homogeneous model which defines the rate constant on the basis of an apparent volume of the solid, may be employed for the mathematical analysis of such systems. Levenspiel's model [36] has been a significant development in this direction.

(C) Reactions controlled by heat transfer rate or those accompanied by phase changes of solid components or by evolution of volatiles: In some cases, because of a rapid exothermic reaction and poor heat conduction, a phase change of the solid component takes place prior to the chemical reaction. The solid reactant simply melts or sublimes before it is brought into contact with fluid reactants. The phase change may proceed with pyrolysis or devolatilization which is often associated with gasification and combustion of solid fossil fuels. In such cases a homogeneous vapour phase reaction takes place either around the periferi of the solid or in the solid product layer formed around the unreacted solid core. Narsimhan's heat transfer model [37] which fitted the experimental data of Satterfield and Feakes [38], is a good example of such systems controlled exclusively by heat transfer rate.

(D) Reactions governed by mixed controls or intermediary controls: In a strict sense, no heterogeneous reaction belongs exclusively to the types A, B or C. This is because no real system can possibly have diffusivity, thermal conductivity or rate constant of zero or infinite value. Therefore, the categories A, B, and C can only be mathematical approximations

to the real situation. On a molecular scale, the distribution of solid reactant in the solid phase cannot be considered homogeneous. At best, it can be considered as an ensemble of small lumps of reactant distributed throughout the solid phase. The overall reaction rate depends on a number of parameters such as the intrinsic reaction rate constants and orders, the sorption characteristics and the transport properties of the fluid reactants in and around the porous solid, the structure of the solid, and the distribution of the small lumps of solid reactant. As has already been pointed out, a master model which incorporates all these factors seems unattainable. In fact most of the cases where the experimental data do not fit into any one of the above three models belong to the category D. To gain better insight into such situations, the recent trend has been not only to isolate kinetic parameters from diffusion parameters, but also various types of diffusion parameters from one another. Gokarn and Doraiswamy [39] have cited a number of examples of mixed controls in an illustrious way.

Inspite of a number of serious short comings of the above classification, almost all phenomenological investigations have relied on it. Each reaction is studied separately at low, intermediate, and high temperatures so that separate analyses for chemical reaction rate controlled regime, mixed control regime, and diffusion controlled regime can be made use of. The presence or absence of an "ash layer" makes a distinct

phenomenological difference and thus the classification based on the phases of reactants and products becomes implicit in the mathematical model.

Gokarn and Doraiswamy [39] have systematically presented the significant developments in the study of ash forming heterogeneous fluid-solid reactions. In most of these reactions, the reacted solid retains its original geometry and dimensions, and the reaction front recedes from the outer surface to the centre. Such topochemical reactions under the quasisteady state conditions are characterized by a linear rate of movement of the reaction zone. A critical review of some shortcomings of the shrinking core model used in these reactions, has been presented in a number of recent publications [3, 18, 40, 41]. Existence of a sharp interface between the reacted and unreacted regions is a fundamental assumption of the shrinking core model. In practice, the demarcation is never sharp. It is not uncommon to find a hemispherical core shrinking into an irregular shaped cone during the course of reaction. A circular ring demarcating the reacted and unreacted zones during the course of reaction may become a wavy ring of any odd shape. Thin line of demarcation may grow into a diffuse structure. With such developments, surface reaction rate constant will have little meaning. Wen [3] has given a quantitative estimate of the accuracy of a pseudo-steady-state approximation which may not be valid for a high pressure and low solid reactant concentration system. In other words, the initial unsteady state time need not always be

negligible compared to the pseudo-steady-state time of reaction. In the case of an unreacted-core shrinking particle, when the rate per unit area decreases as the conversion becomes greater, the nonuniformity of structure will tend to be smoothed out because the rate of reaction is less at a point of deeper penetration. On the other hand, when the rate of reaction per unit area increases as the penetration is deepened, greater unevenness of the reaction surface will result. This is termed the "geometrical instability" and was first pointed out by Cannon and Denbigh [42]. Shrinking core model does not normally account for such instability. The assumption of equimolal countercurrent diffusion through the ash layer or the constancy of effective binary diffusivity may not be valid if there is a change in the number of moles during the course of reaction or if the concentration of diffusing species is high. At times the bulk flow due to pressure gradient cannot be overlooked in the shrinking core model. Moreover the irregular surface boundary of the exterior solid core sets in complex velocity profiles in the adjoining fluid layer. This will result in unpredictable mass transfer coefficients at the fluid-solid interface. Shrinking core model must be used with caution when shifting of rate controlling regimes takes place. For example, a fluid-solid reaction originally under the diffusion-controlled-regime, may shift to the chemical-reaction-controlled regime resulting in an overall rate, many folds lower than the original. In such cases the unreacted-core-shrinking model, of course

represents only a part of the reaction history. The reacting porous solid is considered to be semi-infinite with a macroscopically unidirectional movement of the reaction zone i.e. one dimensional diffusivity. But in practice the propagation of reaction in a porous solid may be multidirectional. Isothermal conditions, uniform pore structure etc. are assumed after careful consideration of the individual system. No generalizations are possible in this respect.

The concept of the order of heterogeneous reactions — though empirical - has been a powerful tool in describing the most complex phenomena in terms of relatively simple expressions. It has been aptly pointed out by Aris and Mehta [43] that "though the concept of reaction order is at best a difficult one to justify - and this is particularly true in the context of heterogeneous catalysis - its undoubted success in organizing data on complex reaction systems has led to its wide spread use". Thus zeroth order reaction, in which the rate is independent of concentration, may be approached in a heterogeneous reaction when the surface is almost completely covered; while at low coverage the reaction may be of the first order. Fractional orders have been found to fit experimental data with tolerable accuracy. Negative orders have been used to represent inhibitory effects. At times an "apparent" order of reaction is used to represent all sorts of physical and chemical factors and possibly "lumping" in complex reaction schemes. The surface rate constant and activation energy which are closely associated

with the concept of order of reaction, invariably are adulterated with pore diffusion. Normally, the order of a surface reaction is based on the concentration of reacting fluid in the gas phase. However, the concentration of solids too has been incorporated in the rate expression by Wen [3]. This will have some advantages in the construction of a homogeneous model. At times structural parameters like solid surface heterogeneity uneven poresize distribution, varying porosity and crystallite orientation are included in the empirical rate equation but satisfactory solutions to such problems are yet to be obtained.

Whenever a heterogeneous reaction takes place in a mixed controlled regime, the concentration gradient of the reacting fluid along the depth of the solid is significant. In such situations, attempts have been made to define and develop the concept of effectiveness factor for noncatalytic reactions. Due to some intrinsic differences in the solid reactivity and the diffusion characteristics, the effectiveness of the effectiveness factor for a noncatalytic reaction has not been as significant as that for a catalytic reaction. Mathematical complexity increases as the changes in pore structure during the course of reaction become more severe. And the most severe changes perhaps are experienced in a reaction with no solid product. Depending on the conditions of a reaction, the basis for the definition of the effectiveness factor may be the void volume of the entire solid or the void volume of the unreacted mass only. Similarly the maximum value of the fluid concentration used in the definition

of the effectiveness factor may vary from system to system. One may consider the concentration at the interface between the reacted and unreacted mass, or the concentration at the fluid-solid interface, or the bulk concentration in the fluid phase. Time dependant pore surface area adds one more dimension to the complexity of the problem. Lewis and Paynter [44] have shown that for most of the catalytic batch reactors, the difference between the steady state and the unsteady state effectiveness factors is less than ten percent. The same is not true for all noncatalytic reactions. Therefore one has to identify the common bases and conditions before making any comparative evaluation of reactive systems in terms of their effectiveness factors.

For the first time, the classical work of Thiele [45] was extended to noncatalytic reactions (gasification of carbon by carbondioxide) by Petersen [46]. Walker [2] gave a formal definition of the "Thiele Utilization Factor" for the first order irreversible reactions of carbon and tabulated the expressions for spherical, cylindrical, and plane blocks in various temperature zones. Weisz and Prater [47] developed a general criterion for the importance of pore diffusion with chemical reaction in porous solids. And this is one of the most useful practical results of the concept of effectiveness factor for first order reactions. Petersen [48] has pointed out that for other order reactions, particularly for adsorption mechanisms, the criterion can be drastically different.

Petersen [49] further gave an asymptotic solution for the generalized effectiveness factor and a generalized criterion for the importance of pore diffusion. Aris [4] then showed how this asymptotic Thiele parameter can be normalised so that the effectiveness factor is asymptotically proportional to the inverse of the Thiele parameter when its value is large. Bischoff [50] has arrived at a still more general criterion of Weisz Prater type but not without the presence of an unevaluated integral in the criterion equation. All such investigations deal with general situations which are common to both catalytic and noncatalytic systems. Recently Ishida and Wen [6] have developed the concept of nonisothermal effectiveness factors exclusively for the noncatalytic reactions. From the effectiveness factor plots, three types of instabilities are identified; the geometrical instability, the thermal instability due to metalable temperature, and the instability resulting from abrupt shiftings of the rate controlling regimes. Calvelo and Cummingham [5] have presented a similar generalization of the effectiveness factor for fluid-solid reactions representing the moving boundary, the continuous layer and the moving layer conditions. However, suitable modifications of such generalizations are yet to be made available for the particular reaction of graphite oxidation.

Existing literature on graphite oxidation runs invariably in two distinctly divisible streams, the first one dealing essentially with thermodynamics, kinetics and mechanism of

oxidation, and the second one confining itself to the process of diffusion of oxidant through porous graphite. Only recently some attempts have been made to combine these two streams to illustrate the effect of simultaneous diffusion and chemical reaction on the continuously changing internal wall profile of a single pore in particular, and on the entire pore structure of graphite in general.[29, 50, 51, 52]. Accordingly, the current review will also follow a similar line i.e. to begin with the two streams will be dealt with separately, and then an attempt will be made to combine the two.

The controversies and difficulties associated with the process of oxidation of carbon and carbonaceous materials are dealt with exhaustively by a number of investigators[53, 54, 55, 56, 57, 58, 59]. In spite of these difficulties and may be because of them, the investigations on gas carbon reactions are really extensive and voluminous extending back to the middle of the nineteenth century[7]. It is neither possible nor necessary to include all the extensive work in a short review. So stress will be laid only on these investigations that are relevant to the present work. Rather, an effort will be made to consider only notable advances in this field. The most extensive review on the subject of Chemistry and Physics of carbon has been made available by Walker[60a, 60b, 60c, 60d, 60e]. In the following part of the review, the thermodynamics of the relevant carbon gasification reactions precede the kinetics and mechanism of such reactions.

THERMODYNAMICS

Oxidation reactions in general are exothermic and are accompanied by highly negative changes in free energy. Graphite oxidation is no exception to this and as such the thermodynamic equilibrium is not likely to be a crucial factor in evaluating the progress of reaction. However, thermodynamic calculations are necessary to choose proper ranges of operating pressures and temperatures so that the product of oxidation is essentially carbondioxide. By doing so, it is possible to neglect the rest of the side reactions, and assume a relatively simple kinetic model for further computations.

TABLE 2-1

No.	Reaction	ΔH K.Cal.	ΔG K.Cal
1.	$C(s) + O_2(g) \rightleftharpoons CO_2(g)$	-94.03	-94.260
2.	$C(s) + \frac{1}{2}O_2(g) \rightleftharpoons CO(g)$	-26.62	-32.808
3.	$CO(g) + \frac{1}{2}O_2(g) \rightleftharpoons CO_2(g)$	-67.41	-61.452
4.	$C(s) + CO_2(g) \rightleftharpoons 2CO(g)$	+40.79	+28.644
5.	$C(s) + H_2O(g) \rightleftharpoons CO(g) + H_2(g)$	+31.14	+21.820
6.	$CO(g) + H_2O(g) \rightleftharpoons CO_2(g) + H_2(g)$	-09.65	-06.817

For a system consisting of carbon, oxygen and water vapour, various possible primary and secondary chemical reactions with their respective heats and free energy changes at 18°C and 1 atmosphere are listed in Table No.2-1. In stochiometric chemical equations, carbon is assumed to be in β form with zero heat of formation. Based on this, various forms of amorphous carbon are reported to have positive heats of formation ranging from 1.7 to 2.6 K.Cal/mole [45] which can be neglected in the preliminary calculations.

Independence of reactions can be worked out by writing the above set of reactions in the following form:

$$
\begin{array}{lllllllllll}
C & + & O_2 & - & CO_2 & + & Z & + & Z & + & Z & = & Z \\
C & + & \tfrac{1}{2}O_2 & + & Z & - & CO & + & Z & + & Z & = & Z \\
Z & + & \tfrac{1}{2}O_2 & - & CO_2 & + & CO & + & Z & + & Z & = & Z \\
C & + & Z & + & CO_2 & - & 2CO & + & Z & + & Z & = & Z \\
Z & + & Z & - & CO_2 & + & CO & + & H_2O & - & H_2 & = & Z
\end{array}
$$

N.B. Z indicates a zero in the above equations.

Therefore the matrix of stoichiometric coefficients is

$$
\begin{array}{cccccc}
1 & 1 & -1 & -0 & 0 & 0 \\
1 & \tfrac{1}{2} & 0 & -1 & 0 & 0 \\
0 & \tfrac{1}{2} & -1 & -1 & 0 & 0 \\
1 & 0 & 1 & -2 & 1 & 1 \\
1 & 0 & 0 & -1 & 1 & -1 \\
0 & 0 & -1 & +1 & 1 & -1
\end{array}
$$

By going through the standard procedure suggested by Aris [61] we obtain the matrix:

$$
\begin{array}{cccccc}
1 & 1 & -1 & 0 & 0 & 0 \\
0 & 1 & -2 & 2 & 0 & 0 \\
0 & 0 & 0 & 0 & 0 & 0 \\
0 & 0 & -0 & 0 & 0 & -0 \\
0 & 0 & -1 & 1 & 1 & -1 \\
0 & 0 & -1 & 1 & 1 & -1
\end{array}
$$

Obviously the number of independent reactions is TWO. Here the reactions 1. and 5. may be considered to occur independently.

From Table 2-1 it is clear that at 18°C and 1 atm., the reactions 4 and 5 are thermodynamically not feasible while the reactions 1,2,3 and 6 are feasible. For some of the reactions free energy changes are nearly zero, and hence it becomes necessary to investigate the effect of temperature and pressure on the equilibria of these reactions. Variation of the equilibrium

constant K_p with respect to temperature is indicated in Figure 2-1. From this one can easily see that the reactions of graphite with carbon dioxide and with water are not likely to be significant within the range of temperature under consideration. Further, reaction 1 has an equilibrium constant which is much higher than that of any other reaction. Therefore, from a limited thermodynamic point of view, complete combustion to carbon dioxide appears to be more favourable.

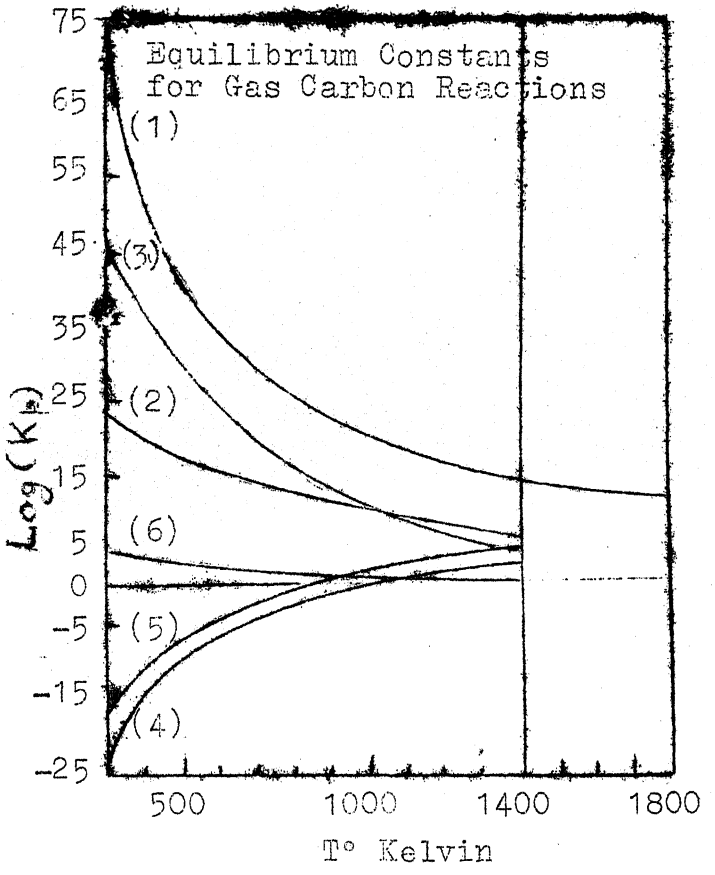

FIGURE 2-1

From the data of reference [62] it is clear that the oxidation of carbon to carbon monoxide and carbon dioxide is not restricted significantly by equilibrium considerations even at temperatures upto 4000°K. It may also be noted that temperatures above 2000°K should be avoided if reactions with carbon monoxide and/or water are to be suppressed.

Again, from table 2-1 it can easily be seen that the effect of pressure on the equilibrium constant can be studied

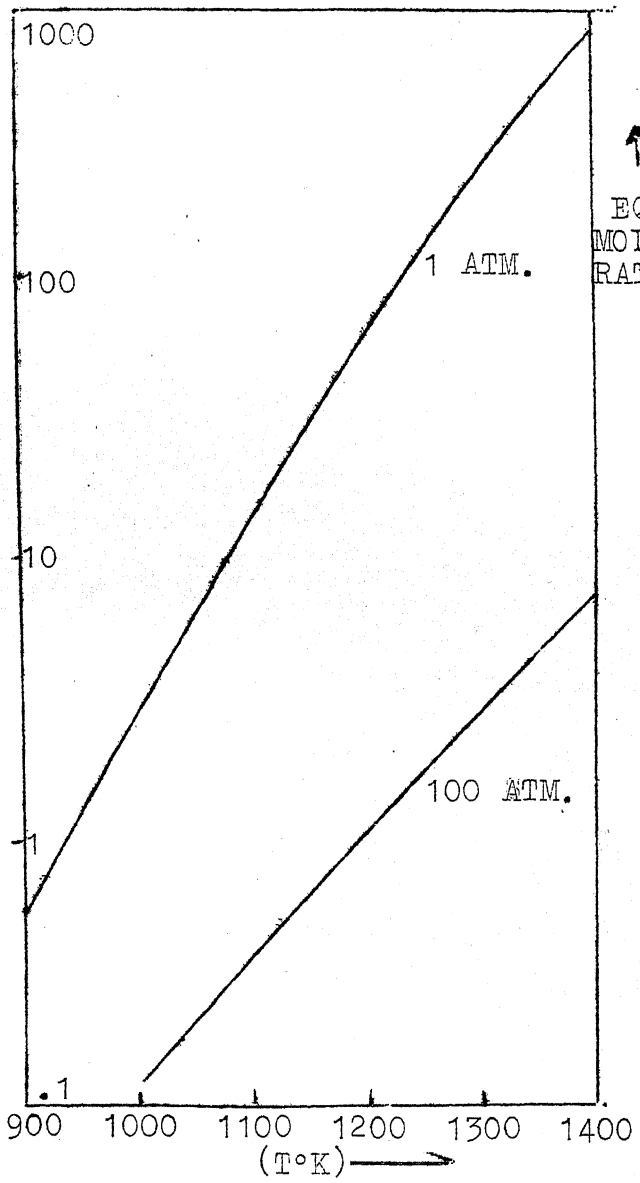

Equilibrium CO/CO_2 ratio as a function of temperature and pressure for the reaction

$$C + CO_2 = 2CO$$

FIGURE 2-2

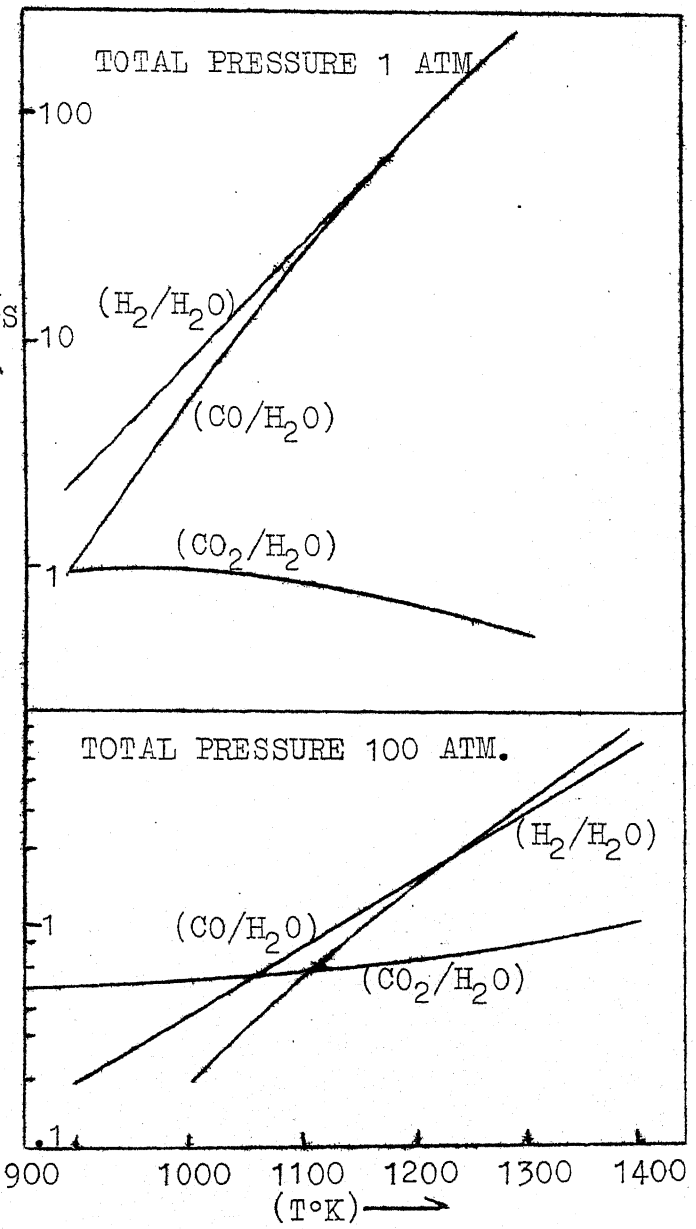

Equilibrium Product Steam Ratios for Reactions 5,6,4.

FIGURE 2-3

only in the case of reactions 2, 3, 4 and 5 where the number of moles does not remain constant during the course of reaction. Over the range of temperature under consideration, the fugacity coefficients of the gases, upto a pressure of 100 atmospheres, remain very close to unity and hence the effect of pressure is not likely to be significant. From actual calculations also we find that the numerical values of K_p do not vary significantly with pressures even upto 1000 atmospheres. However, the variations in equilibrium compositions of carbon monoxide and carbon dioxide are indicated in Figures 2-2 and 2-3 [2]. From Fig. 2-3 it is seen that at temperatures above 1200°K and at atmospheric pressure the conversion of carbon dioxide to carbon monoxide by reaction 4 is unrestricted by equilibrium considerations. At elevated pressures the possible conversion markedly decreases; hence, high pressure is likely to suppress this reaction and promote reaction 1. For the carbon steam reaction, it is seen in Fig. 2-3 that the amounts of carbon monoxide and hydrogen, which can be produced above 1100°K and upto a pressure of 100 atmospheres, are essentially equal, even when the possible side reactions are considered. However, as in the carbon-carbon dioxide reaction, the possible extent of conversion of steam to carbon monoxide and hydrogen decreases with the increasing total pressure. Since the moisture content of the system used in the present investigation is very low, and the steam-carbon reaction is less likely to occur under noncatalytic conditions, the presence

of hydrogen in the gaseous mixture is ruled out. Consequently, the reaction of methane formation is not included in the thermodynamic review.

After considering the effect of temperature and pressure, one may be tempted to go in for the analysis of a complex equilibrium for the reactions 1,2,3 and 4 to arrive at the equilibrium compositions of carbonmonoxide, carbondioxide and oxygen in the multicomponent reaction mixture. But uncertainty of kinetic constants and the inherent coupled diffusion effects associated with porous graphite render the complex analysis less meaningful. This may perhaps be the reason why the analysis of complex equilibrium is not to be found in the vast published literature on this topic.

Since the sorption of gases on the surface of graphite is the primary step - atleast from a chemist's point of view - in all graphite oxidation reactions, the thermodynamics of chemical reaction remains incomplete without the thermodynamics of sorption. The interaction between the graphite surface and the oxygen molecule can be any one of the following:

(a) monolayer adsorption

(b) multilayer adsorption or condensation

(c) chemisorption in presence or absence of other impurities

(d) chemical reaction producing volatile products

Energetics of each of these interactions will naturally be different from one another.

While there exists an abundant literature [22, 26, 63, 64] on adsorption of gases on carbon blacks, very little is reported about the adsorption of gases on graphite [65]. This should be expected because incomplete graphitization has been proved to produce active polar groups on the surfaces of active carbon particles [23]. Correlation of adsorption power and catalytic activity of various finely divided carbons shows that these lie in the sequence: active charcoal > soot > coke or retort graphite. For near ideal graphites, the heat of adsorption has been estimated as few ergs per gramme mole of oxygen, and no calorimetric experiments have been possible in this direction. So, for all practical purposes, the adsorption type of interaction on graphite surface can safely be neglected.

Coming to the next stronger type of interaction of oxygen with graphite, much controversy is found, not only about the physicochemical nature of interaction, but also about the nomenclature used to describe this interaction [64]. The current review follows Ubbelohde's nomenclature [23] to describe these interactions which can be classified into two broad categories.

(i) Graphite Oxide which is the product of chemisorption of oxygen on graphite in presence of hydrogen, which may be represented by a general reaction like $xC + yO + zH \longrightarrow CxOyHz$.

(ii) Surface oxide which is the product of chemisorption of oxygen on graphite in the absence of hydrogen, which may be represented by a general reaction like $xC + yO \longrightarrow C_xO_y$.

Without going into the controversies regarding the precise chemical nature of graphite oxide or surface oxide, it may be worthwhile to recollect some specific instances where the heats of interaction of graphite and oxygen are indicated. A graphon which provides a homogeneous hydrophobic surface of 100 metre^2/gram is supposed to have a medium surface energy of 110 ergs/cm^2 [60b page 221]. Heats of immersion in case of NaDBS solution are of the order of 2.5 cal/gm. of the same graphon [60b page 219]. With N-butanol, in aqueous solutions, it is of the order of 20-80 ergs/cm^2. Bull H.J. and M.H. Hall[66] in a very rudimentary way calculated from bond energy considerations the heat of chemisorption of oxygen as 112 K.cal/gramme mole, which was in reasonable agreement with the experimental values. R. Nelson Smith [67] has reported the variation of the heat of chemisorption with temperature and the amount of oxygen chemisorbed. The first quantities of oxygen admitted to carbon surface at room temperature are chemisorbed with exceedingly high heats of formation (70-100 Kcal/mole) of the same order of magnitude as the heat of formation of carbondioxide. These heats decrease rapidly as additional oxygen is added, finally levelling out to about 55-60 Kcal/mole, when physical adsorption sets in. The heat of formation of complexes formed at 400°C (calculated from heats of combustion) is 32.5 Kcal/gram atom of oxygen, independent of the amount of oxygen combined. All these figures indicate the obvious diversity of thermodynamic data on sorption. Engineering

studies have therefore preferred to group together the steps of sorption and desorption with chemical reaction, thus enabling the usage of a single equation for the entire phenomena.

MECHANISM AND KINETICS

It is needless to say that the doubtful nature of the chemical composition of the surface complex, surface heterogeneity and surface impurities affects the mechanism as much as it does affect the thermodynamics of sorption. However, a broad general scheme of a chain reaction mechanism can be put forward in terms of a "first step" and a series of "succession steps" [68, 69, 70, 71]. Many interesting suggestions regarding "edge attack", "surface attack", foreign element attack at a "claw" or a "hole", breaking off of volatile molecules such as carbon monoxide, chemisorption of atomic oxygen or carbon monoxide, and formation of Lamellar type of compounds, have preceded the development of modern concepts of the nature of defects in solids and the different ways in which foreign atoms can be incorporated in solids. In view of this and because of lack of precision in characterising the defect state of carbon or graphite, the situation regarding the "first step" and the "succession steps" can be considered open for further investigations.

Upto 1960, the major question concerning the mechanism of carbon-oxygen reaction has been whether carbon dioxide is

a primary product of reaction or a secondary product resulting from the gasphase oxidation of carbon monoxide. By now, however, a large majority of workers have agreed that both carbon monoxide and carbon dioxide are primary products, and the primary carbon monoxide-carbondioxide ratio increases with increasing reaction temperature. If high velocities of oxygen are used to avoid stagnation due to molecular diffusion, partial pressure of oxygen does not significantly affect the primary carbon monoxide-carbondioxide ratio. A number of correlations are available for the variation of the primary carbon monoxide - carbon dioxide ratio with temperature, but none of them is really versatile because it has not yet been established that the magnitude of this ratio is solely a function of temperature and is independent of the carbon reacted and the impurities present in it. It is interesting to note that the evidence for the formation of a carbon suboxide (C_3O_2) as a first volatile product at present refers to graphite with considerable radiation damage, and may apply only to highly defective carbon net works [54, 72]. Another suboxide (C_2O) has also been proposed in oxidation mechanisms particularly at low temperatures [73]. The mechanism of carbon-carbon dioxide reaction, which is itself not understood properly, cannot possibly be used to understand the nature of the primary product of oxidation.

Before proceeding with the details of kinetics, it may be useful to list some experimental techniques used in

the study of graphite oxidation. One of the commonly employed methods of following the kinetics of reaction is to observe pressure changes as a function of time [74]. Since the products are volatile, another convenient way of measuring reaction rate is from the loss of weight of the graphite sample [64, 75, 53], as recorded by means of a sensitive microbalance operable at variable temperature, pressure and gas composition. Recently developed instruments provide a gas analyser to continuously record the composition of outgoing gases. Not only can this give information regarding the carbonmonoxide-carbon dioxide ratio, but it also provides a double check on weight loss measurements. Very high velocities of gas have been utilized to eliminate the effects of diffusion while stagnant gas is used to introduce the effect of molecular diffusion only. Inhibitors like phosphorous trichloride are employed in the gas stream to arrest secondary reactions. Radioactive tracers have also been used to follow the reaction [76].

A number of classical techniques have been employed to isolate the effect of catalyst from the crystal defect. An experimental method applied in high temperature studies is to use a carbon filament as a specimen which can be heated by the passage of an electric current and the temperature can be measured by means of an optical pyrometer [77]. This not only solves the problem of material of construction at high temperatures, but also eliminates the parameter of porosity

from experimentation when very thin filaments are employed. Recently [60a] attempts have been made to record the changes in thermo-e.m.f. developed at the junction of graphite crystal, to follow the kinetics of chemisorption of oxygen. Optical and electron microscopy techniques have been very useful in studying the etchpit expansions during the course of oxidation. J.M. Thomas [60a] has reviewed important experimental techniques in this direction, and has indicated how etchpit expansion studies have helped to differentiate between the rate of oxidation in planar and perpendicular directions at the molecular level. Recently,[11], a novel technique of a motion picture study of catalysed and uncatalysed reaction between carbon and oxygen has been effectively employed in Pennsylvania State University. Coming to macrostudies, huge channels and nozzles of graphite are subjected to oxidation studies under flow and nonflow conditions to find out the suitability of graphite as a material of construction in nuclear reactors and rockets[52, 28].

With the available experimental data and the postulated mechanism, various attempts have been made to interpret activation energies, rate constants & order of reaction, at different temperatures. In absence of diffusion effects and secondary reactions, the rate of reaction (weight loss of carbon) can be considered the same as the rate of surface rearrangement of the carbon-oxygen complex to a rapidly desorbable product. In principle, in an equimolal gas solid reaction, the order of reaction with respect to the oxygen pressure should vary

between ONE and ZERO as θ, the fraction of the surface covered by carbon oxygen complex changes from ZERO to ONE. At a constant temperature, θ varies from ZERO to ONE as the pressure is increased from zero to higher values, thus causing a corresponding variation of order from ONE to ZERO. Similarly the reaction temperature can also affect the order. The reaction which is of zero order at low temperatures and at a given pressure can become of first order at the same pressure and sufficiently higher temperatures.

The majority of results [74, 78, 79, 80, 81, 82, 83, 84, 63] under varied experimental conditions show the carbon-oxygen reaction to be first order or close to first order. From the previous discussion, it implies that under all the experimental conditions used by the above authors, the fraction of the total active carbon surface occupied by the oxygen surface complex at any given instant during the reaction approaches zero. Almost all the authors have given experimental evidence to this effect. Two notable exceptions are found to the carbon-oxygen reaction being first order. Gulbransen and Andrew [53], working with spectroscopic graphite, have found that, at reaction temperatures of 450°C and 500°C and at pressures below 0.15 cm. of Hg, the order is nearly zero. They do state further that at pressures above 10 cm. of Hg. the reaction is first order. Blyholder and Eyring [85] reacted extremely thin coatings of graphite, supported on a ceramic base, with oxygen at 800°C and a pressure less than 100 μ Hg.

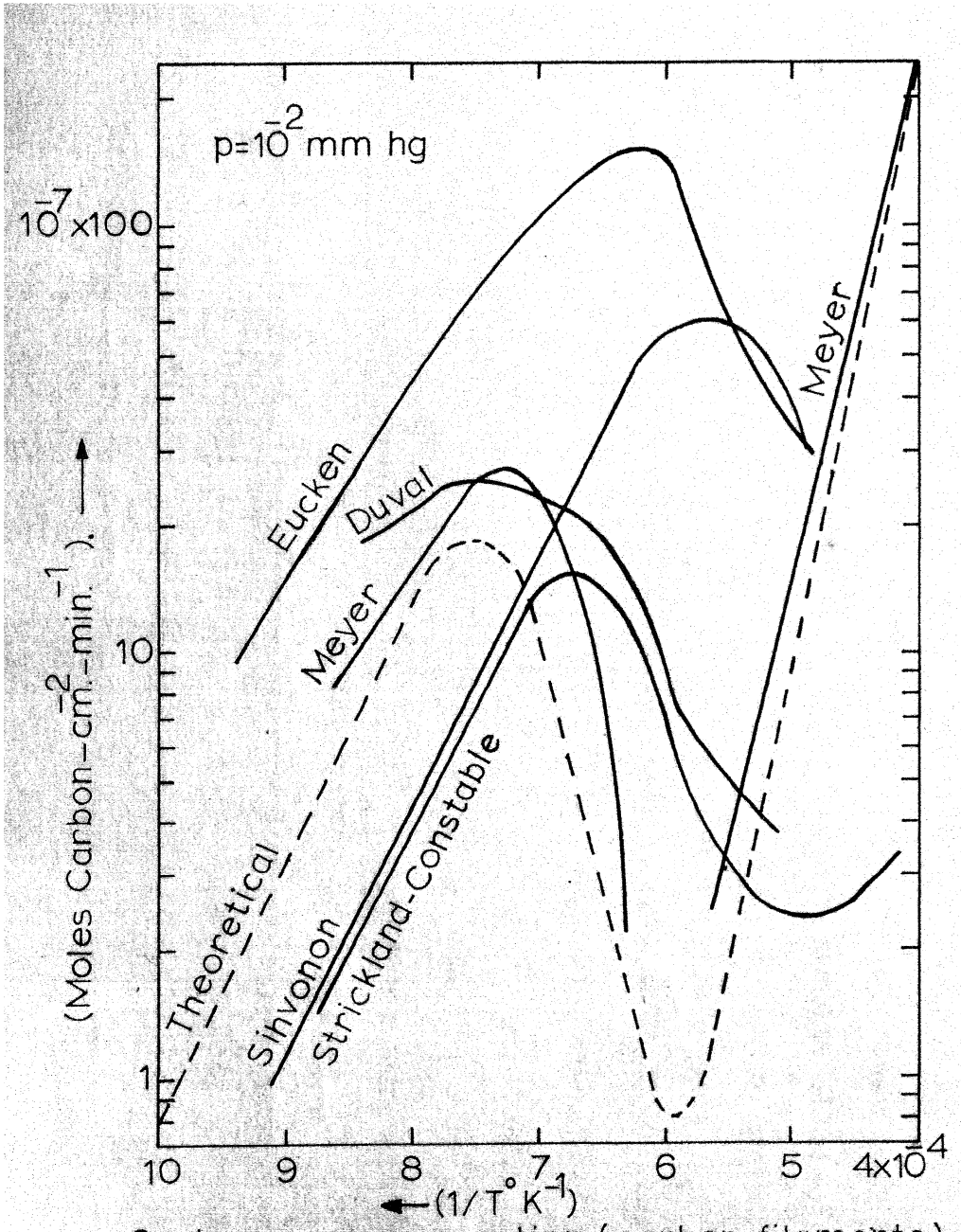

Carbon-oxygen reaction (carbon filaments)

FIGURE 2.4

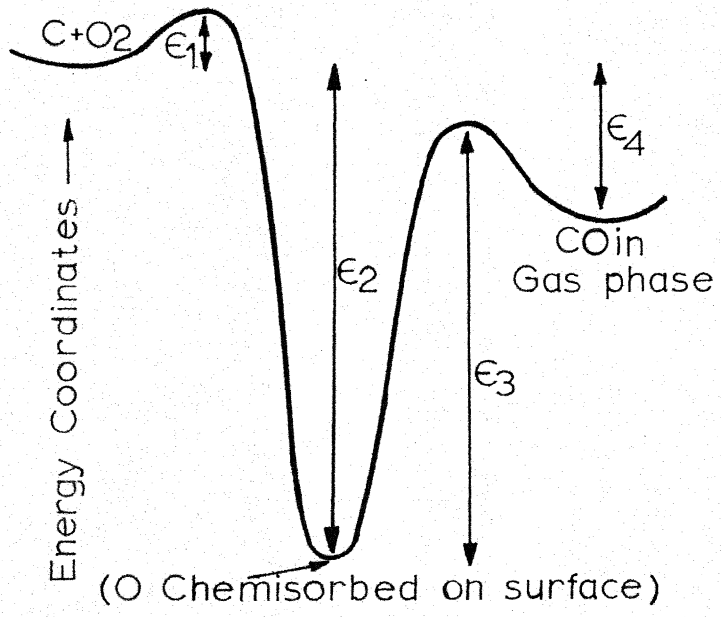

Reaction coordinates for reaction of oxygen with surface

ϵ_1 is the activation energy for chemisorption of oxygen (value unknown)

ϵ_2 is the heat of adsorption of oxygen:
calculated from bond energies 183 kcal/mole,
estimated from calorimetry 97 kcal/mole,

ϵ_3 is the activation energy for desorption of CO, estimated from kinetic measurements (Blyholder & Eyring, 1957) 8 kcal/mole.

ϵ_4 is the heat of formation of CO from solid carbon and gaseous oxygen, 26·8 kcal/mole.

FIGURE 2-5

From limited data they have concluded that the reaction is of zero order. Andrew's statement that the reaction order increases with increasing pressure is difficult to explain on theoretical grounds because, in any heterogeneous reaction, with increasing pressure θ tends to ONE and the order of reaction to ZERO. However, Blyholder and Eyring prescribe a half order reaction for Gulbransen and Andrew's data at 450°C over the entire range of pressure. In the present work, low temperatures have been avoided so that a first order reaction may be uniformly assumed.

The oxidation rates for carbon filaments increase with temperature upto about 750°-1000°C. Between this range and about 1700°C rates remain of first order, but decrease with the rise in temperature. Figure 2-4 illustrates results obtained by different authors who have studied the oxidation of carbon filaments. As the temperature increases, the rate goes through a maxima; at still higher temperatures the rate increase again, but the order now becomes ZERO. Different steps appear to exert their control in different ranges of temperature. From an oxidation rate equation of the form Rate = $A + BPo_2$, where A and B are constants at a particular temperature and Po_2 is the partial pressure of oxygen, a rate controlling activation energy of 37.5 Kcal/g.mole has been inferred [53]. Alternative interpretations can be that this energy refers to the desorption of chemisorbed carbon monoxide molecules, without which the succession steps cannot occur, or to the

breaking of carbon bonds as carbon monoxide is separated from the carbon network. A rate expression of the form Rate = $A\sqrt{Po_2}$ has been proposed as an alternative to fit the same experimental data and also other results [85]. This gives an activation energy of about 42 Kcal/mole. This form of apparent rate expression could originate from the diffusion of oxygen into the cracks and pores of the solid, as a rate controlling process [7]. Attempts to avoid complications of porosity by using natural graphite of high density (2.26 g/cc) still fail to evade the problems of total pore surface area and particle size [86]. Where diffusion of oxygen into graphite controls the rate of oxidation, it has been shown that the order of reaction is (n+1)/2 where n is the true order of the surface reaction [85]. Under these conditions the observed activation energy should be half the activation of the actual surface process. When very thin layers of graphite are oxidized so as to minimize the effect of diffusion into the interior, zero order reaction rates with respect to pressure were obtained with the calculated activation energy of 80 Kcal/mole. Since this value is also found in the zero order oxidation rate that prevails above 1700°C for graphite filaments, this appears to refer to a fundamental step in oxidation such as the breaking of C-C bonds in the surface.

Figure 2-5 illustrates a scheme of activation energies for different steps involved in graphite oxidation when the rate is controlled solely by resistance to chemical reactivity

and not by diffusion. Apparently, step 2 appears the slowest. However, Rossberg [87] suggests that the slowest step in the reaction is the separation of an oxygen atom from the reacting species. He justifies this by comparing the activation energy of the reaction $C + 1/2\ O_2 \longrightarrow CO$ (58 Kcal/g.mole) with the dissociation energy associated with the breaking of half mole of oxygen into an atom of oxygen i.e. $1/2\ O_2 \longrightarrow O$ (59 Kcal/atm of oxygen). This line of argument appears inconsistent because it presumes that irrespective of whether θ is ZERO or ONE, dissociation of oxygen is the slowest step. As discussed before, the implication of the zero order reaction is that the overall gasification rate is being controlled by the rate of removal or rearrangement to a desirable product of the surface oxygen complex and not by the rate of its formation. Even when the reaction is of first order, it is doubtful whether Rossberg's concept has any significance, since it would appear unsound to compare half the dissociation energy of oxygen with the activation energy of reaction. Moreover, the dissociation of oxygen just does not figure in any of the steps mentioned in the reaction mechanism. Perhaps a more reasonable explanation of relative activation energies for the reactions between carbon and oxygen containing gases, is indirectly hinted by Long and Sykes [88]. Their contention that the exothermicity of interaction of a gas molecule with a carbon free site in case of carbon-oxygen reaction is nearly twice that for carbon-steam or carbon-carbon dioxide reactions

fits well in the pattern of activation energies shown in Figure 2-5.

For some carbons it is contemplated that the reaction with carbondioxide proceeds at a measurable rate above 600°C. However, with electrograde graphite of density 1.6 gm/cc, the reaction with carbondioxide is unlikely because excess of carbon monoxide molecules in the gas phase compete with carbondioxide for active sites, thus poisoning the reaction. This is supported by tracer experiments with radiocarbon [89]. But with synthetic graphite diffusion into internal pores could lead to a different explanation of the inhibitory effect [75]. In other words, inhibition is imperative and hence the isolation of reaction of oxygen from that of carbon dioxide is needless. Reaction with water vapour - as has been pointed out in the thermodynamic review - is a more remote possibility than that with carbon dioxide, and hence need not be considered. It is to be noted that while the presence or absence of water vapour makes a difference in the mechanism and kinetics of reaction, there will be no difference in the mechanism once the water vapour content in the oxidizing medium exceeds the limit of a few parts per million. Normal variations, therefore, in the level of humidity of the reacting gas medium will not be a factor in the present experimental work.

EFFECT OF SOLID IMPURITIES AND CRYSTAL DEFECTS

Even spectroscopically pure carbon contains impurities like boron, titanium, calcium, sodium, silicon, iron, magnesium and copper, which can be detected by special means. If these are incorporated in the network, the electron densities of the neighbouring carbon atoms will be perturbed, so as to favour or disfavour attack by oxygen. It, therefore, becomes necessary to study the effect of these solids on the mechanism and kinetics of oxidation. Traditionally, it has been customary to treat the defects in graphite crystals as some solid impurities in the structure. This is probably because crystal defects and solid impurities have similar effects on oxidation; and in some cases it has not been possible to say one from the other [23]. Experiments showing a catalytic influence of solid impurities do not in general establish how they are bounded to the carbon [90]. However, the fact that gaseous impurities such as oxygen, hydrogen and nitrogen atoms can be directly linked to the carbon atoms whereas solid impurities are indirectly linked, probably through acidic groups like -C-OH, is well established. It is also generally agreed that most of the common solid impurities catalyse oxidation, and substances like phosphates, borates, pyrolytic carbon, phenolic resins and metal carbides inhibit the reaction. An exaustive list of references on catalytic activities is given by Walker [2] and Ubbelohde [23]. Most of these investigators have taken a

a common approach of correlating catalytic activity with "nobility" or ionization potential of the elements, obviously without much success. Synergistic catalytic effects are invariably observed when combinations of a number of elements is tried.

The main concern of this review is for the uniformity of samples with respect to composition, electronic state of impurities, distribution of crystal defects and crystallite orientation, both perpendicular and parallel. Fortunately, in macro-oxidation, the number of nonuniformities is so large and randomly distributed that on an average the reacting surface retains its uniformity.

The size and shape of graphite particles are two parameters which are badly mixed up with the effect of crystal defects, impurities and the irregular variation in the effectiveness factors. Armington [80] selected carbon blacks of a wide range of particle size and represented the rate data as shown in figure 2-6.

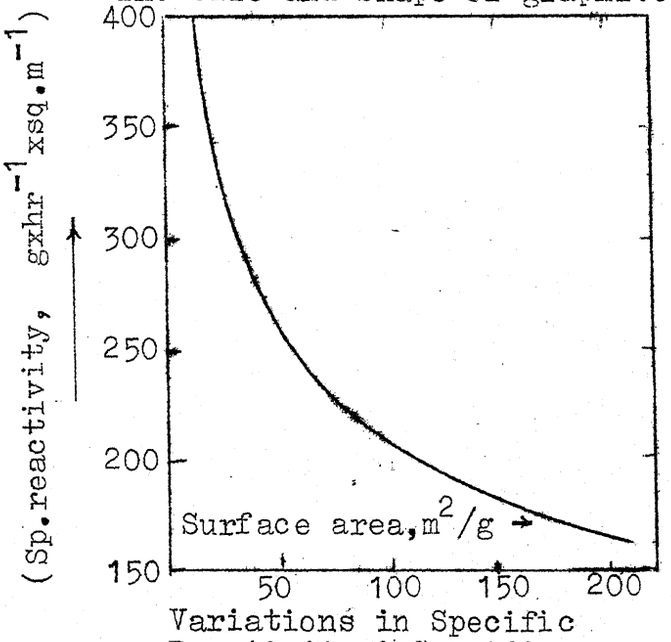

Variations in Specific Reactivity & Specific Surface Area

FIGURE 2-6

He suggests that crystallite edges serve as zones of high resistance to electron flow. The number of edge carbon atoms

per unit volume, and hence the resistance to the spread of electronic effect of an impurity, is more in the case of a smaller crystallite size than in a larger one.

Recently H. Harker and associates [91, 92] have used E.S.R. techniques to study the effect of impurities that are added to the graphite net work before and after irradiation. Hennig's etchpit technique [60a] has also been used to isolate the effect of a defect from that of an impurity. As has already been mentioned [11], microcinematographic techniques have been utilized for similar purposes. With the advent of more powerful microscopes, it is hoped that the effect of impurities will be better understood, thus paving a way for a clearer understanding of the mechanism.

ROLE OF MASS TRANSPORT IN GRAPHITE OXIDATION

The steps involved in graphite oxidation are essentially the same as the ones mentioned earlier for general heterogeneous reactions, and thus the reaction can take place in various control regimes. The apparent values of the order of reaction, activation energy and the effectiveness factor for different zones of temperature are given in Table 2-2.

Peterson [46], for the first time, using an approach similar to the one of Thiele for catalytic reactions, has mathematically treated a single cylindrical pore and a porous solid initially containing uniform cylindrical pores with random intersections. In essentially a similar manner,

TABLE 2-2

Zone	Order of Reaction	Effectiveness factor	Relation between E_a and E_t	Remarks
Zone I (low temperature)	ZERO	ONE	$E_a = E_t$	The diffusion resistance and hence activation energy for diffusion is ZERO
Zone II (Intermediate temperature)	>HALF	>HALF	$E_a = E_t/2$	Relation has shortcomings because of missing kinetic & diffusion parameters
Zone III (High temperature)	ONE	ALMOST ZERO	$E_a > E_t$	Both diffusion and reaction have low activation energies and hence magnitude of E_a is small

N.B. E_a and E_t are apparent and true activation energies

Walker et.al. [2] gave a formal definition of the "Thiele utilization factor" and have derived an equation to predict the criteria for the occurrence of a gas-carbon reaction in Zone II. Equations for a plane sphere and a cylinder are developed on the lines given by Aris [93]. The treatment assumes a first order reaction on the surface of a cylinder of infinite length. A quasisteady state is assumed. The variation of concentration of gas is considered within the solid and not in the gas phase. Volumetric specific rate constant K_v and the effective diffusivity D_{eff} are assumed constant throughout the rod. The equation for simultaneous diffusion

and chemical reaction in cylindrical co-ordinate system is solved for the rate of loss of weight of the cylinder. The "Thiele utilization factor" η, defined as the ratio of the actual rate of reaction to that which would occur if the reacting gas concentration were uniform throughout the material, is expressed in terms of a dimensionless ratio $\varphi = R\sqrt{K_v/D_{eff}}$ which is an empirical index assuming different values in different zones. Results are summarized in Table 2-3.

TABLE 2-3

Criteria for the prediction of gas carbon reactions entering Zone II for samples of various geometry

Geometric shape	φ	η for $\varphi > \Delta\varphi_{II}$		Rate of reaction per unit area of exterior surface for uniform gas concentration throughout the sample.	Rate of reaction per unit area of exterior surface when $\varphi > \varphi_{II}$
		η	φ_{II}		
Plane: thickness R	$R\sqrt{K_v/D_{eff}}$	$1/\varphi$	2	$K_v C_R R$	$\frac{dw}{dt} = C_R\sqrt{K_v/D_{eff}}$
Cylinder: radius R	$R\sqrt{K_v/D_{eff}}$	$2/\varphi$	4	$K_v C_R R/2$	$\frac{dw}{dt} = C_R\sqrt{K_v/D_{eff}}$
Sphere: radius R	$R\sqrt{K_v/D_{eff}}$	$3/\varphi$	6	$K_v C_R R/3$	$\frac{dw}{dt} = C_R\sqrt{K_v/D_{eff}}$

Note that the value of φ_{II} for start of zone II is quite arbitrary. In fact, the changeover from zone I to zone II can cover a considerable range of temperature. This difficulty is not experienced when the reaction passes from zone II to zone III, because the overall rate does not vary appreciably due to small changes in diffusivities.

Without altering this basic background, a large number of investigators have studied graphite oxidation under varying velocities, gas temperature, oxygen concentration, etc. Many a time air at varying velocities, is admitted over the sample and the rate of weightloss is determined. Extrapolation in the region of high velocity gives the rate data which is free from diffusion effects. After considering the heat transfer analogy and after eliminating the effects of variations in viscosity, density, diffusivity and reactivity, many investigators have attempted to correlate the variation of reaction rate with linear gas flow rate as given by the equation $\frac{dw}{dt} = \alpha \left(\frac{V}{R}\right)^n$, where α is a constant, V is the velocity of gas, R is the characteristic dimension of the sample, and n is the exponent which can take values from 0.20 to 0.50. Parker and Hottel [94], reating brush carbon with air at 1227°C have found that the rate varies with 0.37 power of velocity. Mayers [95], using 40- by 60- mesh coke in 1" high beds, obtains a value of 0.5 for the exponent; Chukhanov and Karzavina [96] in their high velocity experiments using beds of particles 3 by 5.5 mm in diameter found a value of 0.4. Kuchta and Co-workers [97] using carbonrods report an exponent of 0.45. Day [78] using carbon and graphite rods reports a value of 0.5, and Tu et.al. [98] a value of 0.49. More and more experiments were done because of the differences in the value of exponent n. However, it was Graham [64] who studied the steam-carbon reaction under high velocity conditions and clearly pointed out that an exponent

less than 0.5 means that the reaction is not in zone III and an exponent of 0.5 indicates that the reaction is well in the high temperature zone. It also goes without saying that under identical reaction conditions (i.e. for a fixed composition and velocity of the gas stream at a fixed temperature) the rate of reaction in zone III is independent of the type of carbon reacted. Some reservation can be expressed regarding the nature of carbon effecting the carbon monoxide-carbon dioxide ratio leaving the surface and hence the reaction rate per unit of oxygen, diffusing to the surface. Even though sufficient data is not available, Day [78] reports that the reaction rates of petroleum coke, graphitized lampblack, and graphitized anthracite rods agree within 12% at a temperature of 1827°C and at a constant gas velocity.

For reaction at the same temperature, P.L.Walker [2] has theoretically predicted the relative rates of the different gas-carbon reactions, in the high temperature zone, when using a sample of fixed dimensions, a constant linear gas velocity and a fixed concentration of reacting gas in the main stream. (Refer Table 2-3). Logically the relative rates should depend on

(i) viscosity and density of gas present in the stagnant film. i.e. the parameters occurring in the expression for film thickness.

(ii) free diffusivity through the stagnant film.

(iii) number of moles of carbon reacting with each mole of the reacting species.

The reaction rate constant does not come into the picture because of the diffusion controlled regime. Surprisingly, very few investigators [52] have tried to exploit this idea to determine one of the above four parameters when the remaining three are known.

Occassionally, the change in physical structure of graphite, in terms of density and area profiles, after degrees of burn off at different temperatures can aid in the understanding of gas-carbon reactions, especially so in deciding the zone of the reaction. This is well illustrated by Walker[2]. Some investigators [60b, 29] have tried to correlate the porosity and the poresize distribution with the percentage degree of burnoff of the sample. Figures 2-7 and 2-8 indicate interesting results of Walker for burning of hollow cylinders of graphite. However, a satisfactory explanation of the extremum points in the curves is not available. Similar multiple extremas seen in the investigations of Griffiths [21] and Thomas [29] are also not well explained.

Most of the recent investigations in the field of mass transfer with chemical reaction of graphite, have been undertaken with one of the following objectives in mind:

(a) To evaluate the properties of graphite as a material of construction for rocket nozzles.

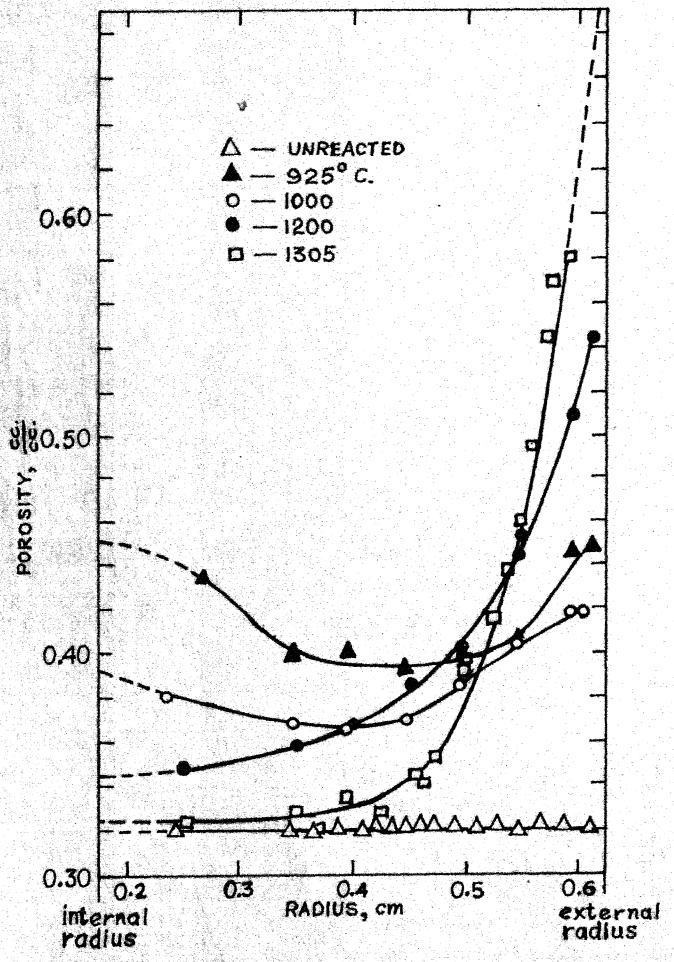

Porosity profiles through spectroscopic carbon rods before and after 11% burnoff at different temperatures.

FIGURE 2-7

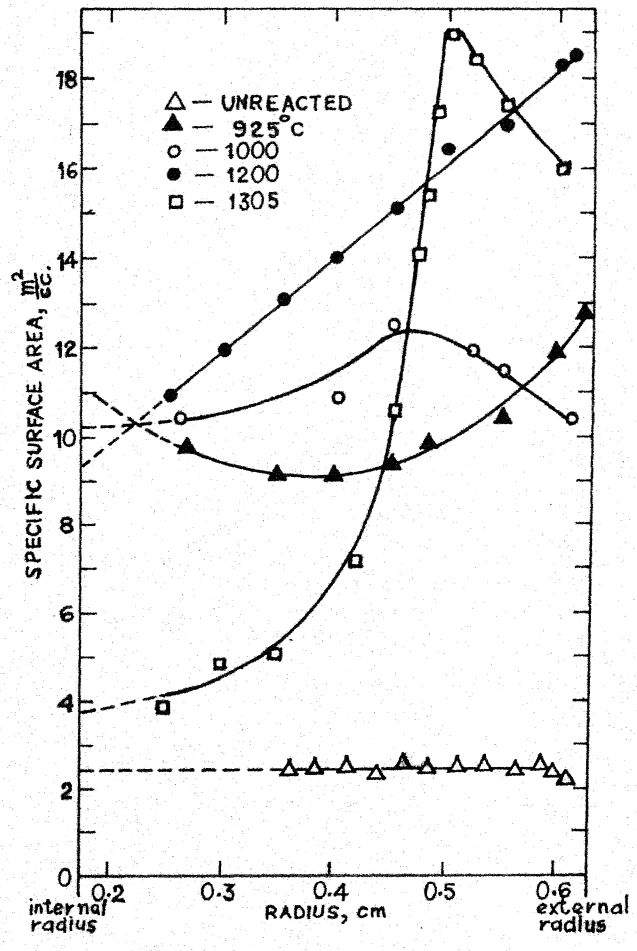

Specific surface area profiles through spectroscopic carbon rods before and after 11% burnoff at different temps.

FIGURE 2-8

(b) To improve the performance of graphite as a moderator in nuclear reactors.

(c) To estimate the time dependent effectiveness factor for noncatalytic reactions.

P. Hawtin and R.A. Huber [52] have studied experimental oxidation of a tubular specimen of nuclear grade graphite in which oxygen access is confined to the bore of the tube and the mathematical model developed has been used to estimate chemical reactivity, utilization efficiency and the effective diffusion coefficient through the porous walls. In fact, this work looks like the starting point for the present work. D.G. Schweitzer, R.M.Singer and Co-authors [51, 99] have studied the simultaneous oxidation and heat transfer in graphite channels with an obvious objective of predicting the stable performance of air cooled BNL graphites in nuclear reactors. They have covered the experimental and theoretical aspects of parameters like temperature, flow rate, channel diameter and chemical reactivity. Two important conclusions arrived at are relevant to the present work. Firstly, the most rapid temperature instability is concluded to be due to the secondary gas phase reaction of carbonmonoxide with oxygen. Secondly, no diameter effect other than that accounted for by the heat transfer coefficient was observed implying thereby the absence of radial concentration gradients in the system. Maberry et.al,[28] have tried to evaluate the performance of a graphite nozzle subjected to internal errosion and corrosion. Straight-

forward dimensional analysis is carried out by using several parameters like nozzle diameter, length, gasflow rates, fuel to oxygen ratio, mach number, temperature, throat to mouth pressure ratio, and the diameter ratios. The exponents for various dimensionless groups are estimated. As late as in 1970 [100], ablation performance of various types of graphites have been tested with a view to assess the potentialities of these materials for the use in dynamic aerospace environments. Hemispherical samples during the course of diffusion controlled reaction, turn out into conical shapes, but unfortunately no mathematical model is proposed. The models given by Scala [101, 102] do not agree with the experimental results. Maahs [100] attributes this to a probable reduction in reaction rate at high temperatures than the ones predicted by the extrapolated Arrhenius plot. G.L. Tingey et.al.[30] have studied the thermal and radiolytic reactions of coolant impurities with graphite in a high temperature gas cooled reactor. The Bessel function solution of an equation for diffusion-limited reaction is numerically solved on the computer. Even though the temperature variations along the length and radius are considered, variations in wall profiles have not been determined owing to an extremely slow rate of gasification of the moderator. Ralph Norman [103] has treated the problem of mass loss as a function of time and position, but the sample geometry is a flat plate and that too with an assumption of one dimensional slug flow and a quasisteady state condition.

In most of the aerospace applications, sublimation of graphite plays an important role in the diffusion controlled regime. Under such conditions new mathematical models are presented to take into consideration supersonic environments and high temperature sublimations. In the field of chemical engineering kinetics, repeated attempts are made to express the effects of diffusion in terms of a generalized effectiveness factor for noncatalytic reactions [5, 6, 49]. However, the treatment given is of a general nature and serious difficulties are experienced when attempts are made to apply this general treatment to the particular case of graphite oxidation, and probably to any specific experimental case.

To end this review, it may be noted that inspite of all the controversies, graphite oxidation forms a reasonably good basis for further experimental investigation because on macroscale the system can be satisfactorily represented by a simple first order surface process.

***

3. MATERIALS AND METHODS

Before going into the details of the experimental procedure, it may be worth mentioning the specifications of the materials used, the list of which is given below:

(1) GRAPHITE: Metallurgical grade graphite which had been used as a melting electrode in a carbon-steel manufacturing furnace for over an year, was used as the starting material for preparing the samples. The apparent density measured by weighing an accurately machined cylinder was found to vary from 1.600 grams/cc to 1.605 grams/cc. Depending on the temperature of graphatization, the theoretical density of nonporous graphite is known to vary between 2.26 gram/cc and 2.10 grams/cc. Based on this, the variation in the porosity of the solid was estimated to be in the range of 0.29 to 0.23. The ash content determined by the standard A.S.T.M. method [104] was found to be less than five hundred parts per million.

(2) METHANOL: BDH analar grade solvent.

(3) PLASTER OF PARIS: No particular specifications.

(4) SILVER GOOP: A patented paste of a silver compound.

(5) NICKEL FOILS: Obtained from 99.99% pure nickel sheets.

(6) SILVER WIRE: Made of 99.99% pure metalic silver.

(7) SILICA: Finely powdered form with no particular specifications.

(8) FELSPAR: Finely powdered form with no particular specifications.

(9) CHINA CLAY: Finely powdered form with no particular specifications.

(10) CALCIUM OXIDE: Finely powdered form with no particular specifications.

(11) SOROSIL CEMENT: A patented paste of a special quality cement dissolved probably in a mineral oil.

(12) BENZOIC ACID: Fine flakes of B.P. grade.

(13) SODIUM HYDROXIDE: Solutions of various strength.

(14) REFRACTORY BRICKS: Fire proof alumina bricks capable of withstanding temperatures upto 1800°C.

(15) COMPRESSED AIR: As available from a compressor or a cylinder.

(16) OXYGEN: 95% purity gas filled in a cylinder.

(17) NITROGEN: 98% purity gas stored in a cylinder.

(18) LIQUID NITROGEN: As available from the liquid air plant.

The entire experimental work can be divided into three parts:

(a) Oxidation of graphite in a single pore.

(b) Reaction of benzoic acid and caustic soda in a pore.

(c) Determination of the first order reaction rate constant.

EXPERIMENTAL PROCEDURE FOR (a)

MACHINING OF SAMPLES: Graphite blocks available in irregular sizes and shapes were machined on a precision lathe to obtain a number of hollow cylinders the dimensions of which are indicated in Table 3-1.

TABLE 3-1

Dimension in Cms.	Set 1	Set 2	Set 3
Length	2.0	4.0	6.0
Internal diameter	0.1	0.2	0.4
External diameter	0.5	1.0	2.0

Some of the guiding principles and constraints which restricted the maximum and minimum dimensions of length, internal diameter and external diameter, are enumerated below. The limiting factor for the maximum length was the operating length of the available precision drills. Holes were drilled from both the ends, and the minor eccentricity resulting therefrom was corrected by sliding and rotating the cylinder over a brass rod of accurate dimensions. In fact, drilling was started with a bore of a smaller size and was gradually increased to a diameter slightly less than the desired value. The minimum length was restricted by the desirability of having an appreciable gas phase concentration gradient in the axial direction. For the same

reasons, the maximum internal diameter had to be restricted to 0.4 cm. As regards the minimum internal diameter, the limiting factors were an unduly long reaction time, a long machine time for computation, and the vibrational stresses causing the breakage of small diameter drills. There were no serious limitations experienced in the choice of the external diameter of the cylinder. While a larger external diameter was suitable for the purpose of coating and material handling, a smaller one was preferable for a short time of reaction and computation.

PREPARATION OF REACTING SURFACE: To obtain uniform surface properties of graphite, samples were washed with methyl alcohol[80]. Machined graphite samples were placed in a conical flask and acid washed methyl alcohol was poured into it. The flask was corked and placed in a constant temperature bath at 40°C for about ten minutes. The samples were removed and dried in an oven at 100°C for two hours; they were now ready for a protective coating. At this stage, the weight of all the samples was recorded. The time lag between the surface preparation and the mounting of the samples in the furnace was not an important factor affecting the initial rate of reaction.

COATING OF EXTERNAL SURFACE: The technical problems involved in the insulation of the external surface against chemical reaction were many and varied. The various methods tried for obtaining a stable protective coating are listed below:

(i) A paste of Plaster of Paris was coated on the external surface and was allowed to "set" in an oven at temperatures varying from 80°C to 300°C. The coating thus obtained was porous and could not act as an airtight covering. As soon as the samples were introduced into the furnace, cracks in the coating became prominent and the samples started burning from outside, at a rate which was much faster than that of the reaction inside the pore. The method, therefore, had to be abandoned.

(ii) Some silver compounds are known [23] to act as inhibitors for graphite oxidation reactions. A patented material "Silver Goop" was coated on the external surface and the sample was dried in an oven at 200°C for two hours. Again, however, when the sample was introduced into the furnace, the coating became unstable and allowed the external surface to react; and this method also had to be discarded.

(iii) Attempts were made to generate a coating of silicon carbide on the external surface so that it remained stable and unreacted even upto a temperature of 1800°C. Solid cylinders were completely covered by finely powdered silica and were introduced into a furnace. Carbide formation normally occurs at temperatures above 1800°C but the porous structure of graphite began crumbling even at 1650°C; so no attempts were made to reach a temperature of 1800°C for obtaining a silicon carbide covering.

(iv) It was contemplated that a metallic sheathing [120] could

act as a protective coating. The graphite cylinder was inserted into a stainless steel sheathing. However, the coefficient of expansion of metal being higher than that of graphite, a tight fitting could not be retained during the course of reaction. Moreover, softening and distortion were added problems. In fact, the softened metal, on entering the latix of graphite, catalysed the surface oxidation instead of inhibiting it. Protection by means of a metallic tube hence was out of consideration.

In order to avoid the problems of softening and distortion of a thick metal coating, attempts were made to deposit very thin layers of nickel and silver vapours on the external surface. Graphite cylinders were rigidly mounted on rotatable shafts connected by aluminium gearwheels, one of which was rigidly fixed on to the shaft of a micromotor. The system was so placed that the tungsten boat of the Veeco vacuum evaporator was centrally located at a point equidistant from the four graphite cylinders, which could freely rotate about their respective axes. The metal foil was placed on the tungsten boat. After closing the belljar of the Veeco evaporator, the two vacuum pumps were started in succession, and when the pressure was 10^{-6} to 10^{-8} cm. of Hg., an electric current was passed through the metal foil. Then the micromotor was switched on so that the graphite cylinders began to rotate, thus enabling a uniform coating of the metal vapour on the external surface. Contrary to our expectations, such a layer did not

adhere to the surface; this in turn rendered the method ineffective.

(v) Next, ceramic protective layers such as frit and glass were tried. Materials were intimately mixed in the proportions indicated in Table 3-2.

TABLE 3-2

Substance	Percentage Composition		Weight in Grams	
	SET 1	SET 2	SET 1	SET 2
Silicon dioxide	80%	80%	200.0	160.0
Felspar	10%	15%	25.0	30.0
China Clay	9%	4%	22.5	8.0
Calcium Oxide	1%	1%	2.5	2.0
TOTAL	100%	100%	250.0	200.0

The mixture of composition mentioned in set 1 was mixed with 300 cc of water and poured into a stone ware ball mill which was then closed and placed on rotating bars. Grinding was continued at 60 r.p.m. for about twenty four hours. The resulting frit was used for coating the external surface of the graphite cylinders, which after drying for 8 hours at room temperature, were introduced into a furnace at 600°C. Nitrogen atmosphere was maintained by constant flow of nitrogen through the furnace. The temperature was allowed to rise to 1000°C in an hour's time. However, the coating thus obtained had developed cracks in it. The frit composition, therefore, was changed to the one mentioned in

set 2, but this also did not yield any favourable results.

(vi) Lastly, a patented paste of "Sorosil Cement" was tried. This coating appeared to be stable and was partially successful in preventing surface oxidation. When the initial adherance was proper, the coating used to serve its purpose but on many occasions, due to improper adherance, the coating allowed the diffusion of oxygen into the space between the outer surface of the sample and the inner surface of the coating. This naturally caused the oxidation on the external surface to produce burnt samples of the shape indicated in Fig.3-1. In such cases, since the rate of burning on the outer surface was much higher than that inside, the results for reaction in the pore could not be obtained satisfactorily.

However, when the coating was stable, the sample was mounted on to a fire proof brick and placed in a furnace in such a way that the axis of the cylinder was perpendicular to the direction of flow of the oxidising medium and parallel to the horizontal direction. The flow of oxygen and nitrogen was adjusted in such a way that the carbon dioxide content in the exit gases remained less than 2%. The outlet composition was checked from time to time by means of a gas chromatograph. After a desired interval of time, the samples were removed from the furnace and allowed to cool. They were then weighed with their coatings. By gentle tapping, the protective shells were broken, and the resulting specimens were cut into a number of rings to measure the radii at various lengths and time intervals.

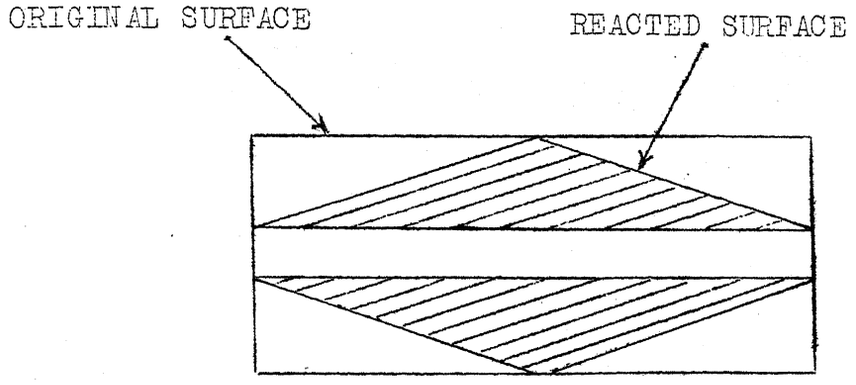

REACTION ON EXTERNAL SURFACE OF GRAPHITE CYLINDER

FIGURE 3-1

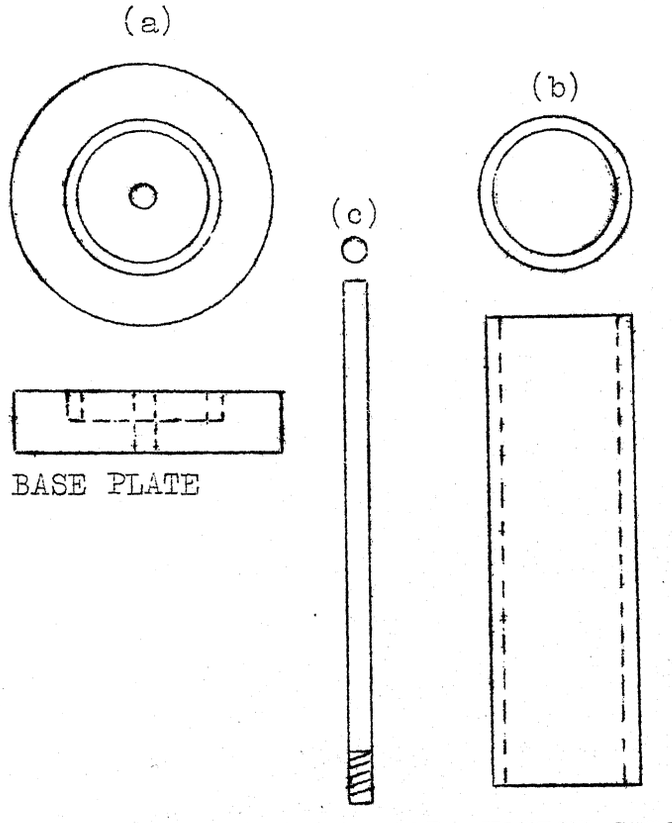

PARTS OF THE BRASS MOULD ASSEMBLY

FIGURE 3-2

Only one of the above experimental runs is reported in the chapter on "Calculations and Conclusions" for the following reasons:

(a) Hardly one out of six sorosil cement coatings adhered properly and hence the results were neither reproduceable nor reliable.

(b) The available furnace - even if operated well below its maximum rated temperature - could not be used continuously for more than 36-48 hours, without running the risk of burning the heating coils. In many cases, meaningful results could be obtained only after a long time of reaction.

(c) While weight loss measurements were somewhat dependable, profile measurements were not accurate enough to have a meaningful comparison with the theoretical values.

EXPERIMENTAL PROCEDURE FOR (b)

In the face of the above difficulties, the possibility of some low temperature reactions was explored. With a view to obtain a hollow cylinder of an organic material, a brass mould indicated in Figure 3-2 was fabricated. A groove was canved on the base plate (a) to allow a pushfit of the brass pipe (b) The threaded portion of the central rod (c) could be fixed in the central hole of the base plate. A layer of silicone oil was applied on the surface of each part of the mould. Molten organic substance was poured into

the annular space of the mould assembly, which was allowed to cool and solidify at room temperature. The cylinder thus prepared was then removed by slow rotary motion of the brass tube and rod.

The above brass mould was used to prepare hollow cylinders of benzoic acid for an experimental illustration of low temperature solid-liquid reaction in a pore. However, the homogeneity of the sample could not be ensured because of nonuniform changes in the chemical structure of benzoic acid during the process of moulding, and because of an uneven distribution of air gaps in the solid phase of benzoic acid. The reaction of benzoic acid with caustic soda was not considered for the main stream of experimentation because it was felt that this combination of low diffusivity (10^{-5} to 10^{-6} cm^2/sec) and high rate constant, may not give a good spread of results. Moreover this diffusivity brings in very low value of the coefficient in the quasilinear parabolic differential equation, introducing serious instability in numerical solution. However,

(a) selection of a suitable low temperature system,

(b) investigating suitable ranges of diffusivity and rate constant,

(c) exploring Dankweirt's criteria for instantaneous reactions,

(d) perfecting a method of moulding solid cylinders in inert atmospheres,

(e) trying pressure pelletization technique for solid moulding.

(f) choosing a proper range of temperature to realize both diffusion and reaction rate controlled regimes,
(g) selection of a proper coating for the external surface, and
(h) exploring the possibility of a homogeneous catalytic reaction, can form a potential field for future research investigations in the area of noncatalytic reactions in porous solids in general a single pore in particular.

EXPERIMENTAL PROCEDURE FOR (c)

In spite of the difficulties experienced in a high temperature operation, and may be because of the limitations of a liquid-solid system which are already indicated in the introductory note, persuit for standardization of a suitable method for the determination of the reaction rate constant was continued. Traditionally a flow system is preferred for the purpose, but in the present situation a static system has been selected with a view to simulate the conditions prevailing in a single pore.

Machined solid cylinders of graphite were cut to obtain a number of cylindrical tablets. Each tablet was rubbed on the surface of a fine sand paper to reduce its thickness to less than 2 millimeters so that the reactions on the curved surface could be neglected. The reacting surfaces of all these samples were again treated with acid washed methyl alcohol as described before. The dried samples

were weighed the cross-sectional area of each tablet was measured by means of a calliper. The samples thus prepared were now ready for reaction.

The furnace associated with the T.G.A. (Thermo Gravimetric Analyser) was switched on for obtaining the desired temperature. The weight loss axis was adjusted to cover a span of 500 mg. Depending on the temperature, the time axis was adjusted to cover a range of half hour to three hours. Cooling water was circulated. Finely powdered silica was filled in a porcelain crucible; the sample was placed on the powder and gently pushed inside so that only one circular face was exposed to the atmosphere. The crucible was then placed in a vertical glass casing which formed an integral part of the T.G.A. Counter weights on the quartz spring were adjusted to obtain the desired position of the pointer on the graph to indicate the initial weight of the sample. As soon as the furnace attained the desired temperature, the glass casing was lowered into the furnace and the temperature over the sample was noted at half minute intervals. When a temperature of 600°C was reached, time and weight recorders were switched on and temperature was noted at regular intervals of time until the sample attained the temperature of the furnace, which was set at a particular value to be taken as the reaction temperature. After permissible levels for weight loss and time were reached, the sample was removed and checked for possible reaction on its other face which was totally covered

by silicon dioxide. The occurance of reaction on the covered surface could be judged by visual observations, and when the sample was found to have been excessively attacked, that particular experiment was repeated. The weight loss curves for temperatures between 600°C and 850°C are shown in figures 3-3, 3-4

At temperatures above 850°C, weight loss recordings on T.G.A. could not be done because of the prolonged severe nonisothermal conditions that prevailed in the initial stages of reaction. On the other hand, if the samples were introduced directly into the furnace without weight loss recording devices, the time for which the nonisothermal conditions existed, i.e. the unsteady state time, was much less. For a higher temperature zone, therefore, this kind of furnace was used, and weightloss measurements were mannually done at discrete intervals of time.

Blind holes, each of one and a half inches depth, were drilled into pieces of refractory bricks, and silica powder was filled into them so as to form a layer of one half inch thickness on the bottom surface. An accurately weighed sample was placed on the powder and was gently pushed inside, so that only one face was exposed to the atmosphere. Eight to twelve identical samples of this kind were simultaneously introduced into a furnace, the temperature of which was set at the desired value. As before, compressed air was passed continuously through the furnace so that the carbon monoxide and carbon dioxide content in the exit gases did not exceed 2%. Exit gas

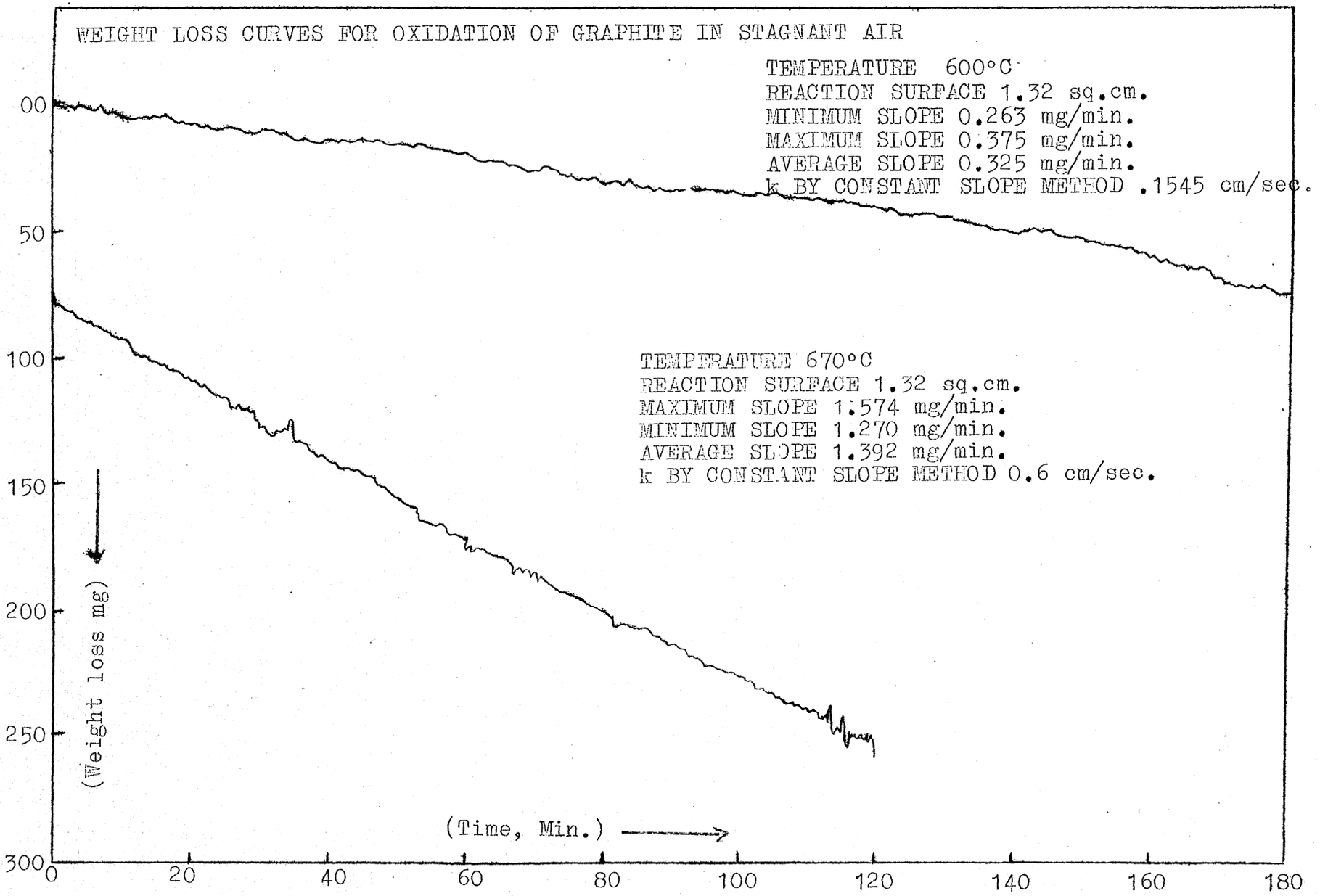
WEIGHT LOSS CURVES FOR OXIDATION OF GRAPHITE IN STAGNANT AIR
TEMPERATURE 600°C
REACTION SURFACE 1.32 sq.cm.
MINIMUM SLOPE 0.263 mg/min.
MAXIMUM SLOPE 0.375 mg/min.
AVERAGE SLOPE 0.325 mg/min.
k BY CONSTANT SLOPE METHOD .1545 cm/sec.
TEMPERATURE 670°C
REACTION SURFACE 1.32 sq.cm.
MAXIMUM SLOPE 1.574 mg/min.
MINIMUM SLOPE 1.270 mg/min.
AVERAGE SLOPE 1.392 mg/min.
k BY CONSTANT SLOPE METHOD 0.6 cm/sec.
00
50
100
150
200
250
300
(Weight loss mg)
(Time, Min.)
0
20
40
60
80
100
120
140
160
180

FIGURE 3-3

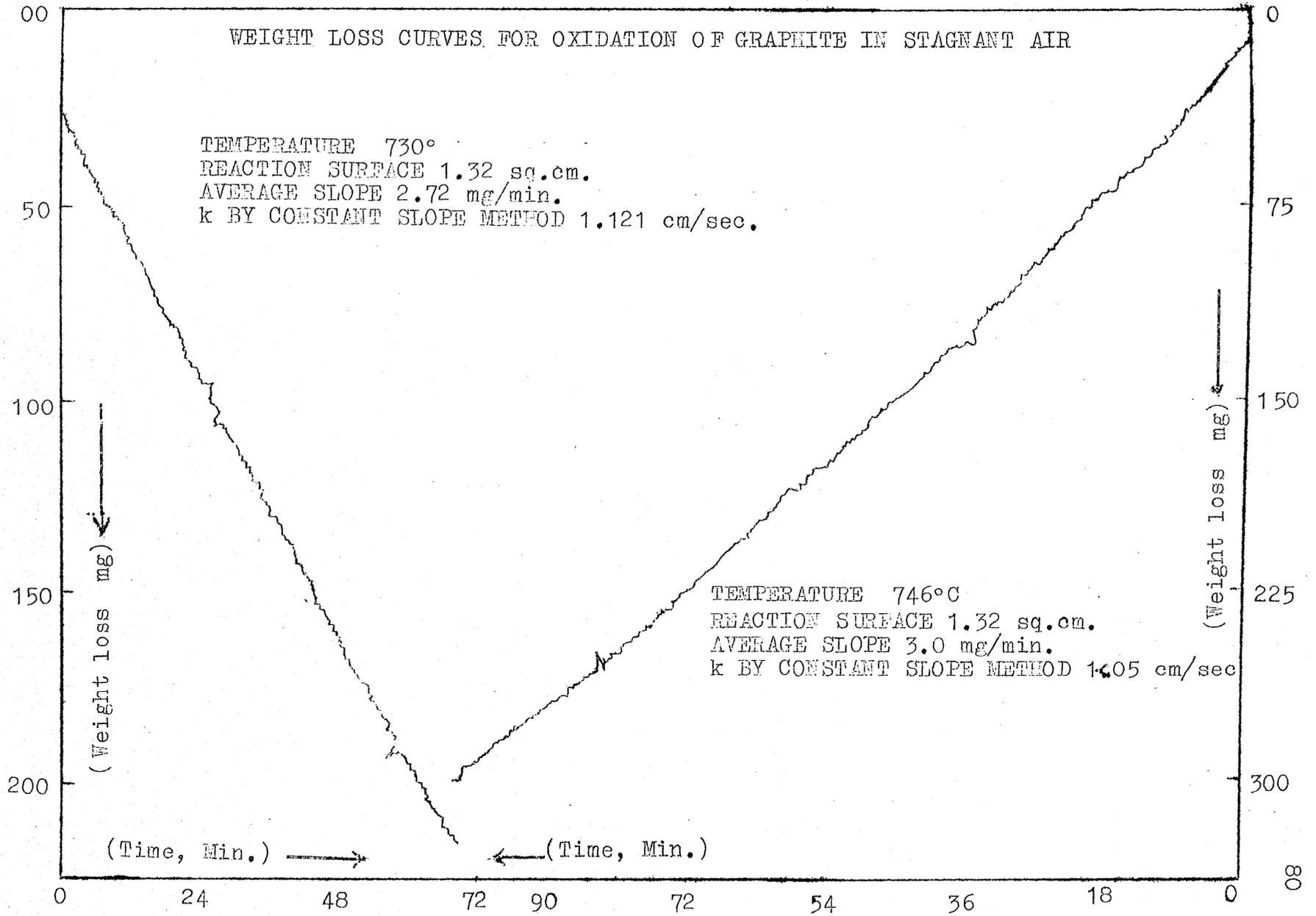
WEIGHT LOSS CURVES FOR OXIDATION OF GRAPHITE IN STAGNANT AIR
TEMPERATURE 730°
REACTION SURFACE 1.32 sq.cm.
AVERAGE SLOPE 2.72 mg/min.
k BY CONSTANT SLOPE METHOD 1.121 cm/sec.
TEMPERATURE 746°C
REACTION SURFACE 1.32 sq.cm.
AVERAGE SLOPE 3.0 mg/min.
k BY CONSTANT SLOPE METHOD 1.205 cm/sec
(Weight loss mg)
(Weight loss mg)
(Time, Min.)
(Time, Min.)
00
50
100
150
200
0
75
150
225
300
80
0
24
48
72
90
72
54
36
18
0

FIGURE 3-4

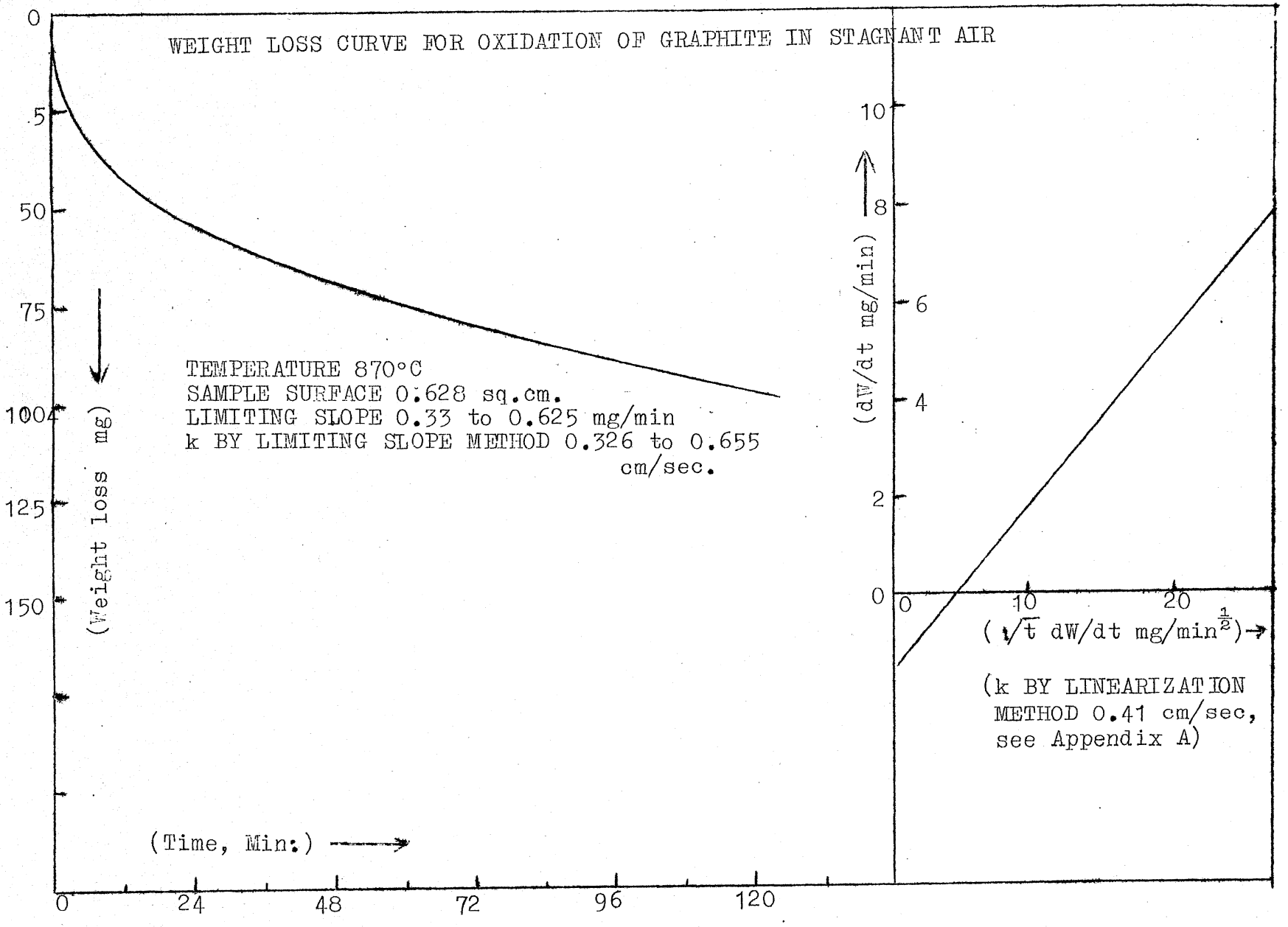
WEIGHT LOSS CURVE FOR OXIDATION OF GRAPHITE IN STAGNANT AIR
TEMPERATURE 870°C
SAMPLE SURFACE 0.628 sq.cm.
LIMITING SLOPE 0.33 to 0.625 mg/min
k BY LIMITING SLOPE METHOD 0.326 to 0.655 cm/sec.
(Weight loss mg)
(Time, Min.)
0
24
48
72
96
120
0
5
50
75
100
125
150
(dW/dt mg/min)
0
2
4
6
8
10
0
10
20
(√t dW/dt mg/min^½)
(k BY LINEARIZATION METHOD 0.41 cm/sec, see Appendix A)

FIGURE 3-5

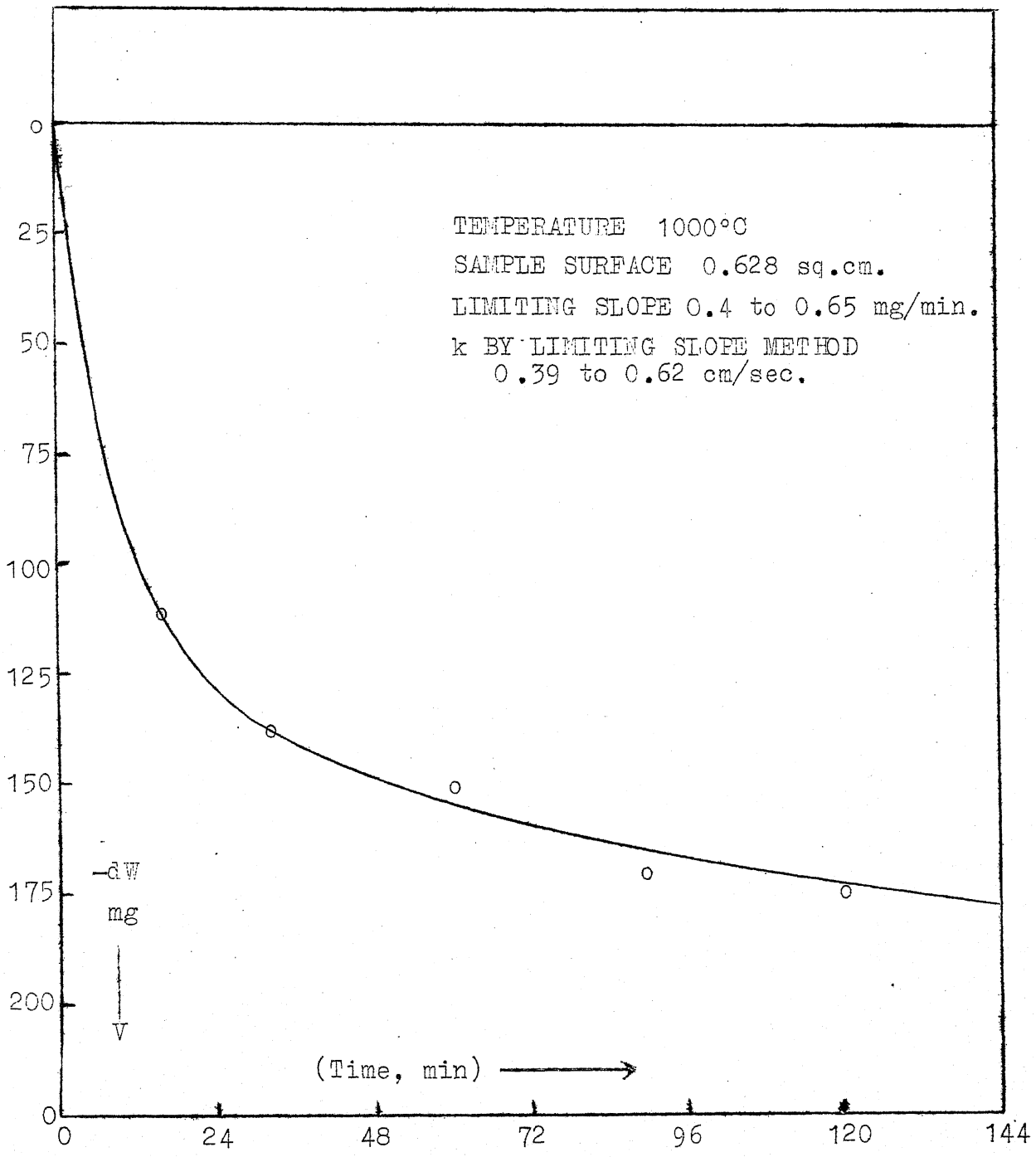

WEIGHT LOSS CURVE FOR OXIDATION OF GRAPHITE IN STAGNANT AIR

FIGURE 3-6

composition was checked by means of a chromatograph from time to time. After every 15-20 minutes of reaction, one sample was drawn out of the furnace; was cooled and then weighed. Weight loss curves drawn from this data are shown in figures 3-5,3-6(p. 82 & 81). More reliable data regarding numerical values of rate constants and limiting slopes was obtained at low temperatures than at high temperatures because the parameters temperature and weight were continuously recorded in the former case.

***

4. MATHEMATICAL MODELLING

There are two aspects of the mathematical formulation of the problem under consideration, the first one dealing with the determination of the first order rate constant for a surface reaction and the second one with the main problem of a heterogeneous fluid-solid reaction in a single pore. Before going into the details of these aspects, it may be worthwhile enumerating the assumptions involved in the mathematical analysis of the system.

(1) ISOTHERMAL CONDITION: There are four possible situations wherein nonisothermal behaviour is likely to occur:

a) At the beginning of the reaction, the temperature of the sample increases from room temperature to the temperature of the furnace.

b) Similarly at the end of the reaction the sample cools from furnace temperature to room temperature.

c) Dissipation of the heat of reaction may result in radial temperature gradients within the solid.

d) Oxygen concentration gradients may cause temperature gradients in the gas phase.

A quantitative or a qualitative analysis of each of these nonisothermal situations will now be made to conclude their insignificance in the system.

To begin with, the time required to raise the temperature of the graphite cylinder from room temperature to furnace

temperature is estimated. The most severe conditions that are likely to occur are assumed. Even though the effective thermal conductivity of graphite increases with temperature, its minimum value is taken for calculations. Also, the maximum numerical values for reaction temperature, specific heat and cylinder radius are assumed. The heating time can be estimated as follows:

Effective thermal conductivity for graphite $K_e = 0.3$ cal./cm.sec.°C [105]

Radius of solid graphite cylinder $R_c = 2.0$ cm.

Room temperature = 20°C

Furnace temperature = 1350°C

Length of the solid graphite cylinder $2H = 6$ cm.

Density of the graphite used = 1.6 gm/cc

Specific heat of graphite $C_{ps} = 2.5/12$ cal/gm.°C

Thermal diffusivity $\alpha_s = K_e/(\rho_s C_{ps})$

$$= \frac{(0.3)(12)}{(1.6)(2.5)}$$

$$= 0.9 \text{ cm}^2/\text{sec.}$$

With the help of a standard Gurney Lurie chart for unsteady state heat conduction, the time required to heat the sample from room temperature to 99.9% of the furnace temperature is estimated to be four seconds. This being true of a solid cylinder, the time required for a hollow cylinder will naturally be still less. No separate calculations need be carried out for the cooling period because it is not likely to exceed the heating period.

In the actual experiment, however, the heating and cooling periods varied from 80 to 135 seconds. This difference between theory and practice might have been due to the extra resistance to heat flow offered by the protective surface coating over the graphite cylinder. An important fact that is revealed by the above estimates is that the heating or cooling period of a few minutes is much less than the reaction time of a few hours. Besides, the temperature does not remain at the maximum level throughout the unsteady state, and hence the error introduced by neglecting the unsteady state time is not as severe as it would have been if the temperature had remained at its maximum level throughout. The only drawback of this assumption is that the severity of error increases with temperature. At high temperatures, the total time of reaction will be less and the period of unsteady state for initial heating and final cooling will be more so that the percentage error will be higher. Taking into consideration all these aspects of unsteady state, the initial heating period is included in the reaction time while the final cooling period is excluded from the same.

Coming to nonisothermal behaviour due to the heat of combustion of graphite, the maximum possible rise in temperature of solid can be calculated as follows: Again, assuming,

Equivalent thermal conductivity of graphite, K_e = 0.3 cal/sec. cm.°C,

Maximum heat of combustion, ΔH = 7831 cal/gm of graphite,

First order rate constant, $k = 10.0$ cm/sec.

Maximum concentration of oxygen in air = 21%,

Density of air $\rho_a = 0.20 \times 4.464 \times 10^{-5}$ gm moles/cc,

External radius of the cylinder $R_e = 1.0$ cm.,

Internal radius of the cylinder $R_i = 0.2$ cm.,

and denoting the external and internal surface area of the cylinder by A_e and A_i respectively, the standard steady state heat transfer equation for a cylinder is given by

$$(12)(2\pi R_i)(\Delta H \; k \; C_A)_{max} = K_e \frac{A_e - A_i}{\ln\left(\frac{A_e}{A_i}\right)} \times \frac{\Delta T}{\Delta R} \qquad \ldots 4\text{-}1$$

Therefore, the maximum possible temperature rise $\Delta T = 1.93°C$. Including the resistance offered by the protective coating, ΔT is not likely to exceed the value of 4°-5°C.

In these calculations, heat transfer in the axial direction is not taken into consideration. This error, however, is on the safer side because if axial transfer is considered, the rate of heat dissipation will be higher. Moreover, the above calculations being valid for most severe conditions, the error in an actual experiment is likely to be less severe than that estimated by equation 4-1. The internal surface area increases during the course of reaction, but at the same time, the thickness of the cylinder and oxygen concentration decrease, so that any adverse effect of the increased reacting surface area is nullified. Thus, from theoretical considerations, it is seen that the nonisothermal condition created by the rise in temperature is insignificant.

In the actual experiment, however, the thermocouple placed in the inner cavity did not register any appreciable change in temperature during the course of reaction. This was because the effect of sluggish heat conduction through the graphite wall has a tendency to counter the nonisothermal effect of heat of combustion. Theoretically, it takes infinite time to raise the temperature of the sample from 99.9% to 100% of the furnace value.

Lastly, the possibility of the existance of an axial temperature gradient resulting from the corresponding axial concentration gradient is considered. However, in the present situation, the temperature gradient is unlikely to occur because the area for heat transfer is much more than that for mass transfer, as indicated in figure 4-1. In other words, the rate of heat dissipation is much higher than that of mass transfer, so that the temperature gradient, if established, will tend to vanish much faster. Even in the actual experiment, no change in temperature was observed when the thermocouple junction was shifted in the axial direction. Therefore, the assumption of isothermal condition in general is not likely to introduce any significant errors in the mathematical analysis of non-catalytic reaction in a pore.

(2) CONDITION OF CONSTANT DIFFUSIVITY: The isothermal condition having been justified, the variation of D need be considered only with respect to the concentration of gas. At room

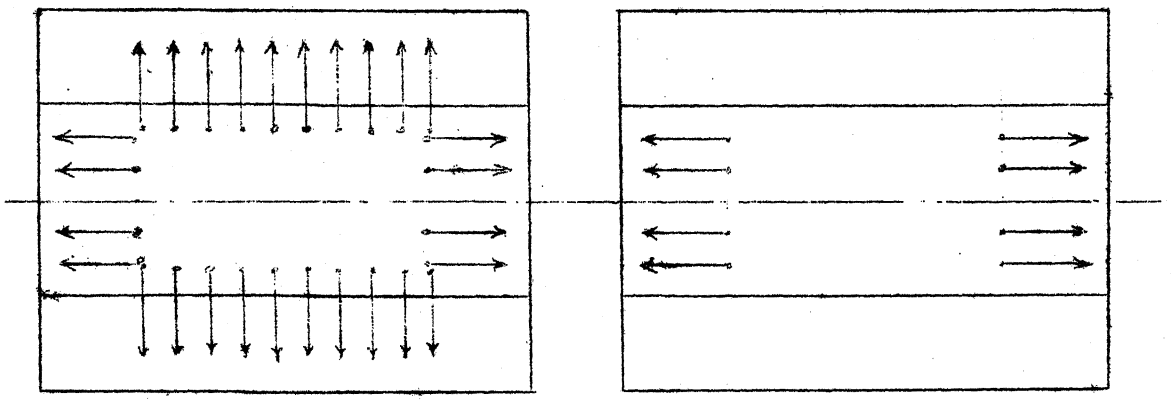

FIGURE 4-1

temperature, the diffusivity of oxygen in air is 0.2 cm^2/sec and that in pure carbon dioxide is 0.18 cm^2/sec [106]. While these numerical values may partially prove the validity of the assumption of constant diffusivity, it is extremely difficult to provide an analytical justification. This is because Fick's law of diffusion in itself is an over simplified mathematical description of the actual process of molecular diffusion. A constant numerical value for the diffusion coefficient is more often a mathematical necessity than a physical reality. In such situations the tradition established by various investigators becomes a good justification for the assumption.

(3) ABSENCE OF CONVECTION: When the axis of the cylinder lies in the horizontal position, there are two ways in which convection currents could be set up:

(a) Gravity: Usually this effect is negligible over small heights and since there is a radial symmetry of temperature and concentration, natural convection is non-existent.

The possibility of convection in the axial direction does not exist because an axial concentration gradient can cause only molecular diffusion.

(b) Flow Past Cylinder: This can set up convective currents near the mouth of the pore. Employing low air velocities minimises convection. Moreover, ceramic protective coatings on the two sides of the cylinder act as dampers for air currents. Computation of a momentum entry region for flow past a hollow cylinder is rather an involved procedure, and is not attempted here. It may, however, be noted that as the cylinder shrinks in its length, the effects of convection will be reduced considerably because of the increased distance between the pore mouth and the source of disturbance.

(4) PRODUCT OF OXIDATION IS CO_2: Sufficient evidence for this has already been given in the review of literature. Even though the assumption looks simple, it considerably reduces mathematical complexity.

(5) FIRST ORDER REACTION: That the surface reaction between graphite and oxygen is of first order with respect to oxygen pressure, has already been concluded in the review discussion. Any deviation from this, if significant, will be discussed in the concluding chapter.

(6) SURFACE AREA FOR REACTION: During the course of reaction, a large number of closed pores open up and there is a considerable change in the surface area available for reaction.

The geometric surface area, in fact, will be a negligible part of the total reacting surface area. First order rate constants are, however, defined on the basis of geometrical surface area throughout the reaction. Various investigators [2] have found this approach satisfactory, and in the present analysis also, a similar procedure is followed. Such an assumption is well justified by the fact that the limiting weight loss curve for each temperature is more or less a straight line. Invariably, the period for which the weight loss curves are nonlinear is much less than the total time of reaction. Therefore, it becomes convenient to define rate constants on the basis of the linear portion of the weight loss curves and the geometric surface area of the sample.

(7) RADIAL DIFFUSION: Almost all the authors have ignored radial diffusion in the analysis of a chemical reaction in a pore, either in an implicit manner or by making a qualitative reference to the negligible transverse gradients in a pore of high length to diameter ratio. However, no quantitative analysis is reported regarding transverse diffusion flux in a reacting pore. A modest beginning in this direction can be made by starting with a two dimensional unsteady state diffusion equation in the cylindrical coordinate system. Let the axial distance be denoted by z, internal radius by R_i, the diffusivity of oxygen in air by D, the time by t, the length of the hollow cylinder by 2H, oxygen concentration by C_A,

the initial oxygen concentration by C_{Ao}.

Defining a dimensionless axial distance* $x = z/R_i$,

a dimensionless concentration $\mathcal{C} = C_A/C_{AO}$,

a dimensionless radial distance $r = R/R_i$,

the two dimensional unsteady state diffusion equation may be written as

$$\frac{\partial^2 C}{\partial x^2} + \frac{1}{r} \frac{\partial}{\partial r} \left(r \frac{\partial C}{\partial r}\right) = \frac{1}{D} \frac{\partial C}{\partial t} \qquad \ldots 4\text{-}2$$

For a quasisteady state the equation 4-2 becomes

$$\frac{\partial^2 C}{\partial x^2} + \frac{1}{r} \frac{\partial}{\partial r} \left(r \frac{\partial C}{\partial r}\right) = 0 \qquad \ldots 4\text{-}3$$

If this pseudo steady state is considred after a time interval t_1, the internal wall radius R will, in general, be a function of both x and t_1, say $R = g(x, t_1)$. The boundary conditions will then be

$$C(o, r) = 1 \qquad \ldots 4\text{-}4$$

$$-D \frac{\partial C}{\partial x}(L, r) = 0 \qquad \text{(where } L = H/R_i\text{)} \qquad \ldots 4\text{-}5$$

$$\frac{\partial C}{\partial r}(x, 0) = 0 \qquad \ldots 4\text{-}6$$

$$-D \frac{\partial C}{\partial r}\{x,\ g(x, t_1)\} = k\, R_i C\{x, g(x, t_1)\} \qquad \ldots 4\text{-}7$$

The functional relation $g(x, t_1)$ being unknown, the boundary condition 4-7 cannot be used to integrate the equation 4-3. As a first approximation, if a linear wall profile i.e. a

---

*In the subsequent analysis, dimensionless axial distance is defined as $x = z/H$. This change in notation will be referred to as and when it appears.

conical pore surface is assumed the boundary condition 4-7 becomes

$$-D \frac{\partial C}{\partial r} (x, ax + b) = k R_i C(x, ax + b) \qquad \ldots 4\text{-}8$$

where a and b are constants for the slant height of the cone. Even with the simplified boundary condition 4-8, an analytical solution of equation 4-3 does not seem possible. However, if the internal wall radius is independent of axial distance, (which is true in the early stages of reaction), the relation 4-8 becomes

$$-D \frac{\partial C}{\partial r} (x,1) = k R_i C(x,1) \qquad \ldots 4\text{-}9$$

By using finite Hankel Transform Technique, the solution in terms of standard Bessel functions, to equation 4-3 with boundary conditions 4-4, 4-5, 4-6 and 4-9 may be obtained as

$$C = 2 \sum_{a_i}^{\infty} \frac{J_1(a_i)\, J_o(a_i r)}{a_i \left[J_o^2(a_i) + J_1^2(a_i)\right]} \frac{\cosh a_i(L-x)}{\cosh a_i L} \qquad \ldots 4\text{-}10$$

where $$a_i J_1(a_i) = \frac{k R_i}{D} J_o(a_i) = \frac{1}{2} \left(\frac{m}{L}\right)^2 J_o(a_i) \qquad \ldots 4\text{-}11$$

and $$m = L \sqrt{\frac{2kR_i}{D}} \qquad \ldots 4\text{-}12$$

Note that the dimensionless parameter "m" represents the standard Thiele modulus for noncatalytic reactions.

To determine the two dimensional effectiveness factor, it becomes necessary to integrate the gasphase concentration both in radial and axial directions. Since the pore mouth

flux gives the actual rate of reaction over half the length of the pore, integration need be done only in the radial direction. Thus average concentration is given by

$$\bar{C} = \frac{\int 2\pi r\, dr\, C}{\int 2\pi r\, dr} = 2\int_0^1 C r dr = 4\sum_{a_i}^{\infty}\left\{a_i^2\left[1+\frac{J_0^2(a_i)}{J_1^2(a_i)}\right]\right\}^{-1}\frac{\cosh a_i(L-x)}{\cosh a_i L} \quad \ldots 4\text{-}13$$

Therefore the two dimensional effectiveness factor becomes

$$\varepsilon_2 = \frac{-D\frac{\partial \bar{C}_A}{\partial z}\pi R_i^2}{2\pi R_i H k C_{Ao}} = \frac{-D\frac{\partial \bar{C}}{\partial x}(0)}{2L R_i k} = \frac{m^2}{L^3}\sum_{a_i}^{\infty}\left[a_i\left(a_i^2+\frac{m^4}{4L^4}\right)\right]^{-1}\tanh(a_i L) \quad \ldots 4\text{-}14$$

Now the error introduced by neglecting the radial diffusion may be estimated by comparing this ε_2 with ε_1, the one dimensional effectiveness factor. For this, a useful approximation to ε_2 for small values of m/L can be obtained by using the relations

$$a_1 \longrightarrow \frac{m}{L} \text{ as } \frac{m}{L} \longrightarrow 0 \quad \ldots 4\text{-}15$$

and

$$a_2 \longrightarrow 3.8 \text{ as } \frac{m}{L} \longrightarrow 0 \quad \ldots 4\text{-}16$$

The equation 4-14 thus reduces to

$$\varepsilon_2 \simeq \frac{\tanh m}{m}\left[1-\frac{1}{16}\left(1+\frac{2m}{\sinh 2m}\right)\left(\frac{m}{L}\right)^2+0\left(\frac{m}{L}\right)^3\right] \quad \ldots 4\text{-}17$$

$$\therefore \varepsilon_2 \simeq \varepsilon_1\left[1-\frac{1}{16}\left(1+\frac{2m}{\sinh 2m}\right)\left(\frac{m}{L}\right)^2+0\left(\frac{m}{L}\right)^3\right] \quad \ldots 4\text{-}18$$

As expected, ε_2 and ε_1 become the same as $m/L \longrightarrow 0$, and from the error term in equation 4-18 it is obvious that ε_2 is always less than ε_1. This is also in accordance with the physical reality that two dimensional diffusion reduces the effectiveness of reaction

As has been aptly pointed out by Aris [107], simplifications of the type 4-17 are not valid, because in the present context, typical numerical values of m/L are of the order of ten. At least in principle, radial diffusion cannot be neglected even for a simple cylindrical geometry. Now, what happens when the pore wall profile is not cylindrical is anybody's guess. A cautious approach is necessary for any intuitive conjecture.

Inspite of these clear indications of importance of radial diffusion, a large number of investigators have made use of the one dimensional effectiveness factor with surprising accuracy. For mathematical simplicity, the present investigation also assumes no radial diffusion. The possible advantages and errors arising out of this assumption in the analysis will be discussed in the concluding chapter.

(8) SAMPLE HETEROGENEITY: As has been pointed out in the review, a number of parameters like porosity, poresize distribution, nature of bonding between impurity and carbon atoms, degree of graphatization, distribution of active sites and defects can and do cause heterogeneity in the sample. However, the number of parameters and the number of sites for each parameter are so large that the problem of heterogeneity acquires a statistical nature and the effect evens out on macro scale. Instances to this effect have already been cited in the review and except in the early stages of reaction, the assumptionof sample homogeneity is not likely to cause any

significant errors.

(9) SECONDARY REACTIONS: The low feasibility of $C-CO_2$ and $CO-O_2$ reactions has already been discussed in the thermodynamic review. Even if secondary changes do take place, a first order rate expression with respect to the concentration of oxygen is satisfactory enough for the empirical description of the gross surface changes.

(10) SUBLIMATION OF GRAPHITE: At the low operating temperatures under consideration, the vapor pressure of graphite is so negligible as to render the possibility of sublimation remote.

With these assumptions in mind, evaluation of various models for determining the first order rate constant from the experimental weight loss curves may be considered. The rate constants thus determined will be used in the main stream of analysis of the problem of a noncatalytic reaction in a pore. As mentioned in the experimental procedure, a system of a stagnant air column over the surface of a reacting graphite pellet is chosen for the determination of rate constant. Mathematically this would mean solving of one dimensional unsteady state diffusion equation with reacting surface boundary condition. The diffusion may be considered (a) in the gas phase (b) in the solid phase or (c) in both the phases. (c) would involve the solution of two simultaneous partial differential equations with common interface boundary condition. (b) requires the knowledge of the effective diffusivity through the reacting

solid and this is not always available. Therefore physically and mathematically (a) becomes a convenient choice. Referring to the figure 4-2, the necessary diffusion equation and boundary conditions may be written as

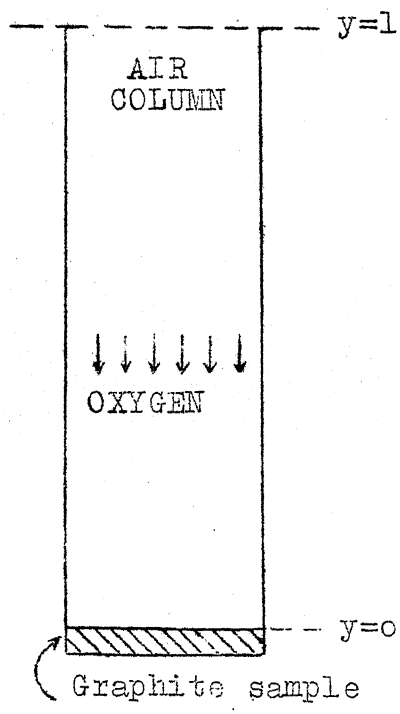

FIGURE 4-2

$$\frac{\partial C}{\partial t} = D \frac{\partial^2 C}{\partial y^2} \qquad \ldots 4\text{-}19$$

$$C(0,y) = 1 \qquad \ldots 4\text{-}20$$

$$C(t,\infty) = 1 \text{ or } C(t,l)=1 \qquad \ldots 4\text{-}21$$

$$D \frac{\partial C}{\partial y}(t,0) = kC(t,0) \qquad \ldots 4\text{-}22$$

If a new variable $f=1-C$ is introduced and further if the Laplace transform of $f(t,y)$ is defined as

$$\mathcal{L}\{f(t,y)\} = \int_0^\infty f(t,y)\, e^{-st} dt = F(s,y) \qquad \ldots 4\text{-}23$$

the solution in Laplace domain for the equation 4-19 with the boundary conditions 4-20, 4-21, 4-22 can be obtained as

$$F(s,y) = \left\{ \frac{k}{\sqrt{D}\, s^{3/2}} - \frac{k\, F(s,0)}{\sqrt{D}\, s^{1/2}} \right\} e^{-y\sqrt{s/D}} \qquad \ldots 4\text{-}24$$

$$F(s,y) = \frac{k[F(s,0)-1/s]}{\left\{1+e^{-2l\sqrt{D/s}}\right\}\sqrt{Ds}} \left[e^{(y-2l)\sqrt{D/s}} - e^{-y\sqrt{D/s}} \right] \qquad \ldots 4\text{-}25$$

Note that the solutions 4-24 and 4-25 are valid for infinite and finite length of the air column respectively.

Inverse transforms of the terms on the right hand sides of the equations 4-25 and 4-24 are not readily available

in the standard tables and it is doubtful whether the closed forms of the same are analytically possible. Efforts to obtain the Laplace inverses and the general solution C(t,y), need not be persued, because in the determination of the surface reaction rate constant, it is sufficient if the variation of concentration with respect to time, only on the surface of the graphite i.e. at y=0, is known. So substituting y=0 in the equations 4-24 and 4-25, we get

$$F(s,0) = \frac{k/\sqrt{D}}{s(\sqrt{s} + k/\sqrt{D})} \qquad \ldots 4\text{-}26$$

and

$$F(s,0) = \frac{k(1 - e^{-2l\sqrt{D/s}})}{s[\sqrt{Ds}(1+e^{-2l\sqrt{D/s}})+k(1-e^{-2l\sqrt{D/s}})]} \qquad \ldots 4\text{-}27$$

In the actual experiment, the length of the stagnant air column l is of the order of 8 cms. By interferometry [60a] it is well established that the significant gasphase concentration variations over the surface of the sample are known to occur within a distance of a few millimeters only. Therefore, for all practical purposes, the distance 8 cms is large enough to be considered as infinite. The inverse transform then need be considered only for the equation 4-26 so that

$$f(t,0) = 1 - e^{k^2 t/D} \operatorname{erfc}(k\sqrt{t/D}) \qquad \ldots 4\text{-}28$$

or

$$C(t,0) = e^{k^2 t/D} \operatorname{erfc}(k\sqrt{t/D}) \qquad \ldots 4\text{-}29$$

Making use of the definition of the heterogeneous surface reaction rate constant, the rate of loss of solid may be given as

$$-\frac{1}{S}\frac{dW}{dt} = k\,C_{Ao}\,e^{k^2 t/D}\,\mathrm{erfc}(k\sqrt{t/D}) \qquad \ldots 4\text{-}30$$

where S is the reacting surface area and W is the weight of the sample. Though in principle, the simultaneous determination of k and D should be possible from the above equation, attempts to use the experimental weight loss curves for this purpose were not fruitful in yielding consistent values of k and D. Therefore, evaluation of k from equation 4-30 was tried by using known values of D from literature, but again inconsistency of k persisted. The root cause of this inconsistency lies in the incompatibility between reliable experimental data and accurate numerical values for error functions. In the initial stages of reaction, i.e. for smaller values of $k\sqrt{t/D}$, the error function evaluation is accurate but the experimental weight loss curves are not reliable, and vice versa operates in the later stages of reaction. Even a special computer programme devised to estimate error functions accurate to the 28th decimal place (for the parameter $k\sqrt{t/D} > 4$) did not prove to be of any use. Yet another way to simplify the equation 4-30 for large values of $k\sqrt{t/D}$, may be to express the error function in the form of an asymptotic expansion. Considering the first two terms in the series, the equation 4-30 may be written as

$$-\frac{1}{S}\frac{dW}{dt} = \frac{C_{Ao}\sqrt{D}}{\sqrt{\pi t}}\left[1 - \frac{D}{2k^2 t}\right] \qquad \ldots 4\text{-}31$$

Integrating this equation, weight loss may be given as

$$W_o - W = \frac{S\,C_{Ao}\sqrt{D}}{\sqrt{\pi}}\left[2\sqrt{t} + \frac{D}{k^2\sqrt{t}}\right] \qquad \ldots 4\text{-}32$$

Again, the weight loss curves could not fit in this equation for any consistent value of k.

From the experimental weight loss curves it can easily be seen that the time for which the curve is nonlinear is much less compared to the time for which it is linear. This suggests that a quasisteady state analysis of the equation 4-19 may be used with advantage in the determination of k without any significant loss of accuracy. The error involved in the quasi-steady state assumption may be estimated with the help of Wen's chart [3]. In the present case, the initial oxygen concentration $C_{Ao} \simeq 10^{-6}$ gm mol/cc, the solid voidage $\varepsilon \simeq 0.3$, the stoichiometric number "a" in the reaction $C+O_2 = CO_2$ is ONE, and the solids concentration $C_{so} \simeq 0.1$ gm.mol/cc. Therefore, the characteristic parameter $(\varepsilon C_{Ao})/(a C_{so}) \simeq 3 \times 10^{-6}$ and the corresponding error is less than ONE percent. For a quasi-steady state, the diffusion equation 4-19 then becomes

$$\frac{d^2C}{dy^2} = 0 \text{ or } \frac{d^2C_A}{dy^2} = 0 \qquad \ldots 4\text{-}33$$

The boundary conditions with reference to figure 4-2 are given as

$$D \frac{d\,C_A}{dy}(0) = kC_A(0) \qquad \ldots 4\text{-}34$$

$$C_A(1) = C_{Ao} \qquad \ldots 4\text{-}35$$

The solution is $C_A = kC_{Ao}y/(1k+D) + DC_{Ao}/(1k+D)$ ...4-36

As before, $(-1/S) \frac{dW}{dt} = kDC_{Ao}/(1k+D)$ ...4-37

Now, $$-dW = \int_s S\, dl \qquad \ldots 4\text{-}38$$

$$\therefore \quad l = (W_o - W + S \int_s l_o)/(\int_s S) \qquad \ldots 4\text{-}39$$

Eliminating l between the equations 4-37 and 4-39 and integrating,

$$t = \frac{(W_o - W)^2}{2S^2 \rho_s D C_{Ao}} + \frac{l_o (W_o - W)}{SD\, C_{Ao}} + \frac{(W_o - W)}{Sk\, C_{Ao}} \qquad \ldots 4\text{-}40$$

and

$$-\frac{dt}{dW} = \frac{W_o - W}{S^2 \rho_s D C_{Ao}} + \frac{1}{S\, C_{Ao}} \left(\frac{l_o}{D} + \frac{1}{k}\right) \qquad \ldots 4\text{-}41$$

The plot of $\frac{dt}{dW}$ versus $(W_o - W)$ should in principle be able to give the value of k, but the intercept contains a term in l_o which seriously affects the accuracy of k. There are a number of empirical methods by which the weight loss curves can be linearized but the mathematical loop holes are toomany. Assumption of a complicated rate expression for the surface process has attracted many investigators but the numerical difficulties associated with the multiconstant system outweigh the possible advantages of linearization. Considering all these difficulties it was decided advisable to fall back upon the conventional method of determining the rate constant from the limiting linear weight loss curves. A number of investigators have found this approach satisfactory [2].

Before proposing, testing, and investigating the merits and demerits of various mathematical models for the main problem of reaction in a pore, it may be advisable to make a precise statement of the problem under consideration. If R_i is the inner radius of the graphite cylinder, R_e is the external radius of the graphite cylinder, C_{Ao} is the concentration of oxygen in the gasphase at the mouth of the pore or the initial concentration of oxygen both inside and outside the hollow

space of the graphite cylinder, C_A is the concentration of oxygen at any time and axial distance, i.e. the variable concentration of oxygen inside the pore, R is the variable radial distance, z is the variable distance along the axis of the cylinder, t is the time of reaction, T is the uniform temperature of reaction, H is half the length of the cylinder, D is the diffusivity of oxygen in the gas phase reaction mixture, k is the first order rate constant for the surface reaction of graphite with oxygen expressed in the units of length/unit time, and further, if the external surface of the cylinder is insulated against chemical reaction and only the internal pore surface is allowed to react, how will the parameters R_i and C_A vary with respect to the axial distance z and the reaction time t and how best can this data be used in the design of heterogeneous reactors?

Since it is a problem of Poiseuille diffusion in the pore space and a heterogeneous reaction on the pore surface, one is naturally inclined to consider the general equation of diffusion and solve it for the reacting wall surface condition. The relevant isothermal unsteady state diffusion equation in cylindrical co-ordinate system is

$$\frac{\partial C_A}{\partial t} = \frac{D}{R} \frac{\partial}{\partial R} \left(R \frac{\partial C_A}{\partial R} \right) + D \frac{\partial^2 C_A}{\partial z^2} \qquad \ldots 4\text{-}42$$

Formulation of the boundary condition for the reaction on the wall surface and the analytical solution of the above equation being difficult, the following simplified models have been considered.

(1) STOICHIOMETRIC MODEL: Neglecting radial diffusion, the unsteady state material balance equation for simultaneous diffusion and chemical reaction of oxygen may be given as

$$D \frac{\partial^2 C_A}{\partial z^2} - \frac{2k C_A}{R_i} = \frac{\partial C_A}{\partial t} \qquad \ldots 4\text{-}43$$

This equation can easily be solved provided R_i is a constant (i.e. independent of t and z), but during the course of reaction R_i does vary, say according to a functional relation

$$R_i = g(t, z) \qquad \ldots 4\text{-}44$$

The nature of this "g" being unknown, the equation 4-43 cannot be solved, and to add to the dilemma, "g" cannot be determined unless the solution to the equation 4-43 is available. Therefore, a straightforward material balance approach will not yield a solution even if numerical techniques are used,

2. AVERAGE RADIUS MODEL (CYLINDRICAL PORE MODEL): In view of the paradigmatic value of the nature of variation of R_i, it should be logical to make some assumption in this direction. If a mean radius $\bar{R}_i$ is assumed, the equation 4-43 becomes

$$D \frac{\partial^2 C_A}{\partial z^2} - \frac{2k C_A}{\bar{R}_i} = \frac{\partial C_A}{\partial t} \qquad \ldots 4\text{-}45$$

Defining a dimensionless axial distance $x = z/H$ and a dimensionless concentration $C = C_A/C_{Ao}$,

$$\frac{D}{H^2} \frac{\partial^2 C}{\partial x^2} - \frac{2k C}{\bar{R}_i} = \frac{\partial C}{\partial t} \qquad \ldots 4\text{-}46$$

By the method separation of variables the general solution of the above equation may be written as

$$C = \left\{ A_1 \cosh(jx\sqrt{1-\beta^2}) + B_1 \sinh(jx\sqrt{1-\beta^2}) \right\} e^{-\frac{2k\beta^2 t}{\bar{R}_i}} \quad \ldots 4\text{-}47$$

where β, A_1 and B_1 are constants and the

Modified Thiele Modulus $j = H\sqrt{2k/(D\bar{R}_i)}$ ...4-48

The relevant boundary conditions are

$$C(t, 0) = 1 \quad \ldots 4\text{-}49$$

$$\frac{\partial C}{\partial x}(t, 1) = 0 \quad \ldots 4\text{-}50$$

$$C(0, x) = 1 \quad \ldots 4\text{-}51$$

$$-\frac{\partial C}{\partial x}(t, 0) = \frac{2k H^2}{D\bar{R}_i}\bar{C} = j^2\bar{C} \quad \ldots 4\text{-}52$$

where $\bar{C}$ is the average concentration over an axial distance H, corresponding to the average radius $\bar{R}_i$, i.e.

$$\bar{C} = \frac{\int_0^1 C\, dx}{\int_0^1 dx} = \int_0^1 C\, dx \quad \ldots 4\text{-}53$$

Since it is difficult to evaluate the constants in equation 4-47 by accommodating four independent boundary conditions 4-49, 4-50, 4-51, and 4-52, the procedure for calculations will be indicated by assuming a solution of the type

$$C = G(x, t, \bar{R}_i, \bar{C}) \quad \ldots 4\text{-}54$$

Now, the change in average radius $\bar{R}_i$ can be related to $\bar{C}$ as

$$\frac{\partial \bar{R}_i}{\partial t}\rho_s = k\, C_{Ao}\, \bar{C} \quad \ldots 4\text{-}55$$

At the start of reaction, the distributionof concentration being uniform, $\bar{C} = 1$ and therefore

$$\rho_s (\Delta \bar{R}_i)_1 = k C_{Ao} (\Delta t)_1 \qquad \ldots 4\text{-}56$$

where $(\Delta \bar{R}_i)_1$ is the change in average radius corresponding to the first time increment $(\Delta t)_1$

$$\therefore (\bar{R}_i)_1 = (\bar{R}_i)_o + (\Delta \bar{R}_i)_1 = (\bar{R}_i)_o + \frac{k C_{Ao}}{\rho_s} (\Delta t)_1 \qquad \ldots 4\text{-}57$$

where $(\bar{R}_i)_o$ and $(\bar{R}_i)_1$ are the average radii at the beginning and after the first time interval $(\Delta t)_1$ respectively.

Using this $(\bar{R}_i)_1$ in equation 4-46, the concentration distribution of the type 4-54 can be obtained, and by going through similar steps, $(\bar{R}_i)_2$, the average radius after the time increment $(\Delta t)_2$, can be evaluated. The procedure can be repeated for further time increments till the pore mouth radius becomes equal to the external radius, However, once this stage is reached H and hence the modified Thiele modulus j assume different values for each incremental cycle. This "forward march technique", with step variations in j, can be employed to determine the distribution of concentration and the average radius at various stages of reaction till the whole cylinder is almost completely reacted.

Obviously, there is a limitation to the utility of this method to the extent that at any time t during the course of reaction, it fails to give the distribution of the radius in the axial direction. This limitation can be overcome by formulating separate sets of differential equations for a number of small grids each of an axial length Δx, and computing $\bar{C}$ and $(\bar{R}_i)_n$ separately for each of the grids. However, it may

be noted that if the total number of grids is N, there will be an N fold increase in the number of computations. Considering all these inadequacies and inaccuracies, it is doubtful whether the average radius model can provide a satisfactory mathematical description of a noncatalytic reaction in a pore.

3. CONICAL PORE MODEL: Having considered an average radius in a cylindrical pore model, the next logical step should be the assumption of an inclined pore wall. Figure 4-3 illustrates a closed pore of a conical shape, the height of which is H and the pore mouth radius R_{im}. Let half the angle subtended at the apex be θ i.e. $\tan^{-1}(R_{im}/H)$, and for convenience, the origin is located at the centre. Keeping the rest of the notations as before, the material balance over the frustrum of an elemental cone of thickness ΔZ isgiven by

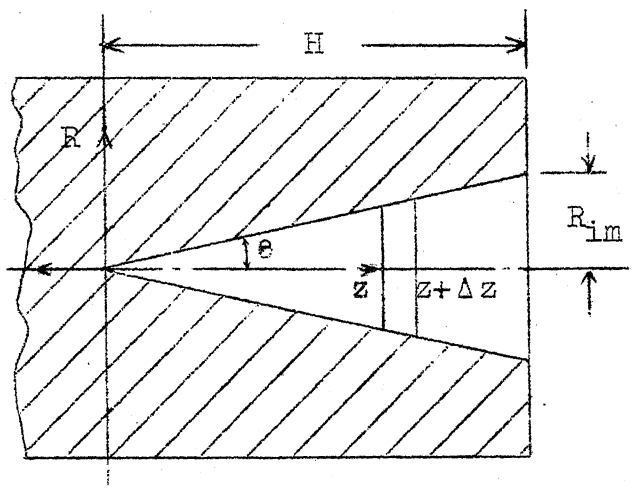

FIGURE 4-3

$$\left(-D\frac{\partial C_A}{\partial z}\pi R_i^2\right)\Big|_z - \left(-D\frac{\partial C_A}{\partial z}\pi R_i^2\right)\Big|_{z+\Delta z} - kC_A\pi(R_i+R_i+\Delta R_i)(\Delta z^2+\Delta R_i^2)^{\frac{1}{2}}$$

$$= \frac{\Delta z}{3}\left\{\pi R_i^2 + \pi(R_i+\Delta R_i)^2 + \sqrt{\pi R_i^2\,\pi(R_i+\Delta R_i)^2}\right\}\frac{\partial C}{\partial t} \quad \ldots 4\text{-}58$$

Substituting $\Delta R_i = \Delta z \tan\theta$ and $R_i = z\tan\theta$, and taking the

limits as $\Delta z \longrightarrow o$,

$$\frac{\partial^2 C_A}{\partial z^2} + \frac{2}{z}\frac{\partial C_A}{\partial z} - \frac{2k\,H^2}{DR_{im}}\sqrt{(1 + \tan^2\theta)}\,\frac{C_A}{z} = \frac{\partial C_A}{\partial t} \qquad \ldots 4\text{-}59$$

For a quasi steady state, the above equation becomes

$$\frac{d^2 C_A}{dz^2} + \frac{2}{z}\frac{d\,C_A}{dz} - h^2\,\frac{C_A}{z} = 0 \qquad \ldots 4\text{-}60$$

where $h^2 = \frac{(2k\,H^2)}{DR_{im}}\sqrt{(1 + \tan^2\theta)}$ $\qquad \ldots 4\text{-}61$

The necessary boundary conditions are

$$C_A(H) = C_{Ao} \qquad \ldots 4\text{-}62$$

$$-D\,\frac{\partial C_A}{\partial z}(0) = kC_A(0) \qquad \ldots 4\text{-}63$$

The solution of the equation 4-60 then becomes

$$\frac{C_A}{C_{Ao}} = \left(\frac{H}{z}\right)^{\frac{1}{2}}\,\frac{I_1\left[2h\sqrt{z/H}\right]}{I_1\left[2h\right]} \qquad \ldots 4\text{-}64$$

where I_1 represents the first order modified Bessel function of the first kind. Thus for a quasisteady state, the above eqn represents the concentration profile of oxygen along the length of the pore. It is also implied that the time required for the pore to change its dimensions significantly is large as compared to the time required to establish the quasisteady state concentration profile within the pore. The rate at which graphite reacts with oxygen may therefore be given by

$$\text{RATE} = k\,C_{Ao}\left(\frac{H}{z}\right)^{\frac{1}{2}}\,\frac{I_1\left[2h\sqrt{z/H}\right]}{I_1\left[2h\right]} \qquad \ldots 4\text{-}65$$

After a finite time interval Δt, the pore radius increases by ΔR_i, and the relevant material balance equation is

$$\rho_s \frac{\Delta R_i}{\Delta t} = \text{RATE} \quad \text{or} \quad \frac{\text{RATE}}{\rho_s} = \frac{\Delta R_i}{\Delta t} \qquad \ldots 4\text{-}66$$

Equating the poremouth flow per unit surface area with the reaction rate within the pore, under a pseudo steady state condition,

$$\text{RATE} = \frac{R_{im} D C_{Ao} h}{H^2 (1+\tan^2\theta)^{\frac{1}{2}}} \left\{ \frac{I_o(2h)}{I_1(2h)} - \frac{1}{h} \right\} \qquad \ldots 4\text{-}67$$

where I_o is the zero order modified Bessel function of the first kind. Combining the equations 4-66 and 4-67,

$$\frac{\Delta R_i}{\Delta t} = \frac{R_{im} D C_{Ao} h}{H^2 \rho_s (1+\tan^2\theta)^{\frac{1}{2}}} \left\{ \frac{I_o(2h)}{I_1(2h)} - \frac{1}{h} \right\} \qquad \ldots 4\text{-}68$$

It may be noted that the equation 4-68 makes the following implicit assumptions:

(a) Small changes in radius R_i do not significantly alter the apex angle of the cone,

(b) The pore is long enough to keep the oxygen concentration at the apex almost zero,

(c) And as a corollary, the apex of the cone does not shift significantly away from the origin.

For $R_{im} \ll H$, the parameter h is so large that the equation 4-68 can be further simplified as

$$\frac{\Delta R_i}{\Delta t} = \frac{C_{Ao}}{\rho_s H} (2kR_i D)^{\frac{1}{2}} \qquad \ldots 4\text{-}69$$

In the initial stages of reaction, the pore geometry being cylindrical, equations 4-68 and 4-69 obtained from a

conical pore model, obviously cannot be applied. Moreover, even if the pore develops a conical shape during the course of reaction, equation 4-68 or 4-69 cannot accurately predict the wall profile because the analysis presented is that for a closed pore while in reality the pore is open at both ends i.e. a divergent-convergent-divergent pore.

However, the equations 4-68 or 4-69, which represent the rate of reaction inside a pore, may be used to formulate an index which gives the ratio of reaction rates on the internal and external surfaces of the solid. If the external surface of the cylinder were also to react simultaneously, the rate at which the external radius Re would decrease may be given as

$$\frac{\Delta Re}{\Delta t} = \frac{k\, C_{Ao}}{\rho_s} \qquad \ldots 4\text{-}70$$

Combining equations 4-69 and 4-70,

$$\frac{\Delta R_i}{\Delta Re} = \frac{(2kR_iD)^{\frac{1}{2}}}{kH} = \psi \qquad \ldots 4\text{-}71$$

where ψ denotes a "predictivity parameter". It can predict whether the burning of graphite takes place essentially on the internal or external surface depending on whether $\psi > 1$ or < 1 respectively. It may be noted that in the equation 4-70 the term C_{Ao} can suitably be modified to accommodate the resistance due to convective mass transfer from the bulk of the gas phase to the solid surface. Standard Nusselt number correlations for geometries other than a cylinder may be used to generalize the predictivity parameter. It is hoped that

this quantitative approach may prove to be useful in the optimum design of operating parameters in a heterogeneous reactor.

4. FINITE DIFFERENCE MODEL: After exploring the possibilities of cylindrical and conical pore models, one could think in terms of various nonlinear geometries in their natural sequence. However, due to the mathematical complexity introduced by these, the analytical solutions of the equations become extremely difficult. Moreover, the assumption of one single nonlinear profile need not necessarily be valid for all time intervals, temperatures and pressures of a single system - let alone different systems - Under the circumstances, the best way would be to consider a suitable numerical method to solve the simultaneous partial differential equations of the system. Irrespective of whether it is a forward march technique or an iterative technique, a stable finite difference scheme forms an essential ingredient of any numerical effort. From time to time, a number of new stable finite difference forms for quasilinear parabolic partial differential equations are reported in the literature, with a view to increase the size of the increments, and hence reduce the computation time required for the numerical solutions [108, 109, 110, 111, 112]. It is probably not possible to make any absolute statement as to the "best" finite difference scheme for solving a particular partial differential equation. However, a good rule

appears to be the following: given a maximum permissible error, use that method which will give an approximate solution within the specified error with the least amount of machine time. It appears unlikely that any single method will be "best" from this point of view even if the choice is restricted to parabolic equations only. It, therefore, becomes necessary to investigate a number of different finite difference schemes so that necessary information is available when needed for the solution of a particular equation. A stability analysis with reference to Lees' finite difference scheme [108] for the most general quasilinear parabolic differential equation, is illustrated below. It could as well be modified and applied to other finite difference forms under consideration.

(i) Milton Lees' Extrapolated Difference Scheme: Let $w(x,t)$ be a smooth solution of the quasilinear parabolic partial differential equation

$$K(x,t,w,\frac{\partial w}{\partial x})\frac{\partial w}{\partial t} = \frac{\partial^2 w}{\partial x^2} + f(x,t,w,\frac{\partial w}{\partial x}) \qquad \ldots 4\text{-}72$$

in the rectangular region $\Omega = \{(x,t) \mid 0 \leq x \leq 1, \quad 0 \leq t \leq T\}$ such that

$$w(x,o) = \phi(x), \qquad o \leq x \leq 1 \qquad \ldots 4\text{-}73$$

$$w(o,t) = \phi^{-}(x), \qquad o \leq t \leq T \qquad \ldots 4\text{-}74$$

$$w(1,t) = \phi^{+}(x), \qquad o \leq t \leq T \qquad \ldots 4\text{-}75$$

where ϕ, ϕ^{-}, ϕ^{+} are specified functions. It is assumed that the functions $K(x,t,p,q)$ and $f(x,t,p,q)$ are defined and smooth for $(x,t) \in \Omega$ and $p^2+q^2 < +\infty$ and that there is a positive

constant μ such that, in this region,

$$K(x,t,p,q) \geq \mu > 0 \qquad \ldots 4\text{-}76$$

It follows from 4-76 that the differential equation 4-72 is uniformly of parabolic type and, consequently, $w(x,t)$ is the only solution of the boundary value problem given by the equations 4-72 to 4-75. Incidentally, the equation 4-72 becomes "semilinear" if the functions K and f are independent of q.

If N is a positive-integer and $h > o$ is defined by the relation $(N+1)h=1$, then $\bar{G}(h) = \{ih \mid i = 0,1,\ldots.N+1\}$...4-77 If $0 < 2k < T$ then we let J be the largest integer such that $kJ \leq T$. Let $\zeta(h)$ be the real linear space of all functions $u(x)$ defined on the finite set $\bar{G}(h)$. Obviously, $\zeta(h)$ has dimension N+2. The concern now is with the construction of a difference scheme for the boundary value problem 4-72 which, for all sufficiently small h and k, determines uniquely a sequence $u_o, u_1, u_2, \ldots, u_J$ of functions from $\zeta(h)$ such that (I) $u_o = \phi$ on $\bar{G}(h)$ and, for each $j \geq 1$, the N numbers $u_j(h)$, $u_j(2h)$, ..., $u_j(Nh)$ are determined directly as the solution of a linear system of equations.

(II) There is a $\delta > 0$ and a constant $A > 0$, independent of h and k, such that $\max_{\substack{0 \leq j \leq J \\ x \in \bar{G}(h)}} |u_j(x) - w(x,jk)| \leq A(h^2+k^2)$ whenever

$$\sqrt{\{h^2 + k^2\}} \leq \delta.$$

It is implied in (I) that the numbers $u_j(h)$, $u_j(2h)$, ...,$u_j(Nh)$ need not be determined by an iterative process

applied to nonlinear system of equations. Condition (II) states that the sequence $u_0, u_1, \ldots, u_j$ furnishes a second order approximation to the solution of the boundary value problem 4-72.

It is known [110] that the standard Crank-Nicolson difference scheme for 4-72 satisfies condition (II). It is also known that it fails to satisfy condition (I), except in the case where 4-72 is a linear differential equation, which in the present context is out of consideration. In 1963, Douglas and Jones [111] formulated two modifications of the standard Crank-Nicolson difference scheme for 4-72, which satisfy condition (I). When 4-72 is a semilinear equation, they proved that their predictor-corrector Crank-Nicolson difference schemes also satisfy condition (II). In a general quasilinear case, however, they obtained only the weaker error estimate

$$\left| u_j(x) - w(x, jk) \right| \leq A(h^2 + k^{3/2}) \qquad \ldots 4\text{-}78$$

In 1967, Milton Lees [108] put forward the forthcoming extrapolated scheme which, in addition to satisfying the conditions (I) and (II) in the general quasilinear case, requires approximately half the number of evaluations of the functions k and f as the predictor corrector methods in [111]. However, it was found necessary to add to condition (II) a mild restriction $k \leq \lambda h$ for some fixed positive constant λ. In 1970, H.B. Keller [109] has presented a new "box scheme" which is

"unconditionally stable, simple and easy to programme, and efficient!." However, this box scheme is excluded from the present consideration because it contains some newly defined derivatives which are useful only when the coefficient of 2nd order derivative is a function of x and t.

Now, coming to the extrapolated scheme, two completely inessential simplifications are made for notational convenience, the first one being the independence of K and f with respect to x and t, and the second one being the identical vanishing of $\bar{\phi}$ and ϕ^{+}. Thus it is supposed that w(x,t) satisfies

$$K\left(w, \frac{\partial w}{\partial x}\right) \frac{\partial w}{\partial t} = \frac{\partial^2 w}{\partial x^2} + f\left(w, \frac{\partial w}{\partial x}\right) \qquad \ldots 4\text{-}79$$

$$w(x,o) = \phi(x) \qquad o \le x \le 1 \qquad \ldots 4\text{-}80$$

$$w(o,t) = w(1,t) = o \qquad o \le t \le T \qquad \ldots 4\text{-}81$$

Defining the standard difference operators D_+, D_- and D_o in the usual way,

$$h\, D_+ u(x) = u(x+h) - u(x) \qquad \ldots 4\text{-}82$$

$$h\, D_- u(x) = u(x) - u(x-h) \qquad \ldots 4\text{-}83$$

$$2h\, D_o u(x) = u(x+h) - u(x-h) \qquad \ldots 4\text{-}84$$

Let $\zeta_\delta(h)$ be the N-dimensional subspace of $\zeta(h)$ consisting of those functions $u \in \zeta(h)$ for which $u(o) = u(1) = o$. Let $G(h)$ denote the intersection of $\bar{G}(h)$ with the open interval $o < x < 1$, and let $\tau = (h^2+k^2)^{\frac{1}{2}}$.

Two sequences $u_o, u_1, \ldots, u_j$ and $u_{\frac{1}{2}}, u_{\frac{3}{2}}, \ldots, u_{J-\frac{1}{2}}$ will now be constructed in $\zeta_o(h)$ by process of induction. Let

$$u_o = \phi \text{ and } u_{\frac{1}{2}} = \phi + \frac{k}{2K(\phi, D_o\phi)} \left[D_+ D_- \phi + f(\phi, D_o\phi) \right] \qquad \ldots 4\text{-}85$$

Now, assume that $u_0, u_1, \ldots, u_j$ and $u_{\frac{1}{2}}, u_{3/2}, \ldots, u_{j+\frac{1}{2}}$ have already been defined. Then u_{j+1} is defined to be the unique solution of the linearized Crank-Nicolson difference equation

$$K(u_{j+\frac{1}{2}}, D_0 u_{j+\frac{1}{2}})(u_{j+1}-u_j) = \frac{k}{2} D_+ D_-(u_{j+1}+u_j) + kf(u_{j+\frac{1}{2}}, D_0 u_{j+\frac{1}{2}}) \quad ..4\text{-}86$$

for $x \in G(h)$, and $u_{j+3/2}$ is defined directly by the linear extrapolation formula

$$u_{j+3/2} = \frac{3}{2} u_{j+1} - \frac{1}{2} u_j \quad ...4\text{-}87$$

It is clear that the two sequences $\langle u_j \rangle$ and $\langle u_{j+\frac{1}{2}} \rangle$ are well defined, and the sequence $\langle u_j \rangle$ satisfies condition (I). It may be noted that the justification for the title "Extrapolated Difference Scheme" stems from the equation 4-87. Incidentally, if f is a linear function of p, it is permissible to replace $f(u_{j+\frac{1}{2}}, D_0 u_{j+\frac{1}{2}})$ by $f((u_{j+1}+u_j)/2, D_0 u_{j+\frac{1}{2}})$ if f is a linear function of q, it is permissible to replace $f(u_{j+\frac{1}{2}}, D_0 u_{j+\frac{1}{2}})$ by $f(u_{j+\frac{1}{2}}, \frac{1}{2} D_0 (u_{j+1}+u_j))$.

By making use of some properties of the linear space $\zeta_0(h)$ and by means of a straightforward but lengthy computation, based on Taylor's formula, Lees has proved the following relations for w.

$$w_{\frac{1}{2}} = u_{\frac{1}{2}} + R_{\frac{1}{2}} \quad ...4\text{-}88$$

$$K(w_{j+\frac{1}{2}}, D_0 w_{j+\frac{1}{2}})(w_{j+1}-w_j) = \frac{k}{2} D_+ D_-(w_{j+1}+w_j) + kf(w_{j+\frac{1}{2}}, D_0 w_{j+\frac{1}{2}}) + kR_{j+1} \quad ...4\text{-}89$$

$$w_{j+3/2} = \frac{3}{2} w_{j+1} - \frac{1}{2} w_j + R_{j+\frac{1}{2}} \quad ...4\text{-}90$$

$$D_0 w_{j+3/2} = \frac{3}{2} D_0 w_{j+1} - \frac{1}{2} D_0 w_j + R^0_{j+\frac{1}{2}} \quad ...4\text{-}91$$

$$D_o w_{\frac{1}{2}} = D_o u_{\frac{1}{2}} + R^o_{\frac{1}{2}} \qquad \ldots 4\text{-}92$$

where, for $0 \leq j < J$,

$$||R_{j+1}||_\infty < ||R_{j+\frac{1}{2}}||_\infty + ||R^o_{j+\frac{1}{2}}||_\infty \leq A_1 \tau^2 \qquad \ldots 4\text{-}93$$

Here A_1 is a constant independent of h,k, and j. Without loss of generality, it may be assumed that

$$||w_{j+1} - w_j||_\infty \leq A_1 k \qquad \ldots 4\text{-}94$$

If error functions $z_j = w_j - u_j$ and $z_{j+\frac{1}{2}} = w_{j+\frac{1}{2}} - u_{j+\frac{1}{2}}$ are introduced, z_j and $z_{j+\frac{1}{2}}$ belong to $\zeta_o(h)$. It follows from equations 4-85 to 4-94 that

$$z_{\frac{1}{2}} = R_{\frac{1}{2}}, \quad D_o z_{\frac{1}{2}} = R^o_{\frac{1}{2}} \qquad \ldots 4\text{-}95$$

$$z_{j+3/2} = \tfrac{3}{2} z_{j+1} - \tfrac{1}{2} z_j + R_{j+3/2} \qquad \ldots 4\text{-}96$$

$$D_o z_{j+3/2} = \tfrac{3}{2} D_o z_{j+1} - \tfrac{1}{2} D_o z_j + R^o_{j+3/2} \qquad \ldots 4\text{-}97$$

$$K(w_{j+\frac{1}{2}}, D_o w_{j+\frac{1}{2}})(z_{j+1} - z_j) = \frac{k}{2} D_+ D_- (z_{j+1} + z_j) + k\left(\frac{\partial f}{\partial p}\right) z_{j+\frac{1}{2}}$$

$$+ k\left(\frac{\partial f}{\partial q}\right) D_o z_{j+\frac{1}{2}} + \left(\frac{\partial k}{\partial p}\right) z_{j+\frac{1}{2}} [\, w_{j+1} - w_j - (z_{j+1} - z_j)] + k R_{j+1}$$

$$+ \left(\frac{\partial k}{\partial q}\right) D_o z_{j+\frac{1}{2}} [\, w_{j+1} - w_j - (z_{j+1} - z_j)] \qquad \ldots 4\text{-}98$$

where the partial derivatives appearing in the above equations are evaluated at points called for by the mean value theorem of the calculus.

For the solution w of the equation 4-79, let

$$m = \max_{\Omega} \left[|w| + \left|\frac{\partial w}{\partial x}\right| \right] \qquad \ldots 4\text{-}99$$

and let A_2 denote the maximum of $\left|\frac{\partial k}{\partial p}\right|$, $\left|\frac{\partial k}{\partial q}\right|$, $\left|\frac{\partial f}{\partial p}\right|$, $\left|\frac{\partial f}{\partial q}\right|$ over the closed bounded region determined by $|p| + |q| \leq 2m$. If $k \leq \lambda h$, then there is a $\delta > 0$ such that $\tau \leq \delta$ implies that

$$2A_1\,\sigma\tau \le 1, \qquad \ldots 4\text{-}100$$

$$2\,\sigma\tau \le m, \qquad \ldots 4\text{-}101$$

$$2A_1\,\tau \le \mu\ , \qquad \ldots 4\text{-}102$$

$$2(A+A_1)\tau \le 1, \qquad \ldots 4\text{-}103$$

where $\sigma = 5 + 4\,\lambda^2$ and

$$A = \frac{(A_1 + A_2)}{\sqrt{\mu}}\left[\,\sigma + 2T(\,\mu^2+1)\,\right]^{\frac{1}{2}}\, e^{\,16(A_1+A_2)^2T/\,\mu} \qquad \ldots 4\text{-}104$$

Now the conditions (I) and (II) will be satisfied if by induction it is proved that, for $\tau \le \delta$,

$$||\,z_{j+\frac{1}{2}}\,||_\infty + ||\,D_o z_{j+\frac{1}{2}}\,||_\infty \le \sigma\tau \qquad \ldots 4\text{-}105$$

$$||\,z_j||_\infty \le A\,\tau^2, \qquad 0 \le j \le J \qquad \ldots 4\text{-}106$$

In view of 4-93, 4-95, and 4-100 to 4-103 it follows that the inequalities in 4-105 and 4-106 hold for j=0. Assuming that 4-105 holds for all integers less than or equal to j, it will be proved that 4-105 also holds with j replaced by j+1. The inductive assumption and 4-101 imply that the modulus of each partial derivative in 4-98 is not greater than A_2. Therefore, forming the l_2 inner product of 4-98 with $2(z_{j+1}-z_j)$ and using 4-76, we get

$$2\mu\,||\,z_{j+1}-z_j\,||^2 \le k(z_{j+1}-z_j,\ D_+D_-(z_{j+1}-z_j)) + 2k(z_{j+1}-z_j,(\tfrac{\partial f}{\partial p})z_{j+\frac{1}{2}})$$
$$+2k(z_{j+1}-z_j,(\tfrac{\partial f}{\partial q})\,D_o z_{j+\frac{1}{2}}) + 2k(z_{j+1}-z_j,\ R_{j+1}) + 2\cdot(z_{j+1}-z_j,(\tfrac{\partial k}{\partial p})$$
$$z_{j+\frac{1}{2}}\,[w_{j+1}-w_j-(z_{j+1}-z_j)]) + 2\cdot(z_{j+1}-z_j,\ \tfrac{\partial k}{\partial q}\,D_o z_{j+\frac{1}{2}}[\,w_{j+1}-w_j$$
$$-(z_{j+1}-z_j)\,]\,) \qquad \ldots 4\text{-}107$$

From 4-107, the following estimate may be given as

$$2\mu \, ||z_{j+1}-z_j||^2 + ||z_{j+1}||_D^2 \leq ||z_j||_D^2 + 2k(A_1+A_2)||z_{j+1}-z_j||$$
$$+ [||z_{j+\frac{1}{2}}|| + ||D_o z_{j+\frac{1}{2}}||] + 2A_1 ||z_{j+1}-z_j|| [||z_{j+\frac{1}{2}}|| + ||D_o z_{j+\frac{1}{2}}||]$$
$$+ k||z_{j+1}-z_j|| \, ||R_{j+1}|| \qquad \ldots 4\text{-}108$$

From the inductive assumption and from equation of 4-108 and from the general inequality relation

$$2ab \leq \varepsilon a^2 + \frac{1}{\varepsilon} b^2, \quad \varepsilon > 0, \qquad \ldots 4\text{-}109$$

another estimate may be obtained as follows:

$$[2\mu - 2A_1 \sigma \tau - 2\varepsilon] ||z_{j+1}-z_j||^2 + ||z_{j+1}||_D^2 \leq ||z_j||_D^2$$
$$+ k^2(A_1+A_2)^2 \varepsilon^{-1} [||z_{j+\frac{1}{2}}||^2 + ||D_o z_{j+\frac{1}{2}}||^2] + k^2 \varepsilon^{-1} ||R_{j+1}||^2$$
$$\ldots 4\text{-}110$$

Now, choose $2\varepsilon = \mu$. Then, in view of 4-102 and the inequality $||R_{j+1}|| \leq A_1 \tau^2$, it follows that

$$||z_{j+1}||_D^2 \leq ||z_j||_D^2 + kA_3 [||z_{j+\frac{1}{2}}|| + ||D_o z_{j+\frac{1}{2}}||]^2 + 2kA_1^2 \tau^4/\mu \qquad \ldots 4\text{-}111$$

where $A_3 = 2\mu^{-1}(A_1 + A_2)^2 \qquad \ldots 4\text{-}112$

Since $z_o = o$, the inequality 4-111 may be iterated to get

$$||z_{j+1}||_D^2 \leq k \sum_{n=0}^{j} \{A_3 [||z_{n+\frac{1}{2}}|| + ||D_o z_{n+\frac{1}{2}}||]^2 + \frac{2A_1^2}{\mu} \tau^4\}$$
$$\leq (kA_3 A_1^2 \sigma^2 + 2\mu^{-1} A_1^2 T) \tau^4 + k \sum_{n=1}^{j} A_3 [||z_{n+\frac{1}{2}}|| + ||D_o z_{n+\frac{1}{2}}||]^2$$
$$\ldots 4\text{-}113$$

where the relation 4-93 and $jk \leq Jk \leq T$ are made use of.

As $||z_{n+\frac{1}{2}}|| + ||D_o z_{n+\frac{1}{2}}|| \leq \frac{3}{2} ||z_n|| + \frac{1}{2}||z_{n-1}|| + \frac{3}{2}||D_o z_n|| +$

$\frac{1}{2}\,||D_o z_{n-1}|| + 2A_1\,\tau^4$, in view of 4-96 and 4-97, it follows from 4-113 that $||z_{j+1}||_D^2 \le A_4\,\tau^4 + 16A_3 k \sum_{n=0}^{j} ||z_n||_D^2$, where

$$A_4 = kA_3A_1^2\,\sigma^2 + 2\mu^{-1} A_1^2\,T + 4A_1^2\,A_3\,\tau^2\,T \qquad \ldots 4\text{-}114$$

Using the discrete version of Gronwall's lemma given in ref. [110],

$$||z_{j+1}||_D^2 \le A_4\,\tau^4\, e^{16A_3T} \qquad \ldots 4\text{-}115$$

$$\therefore \quad ||z_{j+1}||_\infty \le ||z_{j+1}||_D \le \sqrt{A_4}\,\tau^2\, e^{8A_3T} \qquad \ldots 4\text{-}116$$

It follows from 4-100, 4-102, 4-112 and 4-114 that

$$(A_4)^{\frac{1}{2}} \le \frac{A_1+A_2}{\sqrt{\mu}}\left[\sigma + 2T\,(\mu^2+1)\right]^{\frac{1}{2}} \qquad \ldots 4\text{-}117$$

which implies that $||z_{j+1}||_\infty \le A\,\tau^2$; therefore 4-106 holds, with j replaced by j+1. It follows from 4-96 and 4-97 that

$$||z_{j+3/2}||_\infty + ||D_o z_{j+3/2}||_\infty \le 2A\,\tau^2 + 2A_1\,\tau^2 + \tfrac{3}{2}||D_o z_{j+1}||_\infty + \tfrac{1}{2}||D_o z_j||_\infty \le 2(A+A_1)\,\tau^2 + 4h^{-1}\,\tau^2 \qquad \ldots 4\text{-}118$$

Since $||D_o z_j||_\infty \le 4h^{-1}||z_j||_\infty$; hence by 4-103, we have

$$\begin{aligned} ||z_{j+3/2}||_\infty + ||D_o z_{j+3/2}||_\infty &\le 2(A+A_1)\,\tau^2 + 4(1+\lambda^2)h \\ &\le \tau + 4(1+\lambda^2)\,\tau \\ &= (5 + 4\lambda^2)\,\tau = \sigma\tau \end{aligned} \qquad \ldots 4\text{-}119$$

which verifies 4-105, with j replaced by j+1. Thus the extrapolated Crank-Nicolson difference scheme given by equations 4-85, 4-86, and 4-87 satisfies the conditions (I) and (II).

After ensuring the stability of the difference scheme, and after estimating an error bound of the order of $\sqrt{h^2+k^2}$, the basic differential equations 4-46 and 4-55 which describe the system of reaction in a cylindrical pore, may be recalled

in the following form:

$$\frac{\partial C}{\partial t} = \frac{D}{H^2} \frac{\partial^2 C}{\partial x^2} - \frac{2kC}{R} \qquad \ldots 4\text{-}120$$

$$\rho_s \frac{\partial R}{\partial t} = kC_A = kC_{Ao}C \qquad \ldots 4\text{-}121$$

For numerical convenience introduce a new variable f=1-C so that

$$\frac{\partial f}{\partial t} = \frac{D}{H^2} \frac{\partial^2 f}{\partial x^2} + \frac{2k(1-f)}{R} \qquad \ldots 4\text{-}122$$

$$\rho_s \frac{\partial R}{\partial t} = k\, C_{Ao}\, (1-f) \qquad \ldots 4\text{-}123$$

Writing these equations in terms of Lees' extrapolated difference scheme given by equations 4-85, 4-86 and 4-87, and denoting $\underline{f(x,t) = f(n,m)}$ and $\underline{R(x,t) = R(n,m)}$,

$$f(n,m+1) - f(n,m) = \frac{D\,\Delta t}{2H^2\,\Delta x^2} \{f(n+1,m+1) - 2f(n,m+1) + f(n-1,m+1)$$

$$+f(n+1,m) - 2f(n,m) + f(n-1,m)\} + 2k\,\Delta t(1-3/2f(n,m)+\tfrac{1}{2}f(n,m-1))/$$

$$(\tfrac{3}{2} R(n,m) - \tfrac{1}{2}R(n,m-1)) \qquad \ldots 4\text{-}124$$

$$\text{and } R(n,m+1) - R(n,m) = \frac{kC_{Ao}\,\Delta t}{\rho_s}[1-\tfrac{3}{2} f(n,m)+\tfrac{1}{2}f(n,m-1)] \ldots 4\text{-}125$$

Standard computer programmes [113]are available to solve the equations 4-124 and 4-125 simultaneously. The rank of the matrix of coefficients in the equations of the type 4-124, depends on the number of axial grids used in the computations. The method of calculations for $\Delta x = 0.2$ i.e. for five axial grids over half the axial length H, is given below:

The equation 4-124 contains terms at time level m+1, m and m-1. To continue with the "forward march" the terms at time

level m+1 are expressed in terms of those at time level m and m-1. Referring to figure 4-4, the axial grid position n=0 represents the air space outside the cylinder. The positions n=1, 2,3,4,5,6 represent the five grids over half the length of the cylinder H. By virtue of symmetry, the point n=7 forms the mirror image of the point n=5.

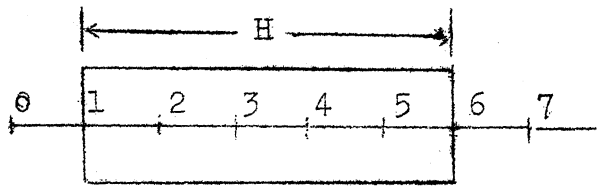

GRID POSITIONS OVER HALF THE PORE

FIGURE 4-4

If $(D\ \Delta t)/(H^2\ \Delta x^2) = b$ ...4-126

$(k\ C_{Ao}\ \Delta t)/\rho_s = a$ ...4-127

the equations 4-124 and 4-125 may be re-arranged as

$$\frac{b}{2} f(n+1,m+1)-(b+1)\ f(n,m+1) + \frac{b}{2}f(n-1,m+1) = -\frac{b}{2}f(n+1,m)+(b-1)f(n,m)$$

$$-\frac{b}{2} f(n-1,m)-2k\ \Delta t(1- \frac{3}{2} f(n,m)+\frac{1}{2} f(n,m-1))/(\frac{3}{2}R(n,m)-\frac{1}{2}R(n,m-1)) \quad ...4\text{-}128$$

and $R(n,m+1) = R(n,m) + a\ (1- \frac{3}{2} f(n,m)+\frac{1}{2} f(n,m-1))$ ...4-129

If at time t=0, m is set at zero, we have

$f(n,-1) = f(n,0)$ ...4-130

and $R(n,-1) = R(n,0)$ ...4-131

and f(n,1) and R(n,1) would then denote the properties at point n and after a time interval Δt. Thus it may be noted that if equation 4-128 is to be used to calculate the properties at time m+1, in terms of those at time m and m-1, there would be three unknowns at positions n+1, n, and n-1. Referring to figure 4-4, the equation 4-128 may be written at positions 1,2,3,4,5 and 6 to obtain six simultaneous linear algebraic equations containing

EIGHT unknowns. However, in view of the fact that f(o,m) is always zero and f(5,m) is always equal to f(7,m) the number of unknowns reduces from EIGHT to SIX. The solution hence can be obtained by means of the following simultaneous equations.

$$\frac{b}{2} f(2,m+1) - (b+1)f(1,m+1)+ \frac{b}{2} f(0,m+1) = - \frac{b}{2} f(2,m) + (b-1)f(1,m) - \frac{b}{2} f(0,m) - (2k\ \Delta t)\ (1- \frac{3}{2} f(1,m) + \tfrac{1}{2}f(1,m-1))/(\frac{3}{2} R(1,m)-\tfrac{1}{2}R(1,m-1)) \quad ...4\text{-}132$$

$$\frac{b}{2}f(3,m+1)-(b+1)f(2,m+1)+ \frac{b}{2}f(1,m+1) = - \frac{b}{2} f(3,m)+ (b-1)f(2,m) -\frac{b}{2} f(1,m) -(2k\ \Delta t)(1- \frac{3}{2}f(2,m)+\tfrac{1}{2}f(2,m-1))/(\frac{3}{2} R(2,m)- \tfrac{1}{2}R(2,m-1)) \quad ...4\text{-}133$$

.....4-134, 4-135, 4-136, ...and

$$\frac{b}{2}f(7,m+1)-(b+1)f(6,m+1) + \frac{b}{2}f(5,m+1) = - \frac{b}{2}f(7,m)+(b-1)f(6,m) - \frac{b}{2}f(5,m)-(2k\ \Delta t)(1- \frac{3}{2} f(6,m)+ \tfrac{1}{2}f(6,m-1))/(\frac{3}{2}R(6,m)-\tfrac{1}{2}R(6,m-1)) \quad ...4\text{-}137$$

There are no difficulties in the calculation of radii at various positions with the help of equation 4-129. Again, referring to figure 4-4, six independent equations for radii may be written as follows:

$$R(1,m+1) = R(1,m) + a\ (1- \frac{3}{2} f(1,m) + \tfrac{1}{2}f(1,m-1)) \quad ...4\text{-}138$$

$$R(2,m+1) = R(2,m) + a\ (1- \frac{3}{2} f(2,m) + \tfrac{1}{2}f(2,m-1)) \quad ...4\text{-}139$$

.....4-140, 4-141, 4-142.....and

$$R(6,m+1) = R(6,m) + a\ (1 - \frac{3}{2}f(6,m) + \tfrac{1}{2}f(6,m-1)) \quad ...4\text{-}143$$

Obviously Lees' extrapolated difference scheme involves an implicit method of solving a set of simultaneous LINEAR

equations to obtain the concentrations after each interval of time. This is a significant advantage over other difference schemes which involve a set of nonlinear simultaneous equations which take greater machine time for numerical solutions.

(ii) Rose's Difference Scheme: Under the constraints and conditions mentioned in Lees' extrapolated difference scheme, Rose [110] approximated the parabolic differential equation

$$\frac{\partial^2 w}{\partial x^2} = F(x,t,w, \frac{\partial w}{\partial x}, \frac{\partial w}{\partial t}) \qquad \ldots 4\text{-}144$$

by means of a family of following implicit difference equations;

$$s\,D_+D_-\,u_j + (1-s)D_+D_-u_{j-1} = F(x,t,u_j,\frac{s}{2}(D_+u_j + D_-u_j)+\frac{1-s}{2}(D_+u_{j-1} + D_-u_{j-1}), (u_j-u_{j-1})/k) \qquad \ldots 4\text{-}145$$

where the parameter s satisfies the condition $0 \le s \le 1$. Following stability analysis argument (to obtain an l_2 error estimate) similar to the one mentioned before, Rose showed that

$$||u - w||_\Omega = 0\,(k+h^2) \qquad \ldots 4\text{-}146$$

for any value of grid ratio $\lambda = k/h^2$ provided that

$$0 \le 2(1-s)\lambda \le 1/a_* \qquad \ldots 4\text{-}147$$

where

$$0 < a_* \le \frac{\partial F}{\partial q} \le a^* \qquad \ldots 4\text{-}148$$

Extrapolating from the known results of linear equations with constant coefficients, Rose also conjectured that $||u-w||_\Omega = 0(k+h^2)$ for all values of mesh ratio provided that $2s-1 \ge 0$. It may be noted that the conditions $s=1$ and $s=\frac{1}{2}$ reduce the relation 4-145 to the standard implicit and Crank Nicolson difference schemes respectively.

New, coming to the problem of reaction in a single pore, equations 4-122 and 4-123 may be written in terms of Rosen's finite difference scheme (4-145) as follows:

$$f(n,m)-f(n,m-1) = s\frac{D\ \Delta t}{H^2\ \Delta x^2}(f(n+1,m) - 2f(n,m) + f(n-1,m))$$

$$+ \frac{(1-s)D\ \Delta t}{H^2\ \Delta x^2}(f(n+1,m-1)-2f(n,m-1) + f(n-1,m-1)) + 2k\ \Delta t(1-f(n,m))/R(n,m) \quad \ldots 4\text{-}149$$

$$\text{and} \quad R(n,m) - R(n,m-1) = \frac{k\ C_{Ao}\ \Delta t}{\rho_s}(1-f(n,m)) \quad \ldots 4\text{-}150$$

Eliminating the nonlinear source term R(n,m) between equations 4-149 and 4-150 and using the same notations for a and b as in equations 4-126 and 4-127,

$$-abs\ [f(n+1,m)\ f(n,m)]+(a+2abs)[f(n,m)f(n,m)]-abs[f(n-1,m)f(n,m)]$$
$$+(abs + bsR(n,m-1))\{f(n+1,m)\}+ ((-1-2bs)R(n,m-1) + (-ab+abs)$$
$$f(n+1,m-1)+(-a+2ab-2abs)\ f(n,m-1) + (abs-ab)f(n-1,m-1) - a-2abs-$$
$$2k\ \Delta t)\{f(n,m)\}+(abs + bsR(n,m-1))\{f(n-1,m)\}+ (a+R(n,m-1))(b(1-s)$$
$$f(n+1,m-1) + (1-2b + 2bs)\ f(n,m-1) + b(1-s)\ f(n-1,m-1)) + 2k\ \Delta t$$
$$= 0 \quad \ldots 4\text{-}151$$

Note that the quantities within the square brackets "[]" represent the nonlinear concentration terms and those within the curved brackets "{}" represent the linear concentration terms, both at time level m. The rest of the terms represent the properties at time level m-1. Thus the equation 4-151 has three unknowns at time level m, (one each at positions n+1, n and n-1) which are to be solved in terms of known terms at time level m-1. The problem now is similar to the one represented by the equation

4-128, with a major difference of the presence of nonlinear terms in the equation 4-151.

Again, referring to the figure 4-4, six simultaneous nonlinear equations of the type 4-151 may be written for axial positions n = 1,2,3,4,5 and 6 in the following manner.

$$-abs[f(2,m)\ f(1,m)]+(a+2asb)[f(1,m)\ f(1,m)]-asb[f(0,m)\ f(1,m)]$$
$$+(asb + bsR(1,m-1))\{f(2,m)\}+ ((-1-2bs)\ R(1,m-1) + (asb-ab)$$
$$f(2,m-1) + (2ab-a-2asb)\ f(1,m-1) + (asb-ab)\ f(0,m-1)-a-2asb-2k\ \Delta t)$$
$$\{f(1,m)\}+ (asb + bsR(1,m-1))\ \{f(0,m)\}+ (a+R(1,m-1))(b(1-s)f(2,m-1)$$
$$+(1-2b+2bs)f(1,m-1) + b(1-s)f(0,m-1)) + 2k\ \Delta t = 0 \qquad ...4\text{-}152$$

.....4-153, 4-154, 4-155, 4-156.....and

$$-asb[f(7,m)f(6,m)]+ (a+2asb)[f(6,m)f(6,m)]-asb[[f(5,m)\ f(6,m)] +$$
$$(asb + bsR(6,m-1))\{f(7,m)\}+ ((-1-2bs)R(6,m-1) + (asb-ab)f(7,m-1)+$$
$$(2ab-a-2asb)\ f(6,m-1) + (asb-ab)\ f(5,m-1)-a-2asb-2k\Delta\ t)\{\ f(6,m)\}+$$
$$(asb + bsR(6,m-1))\{f(5,m)\}+ (a+R(6,m-1))(b(1-s)f(7,m-1) + (1-2b+2bs)$$
$$f(6,m-1)+b(1-s)f(5,m-1)) + 2k\ \ \Delta t = 0 \qquad ...4\text{-}157$$

Again, noting the fact that at position n=0, f is always zero and the position at n=5 is the mirror image of that at n=7, the six unknowns at time level m can be evaluated from the above set of six nonlinear simultaneous algebraic equations, by means of a standard iterative technique given in reference [113]. Once the concentration profile at time level m is known, the radial profile at time m can easily be evaluated by means of equation 4-150, and the "forward march" with respect to reaction time can be continued. Actual computations for s=0.3 and s=0.7 are presented in the chapter on calculations and conclusions.

(iii) Modified Backward Difference Scheme: If $w(x,t)$ is a four times boundedly differentiable solution of the parabolic differential equation

$$\frac{\partial}{\partial x}\left(g(x,t)\,\frac{\partial w}{\partial x}\right) = F\left(x,t,w,\frac{\partial w}{\partial x},\frac{\partial w}{\partial t}\right) \qquad \ldots 4\text{-}158,$$

in the rectangular region $\Omega = \{(x,t) \mid 0 \leq x \leq 1,\ 0 \leq t \leq T\}$ and if the notations assumed in Lees' difference scheme are maintained, the approximation to $w(x,t)$ is given by the solution of the difference equation

$$D_-(G_j D_+ u_j) = F\left(x,t,u_{j-1},\tfrac{1}{2}[D_+u_{j-1} + D_-u_{j-1}],\frac{u_j - u_{j-1}}{k}\right) \ldots 4\text{-}159$$

where G_j is the difference approximation of the smooth function $g(x,t)$ defined in the region Ω. Following a similar line of argument as before, it may be shown that

$$||u - w||_\Omega = 0\,(k+h^2) \qquad \ldots 4\text{-}160$$

The difference equation 4-159 differs from the standard backward difference analogue of 4-158 in that the difference derivatives D_+ and $\frac{1}{2}(D_+ + D_-)$ are evaluated u_{j-1} rather than at u_j. This modified backward difference scheme has special significance in the present context because the parabolic equation 4-122 describing the reaction in a pore belongs to a class of functions F which can be expressed as

$$F(x,t,w,p,q) = F_1(x,t,w,p) + F_2(x,t,w,p)q \qquad \ldots 4\text{-}161$$

It is readily verified that in such cases the solution of the modified backward difference equation requires the inversion of linear system of algebraic equations.

If the difference scheme 4-159 is applied to the particular problem of reaction in a pore, the equations 4-122 and 4-123 become

$$bf(n+1,m)-(2b+1)f(n,m)+bf(n-1,m) = 2k\ \Delta t(1-f(n,m-1))/R(n,m-1) + f(n,m-1) \quad \ldots 4\text{-}162$$

$$\text{and } R(n,m) = R(n,m-1) + a(1-f(n,m-1)) \quad \ldots 4\text{-}163$$

where a & b are constants given by equations 4-126 and 4-127. The problem now is a simplified version of equation 4-128. Following a procedure similar to one used in Lees' difference scheme, the concentration and radial profiles may be given as

$$bf(2,m)-(2b+1)f(1,m) + bf(o,m) = 2k\ \Delta t(1-f(1,m-1))/R(1,m-1) + f(1,m-1) \quad \ldots 4\text{-}164$$

$$bf(3,m)-(2b+1)f(2,m) + bf(1,m) = 2k\ \Delta t(1-f(2,m-1))/R(2,m-1) + f(2,m-1) \quad \ldots 4\text{-}165$$

.....4-166, 4-167, 4-168.....and

$$bf(7,m)-(2b+1)f(6,m)+bf(5,m) = 2k\ \Delta t(1-f(6,m-1))/R(6,m-1)+ f(6,m-1) \quad \ldots 4\text{-}169$$

and

$$R(1,m) = R(1,m-1) + a(1-f(1,m-1)) \quad \ldots 4\text{-}170$$

$$R(2,m) = R(2,m-1) + a(1-f(2,m-1)) \quad \ldots 4\text{-}171$$

.....4-172, 4-173,4-174.....and

$$R(6,m) = R(6,m-1) + a(1-f(6,m-1) \quad \ldots 4\text{-}175$$

In comparison with Lees' difference scheme, computations here are simpler, but the error bound is higher. The computational merits and demerits of the modified difference scheme will be discussed in the chapter on calculations and conclusions.

(iv) Explicit Forward Difference Scheme: Before going into the details of the scheme, it may be noted that no rigorous stability analysis is available for the explicit difference approximations of the nonlinear or seminlinear parabolic differential equations. However, on a number of occasions, [114], the explicit difference forms which are proved stable for the linear parabolic equations are extended to the nonlinear systems without any valid theoretical justification. If the actual numerical calculations are in reasonable agreement with those obtained from the standard stable implicit schemes, the extension is considered acceptable. The scheme is otherwise rejected. Moreover, no guide lines are available to decide whether a particular difference scheme should or should not be extended to a particular kind of nonlinearity. This kind of approach, though not satisfactory, has been widely used in the solution of nonlinear equations with considerable computational advantage. After having reconciled to this empirical procedure, scanning of various possible difference forms may be considered. However, their number being too large and the numerical advantage of one modification over the other being uncertain and marginal, it may be advisable to start with the simplest of the explicit finite difference schemes.

The basic differential equations 4-122 and 4-123 describing the reaction in a cylindrical pore may thus be written in the following difference forms:

$$\frac{f(n,m+1)-f(n,m)}{\Delta t} = \frac{D}{H^2}\frac{f(n+1,m)-2f(n,m)+f(n-1,m)}{\Delta x^2} +$$

$$2k(1-\tfrac{1}{2}(f(n,m+1)+f(n,m))/(\tfrac{1}{2}(R(n,m+1)+R(n,m))) \quad \ldots 4\text{-}176$$

and $$\frac{R(n,m+1)-R(n,m)}{\Delta t} = \frac{kC_{Ao}}{\rho_s}(1-\tfrac{1}{2}(f(n,m+1)+f(n,m))) \quad \ldots 4\text{-}177$$

Eliminating the nonlinear source term R(n,m+1) between equations 4-176 and 4-177 and rearranging the terms as before, the following quadratic equation can be written for f(n,m+1).

$$af^2(n,m+1) - [4R(n,m) + 2a + ab(f(n+1,m) - 2f(n,m) + f(n-1,m)) + 4k\,\Delta t]\, f(n,m+1) + \{f(n,m) + b(f(n+1,m) - 2f(n,m) + f(n-1,m))\}\{4R(n,m) + 2a - af(n,m)\} + 4k\,\Delta t\{2-f(n,m)\} = 0 \quad \ldots 4\text{-}178$$

Denoating the coefficient of f(n,m+1) by -b'(n+1,n,n-1,m) and the constant terms by c'(n+1,n,n-1,m) the above equation may be rewritten as

$$af^2(n,m+1) - \{b'(n+1,n,n-1,m)\}\, f(n,m+1) + c'(n+1,n,n-1,m) = 0 \quad \ldots 4\text{-}179$$

To obtain the concentration at time level m+1 in terms of those at time level m, the equation 4-179 may be solved as

$$f(n,m+1) = (b'(n+1,n,n-1,m) \pm \sqrt{(b'(n+1,n,n-1,m))^2 - 4ac'(n+1,n,n-1,m)})/(2a) \quad \ldots 4\text{-}180$$

and $$R(n,m+1) = R(n,m) + \frac{a}{2}(2-f(n,m+1) - f(n,m)) \quad \ldots 4\text{-}181$$

Referring to figure 4-4, the concentrations at positions n=1,2,3, 4,5 and 6 can now be evaluated by <u>six independent algebraic equations of the type 4-180</u>. This is precisely the advantage of an explicit scheme which avoids the solution of a <u>set of simultaneous</u>

linear or nonlinear equations prevalent in an implicit scheme.

Once the concentration distribution at time level m+1 is known, the radii at various positions can easily be calculated by means of the equations of the type 4-181 and the"forward march" can be continued.

Since the stability of the above difference scheme is dependent on the stability of the corresponding difference scheme for the linear parabolic system, it may be worth analysing the truncation and round-off errors and the constraints placed on the variation of "radius of convergence" in the following linear parabolic differential equation

$$\frac{\partial w}{\partial t} = \frac{\partial^2 w}{\partial x^2} \qquad \ldots 4\text{-}182$$

Discretising the variables in terms of Taylor series.[114],

$$\frac{w(n,m+1) - w(n,m)}{\Delta t} - \frac{\partial^2 w}{\partial t^2}(n,m)\,\frac{\Delta t}{2!} \quad \ldots\ldots\ldots = \frac{w(n+1,m) - 2w(n,m) + w(n-1,m)}{\Delta x^2} - \frac{\partial^4 w}{\partial x^4}(n,m)\,\frac{2\Delta x^2}{4!} \qquad \ldots 4\text{-}183$$

If u(n,m) is the difference approximation of the exact solution w(n,m), the explicit forward difference scheme for the equation 4-182 may be written as

$$u(n,m+1) = u(n,m) + \frac{\Delta t}{\Delta x^2}\,(u(n+1,m) - 2u(n,m) + u(n-1,m)) \ldots 4\text{-}184$$

To start with, von Neumann test may be applied to obtain the criterion of stability of the scheme 4-184. If i,θ, and λ respectively denote $\sqrt{-1}$, a real number and a complex number, the the exponential perturbation expression

$$u(n,m) = e^{in\theta}\, e^{im\lambda} \qquad \ldots 4\text{-}185$$

may be substituted in 4-184 and each term may be divided by $e^{in\theta}\, e^{im\lambda}$ to obtain λ as the root of the equation

$$e^{i\lambda} = 1 - 4\left(\frac{\Delta t}{\Delta x^2}\right) \sin^2\left(\frac{\theta}{2}\right) \qquad \ldots 4\text{-}186$$

The stability criterion requires that the imaginary part of λ be nonnegative, or in other words that for every real θ,

$$|e^{i\lambda}| \leq 1 \qquad \ldots 4\text{-}187$$

This is the case if and only if

$$(\Delta t)/(\Delta x^2) \leq 1/2 \qquad \ldots 4\text{-}188$$

(Note that the corresponding constraint for the nonoscillatory decay in the Crank Nicolson scheme would be

$$(\Delta t)/(\Delta x^2) \leq \{2(2(1-\cos(s\,\Delta x)))\}^{-1} \qquad \ldots 4\text{-}188a)$$

Under the constraint 4-188 concerning the ratio of the mesh sizes, not only should the round off errors generated by the finite difference scheme 4-184 have a stable behaviour, but also the approximate solution u(n,m) should converge towards the exact solution w(n,m) as $\Delta x \to 0$. To prove the same, equation 4-184 may be rearranged as

$$u(n,m+1) = \frac{\Delta t}{\Delta x^2}\, u(n+1,m) + \left(1 - \frac{2\,\Delta t}{\Delta x^2}\right) u(n,m) + \frac{\Delta t}{\Delta x^2}\, u(n-1,m) \qquad \ldots 4\text{-}189$$

so that u(n,m+1) is expressed as an average of u(n+1,m), u(n,m) and u(n-1,m) with nonnegative weighting factors. According to Taylor's theorem with remainder, the differential equation 4-182 provides an analogous relation

$$w(n,m+1) = \frac{\Delta t}{\Delta x^2} w(n+1,m) + (1- \frac{2\ \Delta t}{\Delta x^2})\ w(n,m) + \frac{\Delta t}{\Delta x^2} w(n-1,m) + 0(\ \Delta t\ \Delta x^2) \qquad ...4\text{-}190$$

Subtracting 4-189 from 4-190, and introducing error term

$$z(n,m) = w(n,m) - u(n,m) \qquad ...4\text{-}191,$$

the difference equation for $z(n,m)$ may be written as

$$z(n,m+1) = \frac{\Delta t}{\Delta x^2} z(n+1,m) + (1- \frac{2\ \Delta t}{\Delta x^2})\ z(n,m) + \frac{\Delta t}{\Delta x^2} z(n-1,m) + 0(\ \Delta t\ \Delta x^2) \qquad ...4\text{-}192$$

Noting the fact that for an initial value problem,

$$z(n,0) = 0 \qquad ...4\text{-}193,$$

the difference equation 4-192 together with the constraint 4-188 gives

$$z_{m+1} \leq z_m + G\ \Delta t\ \ \Delta x^2 \qquad ...4\text{-}194$$

where $z_m = \sup_n |z(n,m)|$ ...4-195,

and G is some sufficiently large positive constant. Moreover, the condition 4-193 implies that $z_o = 0$, whence from 4-194, the basic inequality may be derived as

$$z_m \leq\ G\ m\ \Delta t\ \ \Delta x^2 \qquad ...4\text{-}196$$

Also if rounding-off errors occur because only 1 decimal places are used in computing an actual numerical solution of the difference equation 4-189, then an additional term ofthe form $10^{-1}G$ ought to be included on the right had side of the in equality 4-194. Therefore the final estimate of the total error becomes

$$z_m \leq G\ m\ \Delta t\ (\ \Delta x^2 + 10^{-1}\ \Delta t^{-1}) \qquad ...4\text{-}197$$

The result 4-196 implies that for any mesh ratio in the range 4-188 the solution $u(n,m)$ of the finite difference approximation

4-184 to the basic initial value problem 4-182 converges towards the exact answer w(n,m) in the limit as $\Delta x \to 0$. However, 4-197 indicates that in order to retain control over the round-off errors generated by a numerical calculation of u(n,m), choice of an unduly small time increment (Δt) should be avoided. In this connection, it may be emphasized that the relationship between estimates of the truncation and of the round-off errors is closely interlinked despite the diversity of the sources from which they arise. Thus in the ultimate analysis, the advantage of independent equations in an explicit form is countered by the restriction placed on the choice of mesh ratio and on the other hand, the advantage of unrestricted mesh ratio is an implicit form is countered by the occurance of simultaneous equations. Thus in a particular problem, it becomes necessary to investigate both explicit and implicit forms and then choose the best one.

(v) Modified Richardson Difference Scheme: Even though Richardson's "unconditionally unstable" difference scheme which uses a central difference for the first order time derivative, is only of historic importance [114], a number of modifications over this classic scheme have been suggested from time to time[115] and some of them are stable too. In the present context, however, only one important modification proposed by DuFort and Frankel [116] is considered for investigation.

Retaining the same notations as in equations 4-182 and 4-184, the original Richardson's scheme for the parabolic

differential equation 4-182 may be written as

$$\frac{u(n,m+1) - u(n,m-1)}{2\,\Delta t} = \frac{u(n+1,m) - 2u(n,m) + u(n-1,m)}{\Delta x^2} \quad \ldots 4\text{-}198$$

DuFort and Frankel [116] modified the above scheme by using the relation $2u(n,m) = u(n,m+1) + u(n,m-1)$ ...4-199, and obtained the following difference form for 4-182.

$$\frac{u(n,m+1) - u(n,m-1)}{2\,\Delta t} = \frac{u(n+1,m) - u(n,m+1) - u(n,m-1) + u(n-1,m)}{\Delta x^2} \quad \ldots 4\text{-}200$$

The advantage of this modification is that it is an explicit scheme which is convergent and stable for all finite values of the mesh ratio $\Delta t/\Delta x^2$. Forsythe and Wasow [114] have given an elaborate stability analysis and have concluded that the discretization error involved in the approximation 4-200, is of the order $O(\Delta x^2)$ for any fixed value of the mesh ratio $\Delta t/\Delta x^2$. However, like in any other explicit form, the proof has not been completely extended to the nonlinear cases. If the parabolic equation is of the more general type (4-122 coupled with 4-123), at other places too, the term u(n,m) should be replaced by the average $\frac{1}{2}(u(n,m+1) + u(n,m-1))$ [114]. As in Richardson's method the value of u after the first increment of time i.e. u(n,1) must be calculated by some independent procedure before the calculation by equation 4-200 can be started.

Coming to the basic problem of simultaneous diffusion and chemical reaction in a pore, the modified Richardson scheme 4-200 may be applied to the system of equations 4-122 and 4-123 to obtain the following difference forms:

$$f(n,m+1) - f(n,m-1) = \frac{2D\,\Delta t}{H^2\,\Delta x^2}\,(f(n+1,m) - f(n,m+1) - f(n,m-1) + f(n-1,m)) + 4k\,\Delta t(2-f(n,m+1)-f(n,m-1))/(R(n,m+1)+R(n,m-1)) \quad \ldots 4\text{-}201$$

$$\text{and } R(n,m+1) - R(n,m-1) = \frac{kC_{Ao}\,\Delta t}{\rho_s}\,(2-f(n,m+1)-f(n,m-1)) \quad \ldots 4\text{-}202$$

Eliminating the nonlinear source term R(n,m+1) from the equations 4-201 and 4-202 and retaining the same notations for a and b as before, the following quadratic equation may be obtained for f(n,m+1):

$$(a+2ab)[f(n,m+1)]^2 - \{2ab\,f(n+1,m) + 2ab\,f(n-1,m) + (2+4b)\,R(n,m-1) - 4ab\,f(n,m-1) + 2a + 4ab + 4k\,\Delta t\}f(n,m+1) + \{2b\,f(n+1,m) + 2b\,f(n-1,m) + (1-2b)\,f(n,m-1)\}\{2R(n,m-1) + 2a - af(n,m-1)\} - 4k\,\Delta t\,f(n,m-1) + 8k\,\Delta t = 0 \quad \ldots 4\text{-}203$$

As before, denoting the coefficient of f(n,m+1) by -B'(n+1,n,n-1, m,m-1) and the constant terms by C'(n+1,n,n-1,m,m-1), the equation 4-203 may be rewritten as

$$a[f(n,m+1)]^2 - (B'(n+1,n,n-1,m,m-1))\,f(n,m+1) + C'(n+1,n,n-1,m,m-1) = 0 \quad \ldots 4\text{-}204$$

$$f(n,m+1) = \frac{1}{2a}\{B'(n+1,n,n-1,m,m-1) \pm ((B'(n+1,n,n-1,m,m-1))^2 - 4a\,C'(n+1,n,n-1,m,m-1))^{\frac{1}{2}}\} \quad \ldots 4\text{-}205$$

Again, the concentrations at positions n=1,2,3,4,5, and 6 may be evaluated by six independent equations of the type 4-205. Once the concentrations at time level m+1 are known, the radii at various positions can easily be evaluated by means of equation 4-202. The procedure is similar to the one used in the explicit forward difference scheme except that the term f(n, m) does not appear in the expression for f(n,m+1). In fact, it is this

difference which renders the scheme numerically stable.

Presuming that the distribution of concentration and radii at any time is obtained by the use of one of the five finite difference schemes mentioned above, the problem then would be to formulate a model to determine the weight loss during the course of reaction. For this, a linear wall profile between the radii R(n,m) and R(n+1,m) is assumed. Referring to the figure 4-5, the weight loss over an elemental cylinder of thickness Δz is given by the weight of the elemental frustrum of a cone of thickness Δz enclosed between the radii R(n,m) and R(n+1,m), minus the weight of the elemental cylinder of thickness Δz and of constant radius R(n,o), the internal radius of the cylinder at time t = 0.

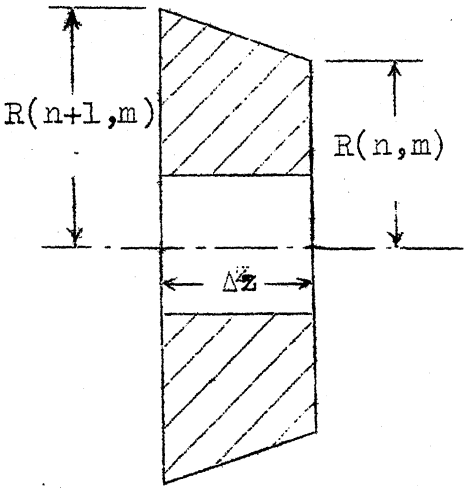

FIGURE: 4-5

$$\therefore \quad \Delta W = \frac{\rho_s \pi \Delta z}{3} \{(R(n,m))^2 + R(n,m)\, R(n+1,m) + (R(n+1,m))^2\}$$

$$- \pi (R(n,0))^2 \rho_s \Delta z \qquad \ldots 4\text{-}206$$

Summing these "ΔW"s over half the length of the pore H,

$$\Sigma \Delta W = \sum_{n=1}^{5} \frac{\rho_s \pi \Delta z}{3} \{(R(n,m))^2 + R(n,m)\, R(n+1,m) + (R(n+1,m))^2\}$$

$$- \sum_{n=1}^{5} \rho_s \pi \Delta z (R(n,0))^2 \qquad \ldots 4\text{-}207$$

Since the reaction is symmetrical about the centre of the pore,

the total loss over the entire pore is given by

$$(W-W_o) = \frac{2\rho_s \pi \Delta z}{3} \sum_{n=1}^{5} \{(R(n,m))^2 + R(n,m)\, R(n+1,m) + (R(n+1,m))^2\}$$

$$-2\rho_s \pi H(R(n,o))^2 \qquad \ldots 4\text{-}208$$

As will be seen in the conclusions, the equation 4-208 gives a fairly accurate estimate of the weight losses at higher temperatures of reaction, i.e. when the wall profiles are linear. At low temperatures, however, a larger number of axial grids have to be considered to obtain more accurate results from the equation 4-208. Graphical interpolation over the curved portion of the wall profile, serves as a convenient method of increasing the number of axial grids.

While investigating the finite difference model, it is important and interesting to attempt a mathematical model for a general pth order non-catalytic reaction in a pore, on the lines similar to those followed by Mehta and Aris [43] for catalytic reactions. The basic differential equations (4-120, 4-121) for a pth order reaction in a cylindrical pore would then take the following forms:

$$\frac{\partial C}{\partial t} = \frac{D}{H^2} \frac{\partial^2 C}{\partial x^2} - \frac{2k' C^p C_{Ao}^{p-1}}{R} \qquad \ldots 4\text{-}209$$

$$\rho_s \frac{\partial R}{\partial t} = k' (C_{Ao})^p C^p \qquad \ldots 4\text{-}210$$

where k' is the pth order heterogeneous surface reaction rate constant having the dimensions of $(\text{moles})^{1-p}\ (\text{length})^{3p-2} (\text{time})^{-1}$.

A typical implicit scheme of Lees applied to the equations 4-209 and 4-210, gives the following relations:

$$C(n,m+1) - C(n,m) = \frac{D\,\Delta t}{2H^2\,\Delta x^2}\{C(n+1,m+1) - 2C(n,m+1) + C(n-1,m+1) + C(n+1,m) - 2C(n,m) + C(n-1,m)\} - 2k' C_{Ao}^{p-1}\{\tfrac{3}{2}C(n,m) - \tfrac{1}{2}C(n,m-1)\}^{p} /$$

$$\{\tfrac{3}{2}R(n,m) - \tfrac{1}{2}R(n,m-1)\} \qquad \ldots 4\text{-}211, \text{and}$$

$$R(n,m+1) - R(n,m) = \frac{k' C_{Ao}^{p}\,\Delta t}{\rho_s}\{\tfrac{3}{2}C(n,m) - \tfrac{1}{2}C(n,m-1)\} \qquad \ldots 4\text{-}212$$

The method of computations now would be identical to the one followed for the equations 4-124 and 4-125, in Milton Lees' extrapolated difference scheme. The only difference is the presence of pth order terms in the constants of the simultaneous equations which alter the shape of the wall profiles.

On the other hand, if a typical explicit forward difference scheme is used, the equations 4-209 and 4-210 become

$$C(n,m+1) - C(n,m) = \frac{D\,\Delta t}{H^2\,\Delta x^2}\{C(n+1,m) - 2C(n,m) + C(n-1,m)\} - k'\,\Delta t(2)^{2-p}(C_{Ao})^{1-p}\{C(n,m+1) + C(n,m)\}^{p}/\{R(n,m+1) + R(n,m)\} \qquad \ldots 4\text{-}213$$

$$\text{and } R(n,m+1) - R(n,m) = \frac{k'\,\Delta t}{\rho_s}\left(\frac{C_{Ao}}{2}\right)^{p}\{C(n,m+1) + C(n,m)\}^{p}. \qquad 4\text{-}214$$

As before, if an attempt is made to eliminate the nonlinear source term R(n,m+1) between 4-214 and 4-213, it results in a (p+1)th degree polynomial in C(n,m+1). Computations obviously would be complicated and inspite of the independent equations the explicit scheme may not have an edge over the implicit scheme. It would be of academic interest to note that a half order

reaction would give a 3/2 degree equation in C(n,m+1) which can be simplified to obtain a cubic equation in C(n,m+1). In the present context, however, no half order reaction between graphite and oxygen is contemplated and therefore the precise form ofthe cubic equation for various explicit difference schemes need not be worked out. It goes without saying that further calculations for the effectiveness factor for the pth order reaction would be still more complicated.

The whole exercise in mathematical modelling may appear meaningless if reference is not made to the possible use of weight loss and profile data in heterogeneous systems. Attempts have been made to use single pore profile data for building a model to predict the overall rate of reaction on the inner and outer surfaces of a lump of a heterogeneous mass of any irregular shape and size. If A_m is the maximum cross sectional area of the solid lump, and if R_{av} is the average radius of the internal pores, the given lump of mass may be imagined to be a cylindrical pellet with right circular area A_m and with thickness 2H so that the volume of the imaginary pellet equals the original volume of the solid lump. The voidage is so adjusted that the volume of all the pores (of radii R_{av}) imagined to be running parallel to the axis of the cylindrical pellet equals the original void volume of the solid lump. The overall rate of reaction of the solid lump may then be expressed in terms of the rate at which the imaginary axial length of the pellet recedes during the course of

reaction. However, the major difficulty in such a scheme, is the absence of an analytical expression for the rate of reduction of the length of the pellet. Numerical data alone, may not be able to establish the complete validity of this new approach. It may be interesting to obtain approximate solutions by method of residuals and test the validity of the above parallel pore model.

.....

5. CALCULATIONS AND CONCLUSIONS

The accuracy of the calculations and the validity of the conclusions are primarily dependent upon the choice of realistic values of rate constant, diffusivity and density, and upon the judicious selection of the time increment Δt, the axial grid Δx and the radius of convergence b. Since the variation of the overall rate of reaction with temperature in a porous media or in a single pore is closely interlinked with the changes in rate constant, diffusivity and density, any error in these is bound to have a significant effect on the quantitative predictions. For instance, increased temperature has a positive effect on k and D so as to enhance the overall rate of reaction while the same change in temperature has a tendency to decrease the density and hence the overall rate. Even the extent of relative variations in k and D have a profound effect on the establishment of unsteady state concentration gradients in the direction of axis of pore and hence of the axial diffusion fluxes. Therefore, as far as possible, attempts are made to select the experimentally determined values of density, diffusivity and rate constant.

Reference [117] gives a fairly accurate and exhaustive data on the density of air and on the binary diffusivity of oxygen in air, at temperatures upto 5000°K. Theoretically predicted values are compared with the best available experimental data, and the errors reported are not more than 2.4%. Selected

TABLE 5-1

Temperature Degree Kelvin	$\rho_a/(4.464 \times 10^{-5})$ g moles/cc	D cm^2/sec (from $T^{3/2}$ law)	D cm^2/sec from $D = k_a/(\rho_a C_{pa})$	k cm/sec (experimental & extrapolated)	k cm/sec (from [2,30] & extrapolated)
873	0.31200	1.032	1.360	0.1545	
923	0.29580	1.122	1.470	0.4730	
973	0.28030	1.221	1.605	0.8605	
1023	0.26600	1.310	1.730	1.6000	
1073	0.25400	1.416			3.316
1123	0.24270	1.520			5.010
1173	0.23236	1.608			11.340
1223	0.22287	1.715			14.800
1273	0.21413	1.810			28.600
1373	0.19855	2.040			53.700
1473	0.18508	2.265			62.400
1573	0.17333	2.490			68.300
1673	0.16297	2.740			79.800
1773	0.15379	2.985			100.000
1873	0.14558	3.105			120.000
1973	0.13820	3.520			180.000
2073	0.13151	3.770			229.000

NOT USED IN CALCULATIONS

values of densities at temperature between 873°K and 2073°K are indicated in Table 5-1. The contribution due to dissociation of oxygen at temperatures above 1400°K has already been included. Tabulated values of diffusivity at various temperatures are not directly available in literature. However, reference [117] gives the thermal conductivity, specific heat and density and their dependence on temperature so that diffusivity can be calculated from the ideal gas equation

$$D_{AB} = \frac{k_a}{\rho_a C_{pa}} \qquad \ldots 5\text{-}1$$

The diffusivity values obtained from the equation 5-1 are slightly higher than the experimental values not so much because of the assumption of ideality but because the self diffusivity of air has been equated with the binary diffusivity of oxygen in air. One way of overcoming this flaw would be to calculate the binary diffusivity from the individual self-diffusivities, but a more convenient method would be to follow a "$T^{3/2}$ law" which is adequately accurate [106] within the range of temperature under consideration. In fact this is equivalent to assuming an ideal behavior at high temperatures which is quite valid. The actual numerical values obtained from "$T^{3/2}$ law" are given in Table 5-1. The base value of diffusivity at room temperature is taken from reference [105].

Coming to the computation of rate constant from the experimental weight loss curves, it has already been pointed out in the chapter on mathematical modelling that consistent

values of k cannot be obtained from the fundamental equations of the type 4-30, 4-32, 4-41, and A-2. Since the weight loss curves at temperatures 600°, 670°, 730° and 746°C are linear, it is convenient to calculate the first order heterogeneous rate constant by the method of constant slope using the equation

$$\frac{1}{S}\left(-\frac{dW}{dt}\right)\frac{10^{-3}}{(12)(60)} = k\,C_{Ao} \qquad \ldots 5\text{-}2$$

where S = reaction surface area square centimeters,

W = weight of the reacting sample milligrammes,

t = time of reaction seconds,

C_{Ao} = initial concentration of oxygen in air gm moles/cm.^{3}

The numerical values of rate constants thus calculated are indicated on the respective graphs (page number 79 to 82). At temperatures 870° and 1000°C the limiting slope method has been used on account of the presence of obvious nonlinearities in the initial portions of the weight loss curves. This method too uses the equation 5-2 in the calculations.

Attempts were made to obtain k at high temperatures from the reliable experimental data at low temperatures i.e. experimentally determined values at 600°C, 670°C and 746°C were used to calculate the preexponential factor and activation energy which in turn were used to predict k's at temperatures 870°C and 1000°C. The predicted and experimental values differed by a few hundred percent. This could be due to a number of reasons as discussed in the review of literature. Therefore, wherever possible, the rate constants at high temperatures

are taken from literature or are calculated by judicious extrapolation. Even though several numerical values of k (determined experimentally) are reported in literature, it is rather difficult to establish a precise scientific method for the selection of k for the particular variety of graphite used in the present investigation. Therefore the conclusions drawn hereafter should be viewed as applicable to a system with the properties mentioned in Table 5-1 rather than to a system of graphite and air used in the experiment.

Besides the concept of a first order surface rate constant, there are other methods which enable a proper correlation of the rate constant with temperature and porosity. The rate constant (k_v) may be expressed on the basis of reaction per unit volume of the porous solid. Levenspeil model [36] makes an effective use of k_v to describe a chemical reaction controlled regime, but the same does not hold true for a diffusion controlled regime. Moreover, the definition of k_v introduces extra terms describing the geometry of the solid in the basic equations 4-120 and 4-121. This increases the computation time considerably. At times, attempts are made to correlate k with porosity or percentage burn off of the solid. This, however, is an over simplification of the actual process of change in porosity during the course of reaction. Yet another way of incorporating the porous medium reactivity into the surface rate constant is to model the reaction in a macropore by considering the axial diffusion in the gas phase

and the radial diffusion in the solid phase. This not only involves the determination of equivalent diffusivity in solid, but also increases the computation time - even greater than the concept of k_v. Since at high temperatures it is only diffusion which counts, attempts can be made to plot log k versus log T so that the slope of the curve which is approximately equal to the index of variation of D with respect to temperature, can predict the relation between k and T. This again has its limitations in the unsteady state. And lastly, separate equations may be formulated for different ranges of temperature. This obviously has limited utility because of large number of constants involved in the description of the system, and extrapolation could be highly erroneous. Thus none of the above methods is really satisfactory for computational adoption in the present system.

It is of importance to note that, at high temperatures, there is no significant change in k because the reaction lies well in the diffusion controlled regime where k is adultrated by D. However, the present interest is unquestionably in an unadultrated k since the entire effort is to isolate the effect of k from that of D with special reference to the reaction in a pore. It, therefore, becomes necessary to hypothetically consider a nonporous solid at high temperatures and hence the exponentially increasing rate constant. To this extent, even at low temperatures, the porous graphite used in the experiment is equivalent to a nonporous solid with the surface rate constant

determined by the weight loss curves. The actual values of k used in the numerical calculations are indicated in Table 5-1. In fact, it would be ideal to undertake an elaborate investigation by considering all conceivable values of k for one particular value of D and vice-versa.

Coming to the model evaluation for the reaction in a pore, various finite difference schemes have to be tested with special reference to the stability, accuracy and the time of computation. In this connection, it may be noted that even though two finite difference schemes for the two equations 4-122 and 4-123 are independently proved to be stable, the stability of the simultaneous solution is not guaranteed [118]. Moreover, there are no fixed rules as to which ofthe two equations should determine the choice of the grid. The boundary conditions may influence this decision. In the present system, however, the nonlinear term being present in the parabolic equation, the whole stability analysis and the choice of the grid is centred around the equation 4-122.

Besides the common problems associated with the finite difference approximation for a set of simultaneous partial differential equations, there is an additional uncertainty involved in the system of equations 4-122 and 4-123 regarding the time varying wall profile. Although equation 4-122 is formulated for a strictly cylindrical geometry, it is used during the entire course of reaction inspite of the fact that the geometry of the pore does not and cannot remain cylindrical

throughout. Such usage is valid only when the profile of the type given in figure 5-1A can be approximated by the curved surfaces of a number of right circular cylinders indicated in Figure 5-1B. Equation 4-122 then becomes applicable to each right circular cylinder separately. The stability

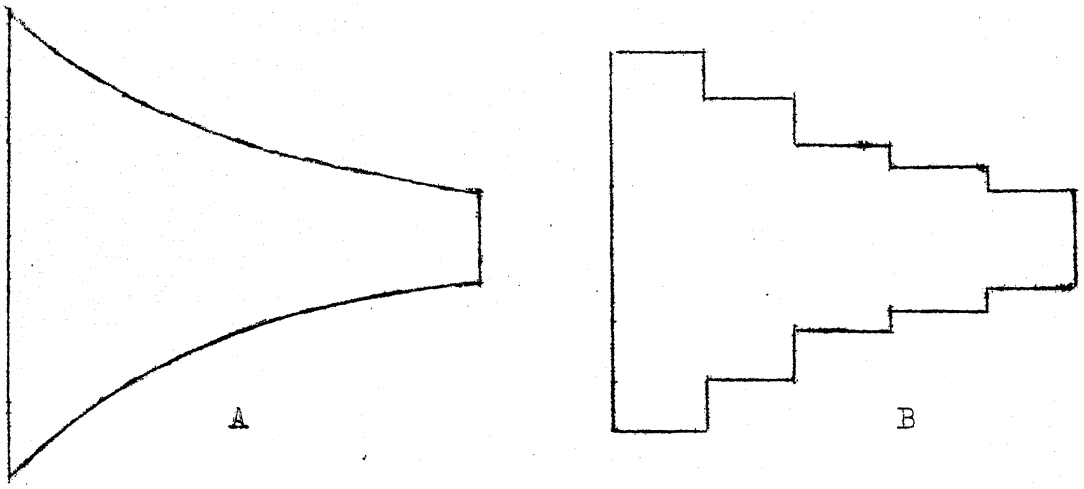

FIGURE 5-1

of the finite difference scheme thus becomes dependent upon the stability of the above approximation which can be justified by the actual numerical calculations alone.

Among the various finite difference schemes discussed, it is only in the explicit forward difference scheme that the size of the mesh ratio is constrained by the criterion of stability. In the rest of the schemes, practically any mesh ratio is permissible provided the accuracy can be compromised. Thus it would be advisable to search for the guide lines to first decide the mesh ratio for the explicit forward difference scheme and then test the accuracy of other schemes by utilizing

the same mesh ratio and mesh sizes.

According to Keller [109], when a nonlinear parabolic differential equation of the type 4-122 is coupled with a first order linear partial differential equation of the type 4-123, it is preferable to choose the distance grid Δx first and then decide the value of time increment Δt according to the rules of stability. The axial grid Δx for an explicit forward difference scheme is chosen on the basis of the following considerations.

(i) Von Numann's Stability Criterion: The constraint 4-188 applied to equation 4-122 gives the condition

$$b = (D\ \Delta t)/(H^2\ \Delta x^2) \leq 1/2 \qquad \ldots 5\text{-}3$$

Since Δt and Δx are two unknowns in 5-3, one more relation for Δx is necessary. Normally, the boundary conditions form the qualitative guide lines for the choice of Δx. However, no quantitative relations are available for the particular system under consideration. Therefore, as a starting point, the condition for nonoscillatory decay (5-4) for the Crank Nicolson scheme may be borrowed and applied to evaluate Δx in the explicit forward difference scheme. Therefore, from 4-188a,

$$b = \frac{(D\ \Delta t)}{H^2\ \Delta x^2} \leq [\sin(\pi\ \Delta x)\ ]^{-1} \qquad \ldots 5\text{-}4$$

Assuming a critical value of radius of convergence (b=1/2), the equations 5-3 and 5-4 can be used to determine the lower limit for Δx as follows:

$$\Delta x \geq 1/6 \qquad \ldots 5\text{-}5$$

The restriction 5-5 is normally applicable to a system in which partial derivatives of f do not occur in the boundary conditions, but if they do occur the number of unknowns at time level m+1 in equation 4-176 should not exceed the number of axial grids. There being only one unknown is 4-176, the question of violation of this condition does not arise.

(ii) Accuracy: The error bound as given by the relation 4-196 is of the order $O(\Delta t\ \Delta x^2)$, and at times a weaker error estimate of the order $O(\Delta t + \Delta x^2)$ is also reported [115]. Smaller values of Δx and Δt will without doubt give more accurate result but the stability condition given by equation 5-5 does not permit infinitely small values of Δx. Thus the maximum number of axial grids given by the relation 5-5 fixes the size of Δx. Therefore, qualitatively speaking, there does not seem to be much scope for the variation of Δx to increase the accuracy.

(iii) Physical and Boundary Conditions: A typical cylindrical sample used in the experiment has a length of 4 cms, an inner diameter of 0.4 cm and an outer diameter of 1.0 cm From physical considerations, ten axial grids over half the length of cylinder (i.e. 2.0 cms.) should give results that are fairly satisfactory, but the maximum limit for the number of axial grids being six, a compromise is called for the use of axial grids less than six, say five (i.e. $\Delta x = 0.2$). On the other hand, an attempt to reduce the number of grids below five will no doubt decrease the machine time of computation.

but the results are not likely to yield accurate wall profiles. The given boundary condition demands that the concentration at the pore mouth remains C_{Ao} throughout the course of reaction In most cases, the reaction being diffusion controlled, the fall of pore mouth concentrations across the axial distance is very rapid. This would call for the use of a smaller size of axial grids and perhaps a different finite difference scheme near the pore mouth, thus leading to an increase in the computation time which is already on the higher side. The size of the grids, therefore, cannot be altered on the basis of the boundary conditions.

Taking into consideration all the above factors, $\Delta x \simeq 0.2$ appears to be a judicious choice for the axial grid. Now, using the Von Neumann condition 5-3, the maximum value of Δt can be chosen on the basis of b=0.5. The lower limit for Δt is decided by the magnitude of the round off errors in the computations. (see equation 4-197). It can be proved [119] that for b=1/6, the error is of the order Δx^4, and for all practical purposes, the corresponding value of Δt gives results which are very close to the analytical solution if it exists. Thus the proper range of variation of Δt for the purpose of numerical trials appears to correspond to the variation of b between 1/6 and 2/5. In the ultimate analysis, the most suited values of Δx, Δt, and b are decided by a trial and error procedure so as to obtain maximum accuracy and minimum time of computation. The relative merits and demerits are illustrated

by means of numerical data given in Table 5-2.

It is clear from Table 5-2 that the difference between the maximum (0.238464 cms) and minimum (0.216568 cms) values of pore mouth radius calculated independently by means of various finite difference schemes after half an hour of reaction at 1373°K is 9.18%, which is fairly reasonable considering the range of variation of Δx between 0.1 and 0.2 and the radius of convergence b between 1/6 and 1/2. A comparison of the results of various difference schemes for the same mesh sizes ($\Delta x = 0.2$ and $b = 1/6$) shows that the Modified Rechardson Difference scheme gives the maximum value of 0.231001cms. and the modified backward difference scheme gives the minimum value of 0.229986 cms. The variation is therefore 0.866%. Similarly, for $\Delta x = 0.2$ and $b = 0.4$, this variation is 1.43%. Presuming that the value $b = 1/6$ yields results very close to the analytical solution, the round-off and discretization errors involved in a numerical solution with b=0.4 may be estimated to be of the order of 5%. A similar trend is noticed in the results of the calculations for the reaction at 873°K.

As regards the machine time [IBM-7044]for computation, it can be easily seen from Table 5-2 that the Explicit Forward Difference scheme with $\Delta x = 0.2$ and $b = 0.4$ takes the minimum time of 835 seconds. This also includes the compilation time (of the order of few seconds) which however is negligible. It may be noted that convergence for the nonlinear simultaneous

TABLE 5-2

COMPUTATIONS FOR REACTION IN A CYLINDER OF I.D.=0.4cm.,O.D.=1 cm., 2H=4 cms.

Difference Form	Error Estimate	Equations	b	Δ X	Δt Sec.	Poremouth Radius after 1/2 hour reaction, cm.	Computation time, secs.
	TEMPERATURE OF REACTION IS	1373°K					
Milton Lee's Difference Scheme	$\sqrt{\Delta t^2 + \Delta x^2}$	4-132 to 4-143	2/5	0.2	0.0314	0.228634	1211
-do-	-do-	-do-	1/6	-do-	0.01307	0.230201	3343
Rose's Scheme (S=0.3)	$\Delta t + \Delta x^2$	4-150 to 4-157	2/5	-do-	0.0314	Not convergent	High
Rose's Scheme (S=0.7)	-do-	-do-	-do-	-do-	-do-	-do-	-do-
Modified Backward Difference Scheme		4-164 to 4-175	-do-	-do-	-do-	0.227433	1123
-do-	-do-	-do-	1/6	-do-	0.01307	0.229986	2688
Modified Richardson Difference Scheme		4-205 to 4-202	2/5	-do-	0.0314	0.228999	880
-do-		-do-	1/6	-do-	0.01307	0.231001	2000
Explicit Forward Difference Scheme	$\Delta t\ \Delta x^2$	4-180 to 4-181	2/5	0.1	0.00785	0.238464	1586
-do-	-do-	-do-	-do-	0.2	0.0314	0.227966	835
-do-	-do-	-do-	1/6	-do-	0.01307	0.230245	1989
-do-	-do-	-do-	1/2	-do-	0.0392	0.216568	672
	TEMPERATURE OF REACTION IS	873°K					
-do-	-do-	-do-	2/5	-do-	0.06202	0.203166	1660
-do-	-do-	-do-	1/6	-do-	0.02580	0.204044	3980

$T = 873^{\circ}K$ $k = 0.1545$ cm/sec $D = 1.032\ cm^2/sec$

$R_i = 0.2$ cm $R_e = 0.5$ cm $H = 2.0$ cms

$W_O = 4.25$ gms $C_{AO} = 0.292 \times 10^{-5}$ gmoles/cc $\Delta X = 0.2$

$\Delta t = 0.06202$ sec Convergence factor $= 0.4$

t HOURS	3.0	28.0	3.0
$(W_O - W_t)$ gm	0.058	0.695	0.023(exptl.)

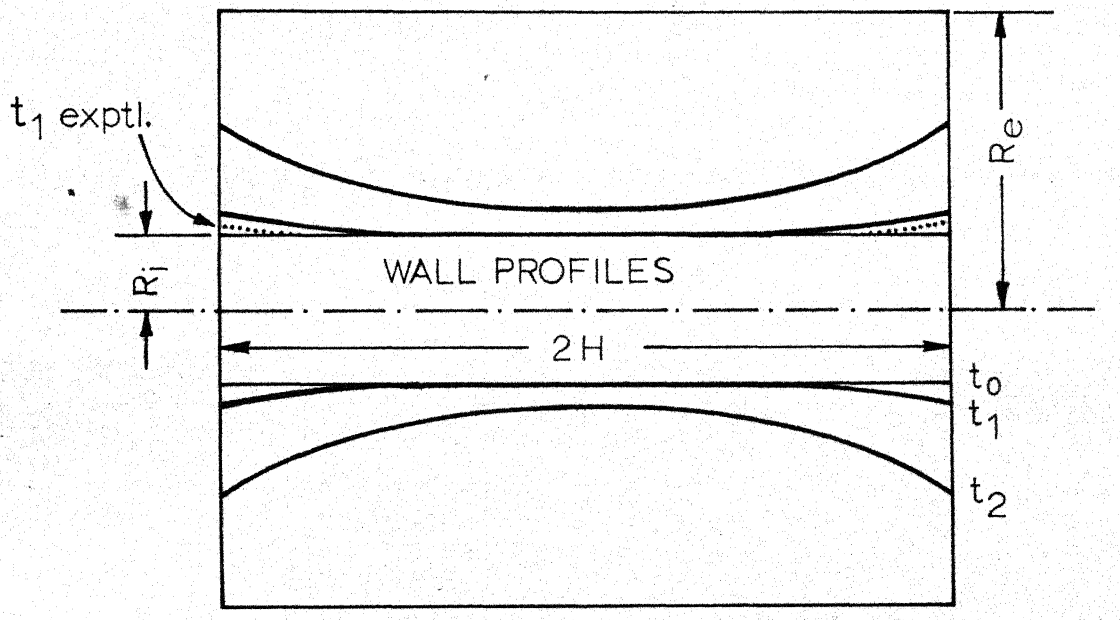

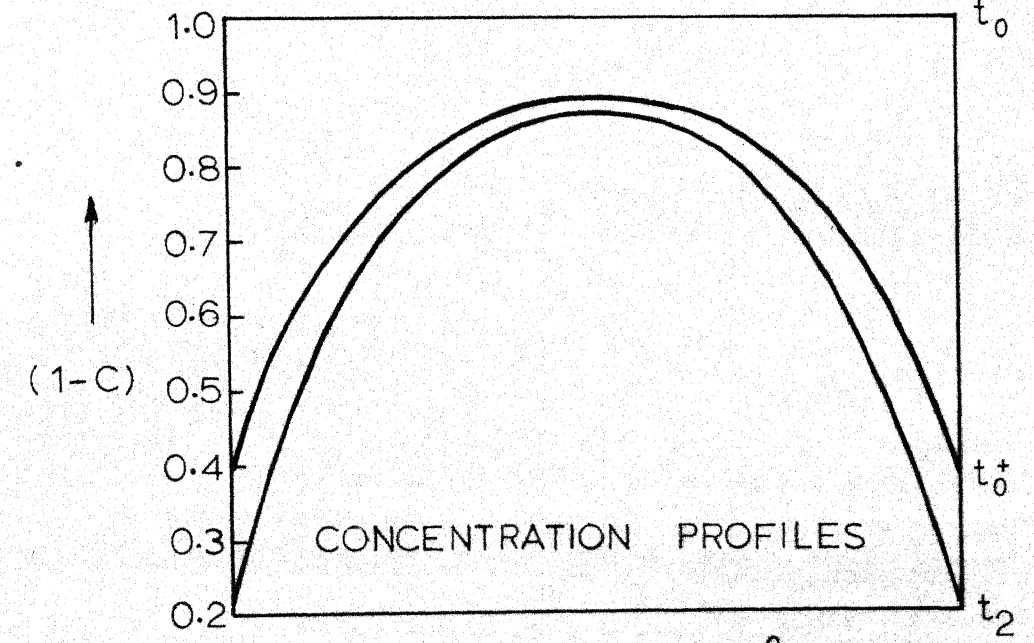

PROFILE DATA FOR 873° K

FIGURE 5-6

$T = 1123^{\circ}K$ $k = 5.01\ cm/sec$ $D = 1.52\ cm^2/sec$

$R_i = 0.01\ cm$ $R_e = 0.02\ cm$ $H = 2.0\ cms$

$W_o = 0.0162\ gm$ $C_{Ao} = 0.2275 \times 10^{-5}\ gmoles/cm^3$ $\Delta X = 0.2$

$\Delta t = 0.04211\ sec$ Convergence factor = 0.4

t HOURS	0.5	1.0	2.0	3.23
$(W_o - W_t)$ gm	4.2×10^{-5}	9.7×10^{-5}	2.2×10^{-4}	5.8×10^{-4}

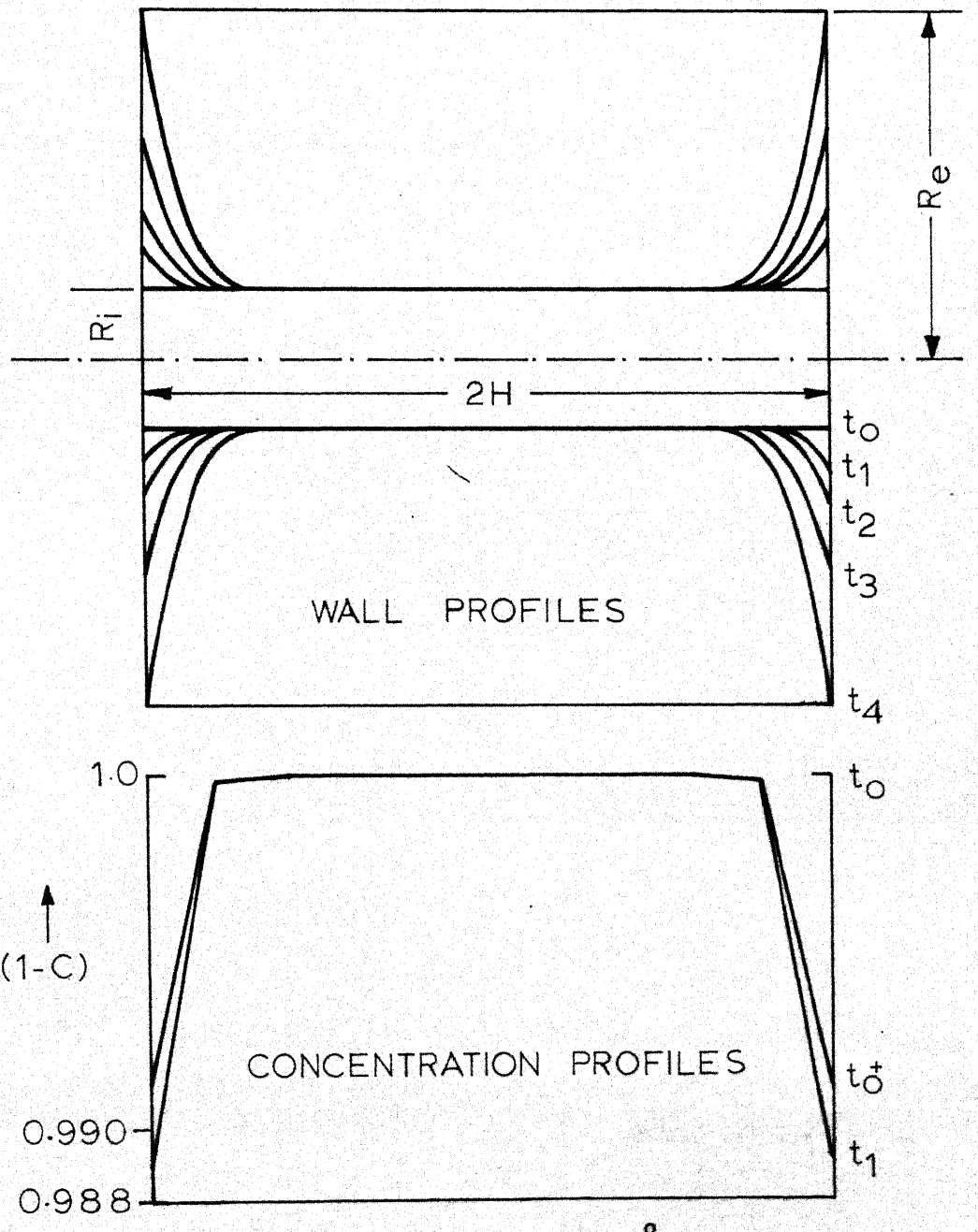

PROFILE DATA FOR $1123^{\circ}K$

FIGURE 5-7

$T = 1373^{\circ}K$ $k = 53.7 cm/sec.$ $D = 2.04 cm^2/sec.$

$R_i = 0.2$ cm. $R_e = 0.5$ cm. $H = 2.0$ cms.

$W_O = 4.25$ gms. $C_{AO} = 0.186 \times 10^{-5}$ gmoles/cc $\Delta X = 0.2$

$\Delta t = 0.03156$ sec. Radius of covergence $= 0.4$

t HOURS	1	2	3	3.5
$(W_O - W_t)$ gm	0.053	0.139	0.255	0.362

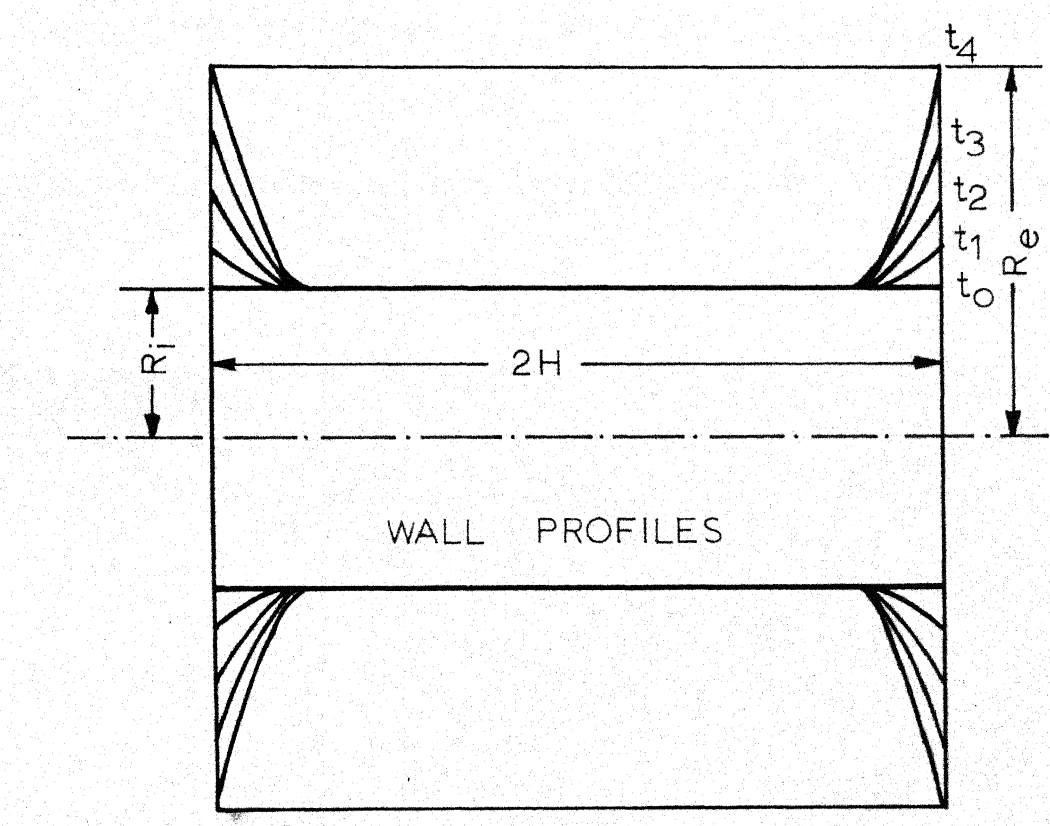

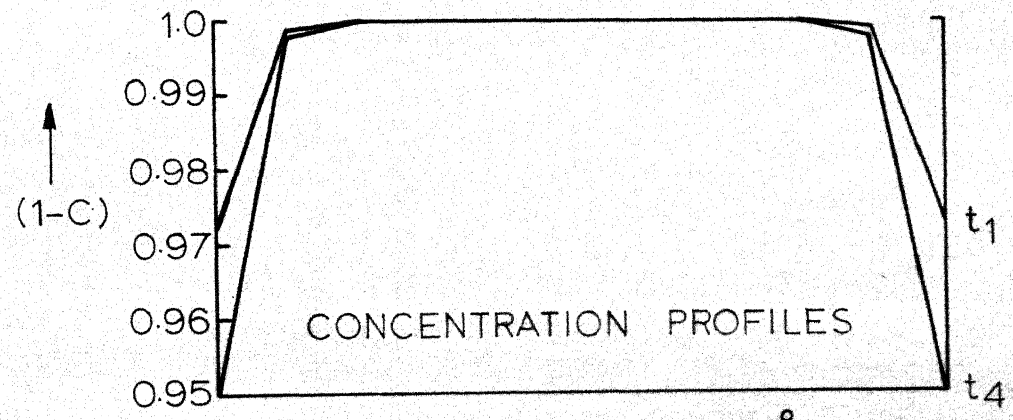

PROFILE DATA FOR $1373^{\circ}K$

FIGURE 5-8

$T = 1573^{\circ}K$ $k = 68.3$ cm/sec. $D = 2.49 cm^2/sec.$

$R_i = 0.01$ cm. $R_e = 0.02$ cm. $H = 2.0$ cms.

$W_o = 0.0162$ gm. $C_{Ao} = 0.1623 \times 10^{-5}$ g.moles/cc $\Delta X = 0.2$

$\Delta t = 0.0257$ sec. Convergence factor = 0.4

t HOURS	0.50	1.0	1.50	1.8
$(W_o - W_t)$ gm	0.79×10^4	1.835×10^4	3.5×10^4	5.4×10^4

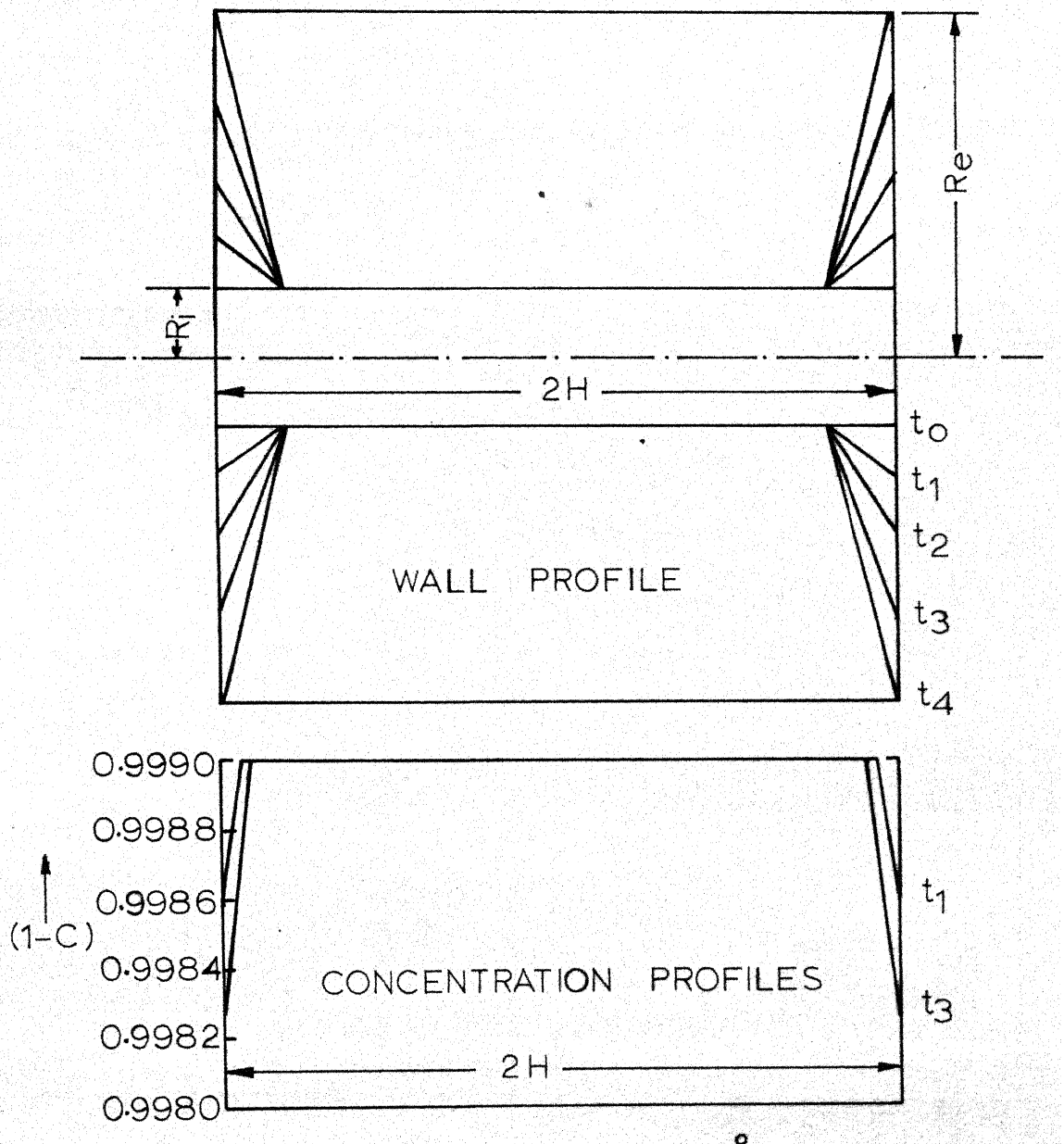

PROFILE DATA FOR $1573^{\circ}K$

FIGURE 5-9

$T = 2073^{\circ}$ K. $k = 229$ cm/sec. $D = 3.77 \text{ cm}^2/\text{sec}$.

$R_i = 0.01$ cm $R_e = 0.02$ cm $H = 2.0$ cms.

$W_o = 0.0162$ gms. $C_{Ao} = 0.1232 \times 10^{-5}$ gmoles/cc $\Delta X = 0.2$

$\Delta t = 0.01698$ sec Convergence factor = 0.4

t HOURS	0.472	0.954
$(W_o - W_t)$ gm	3.6×10^{-4}	5.4×10^{-4}

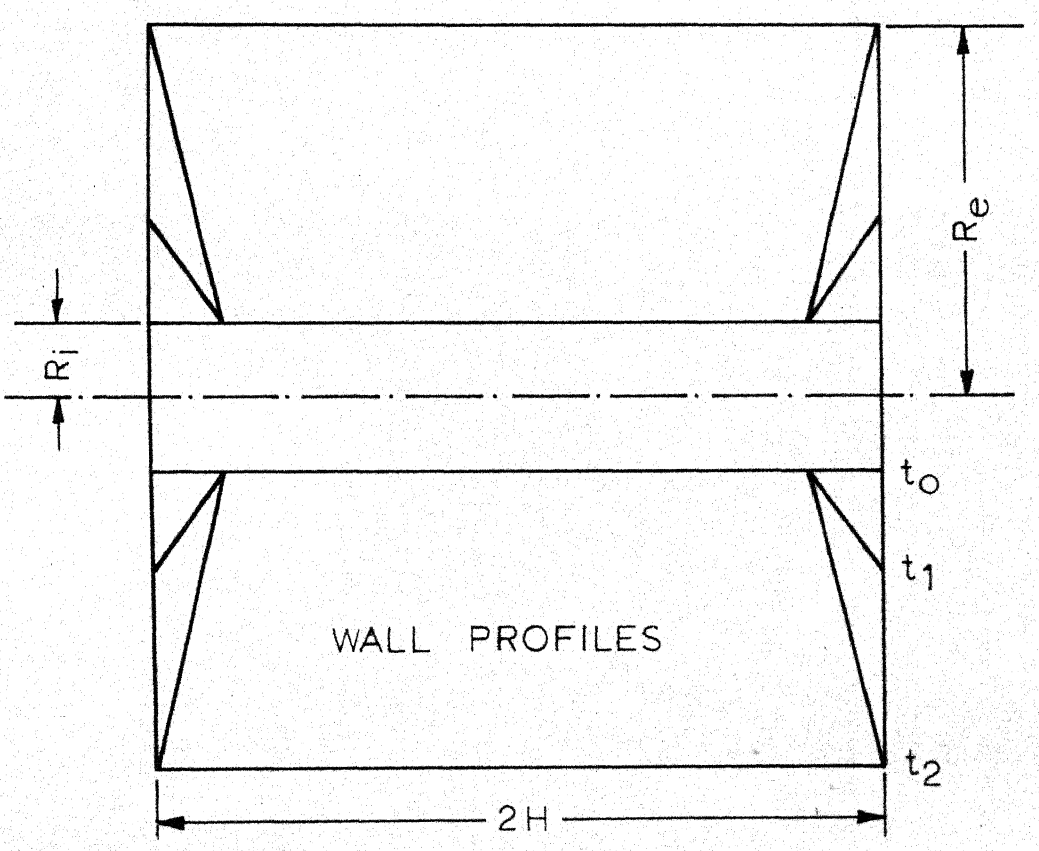

Concentration was almost zero throughout the length. At the pore mouth C = .0001
2073° K

FIGURE 5-10

T = hypothetical k = 100 cm/sec. $D = 2.0\ cm^2/sec.$

$R_i = 0.2$ cm $R_e = 0.5$ cm H = 2.0 cms.

$W_o = 4.25$ grms. $C_{Ao} = 1.595 \times 10^{-6}$ gmoles/c.c. $\Delta X = 0.2$

$\Delta t = 0.032$ sec. Radius of convergence = 0.4

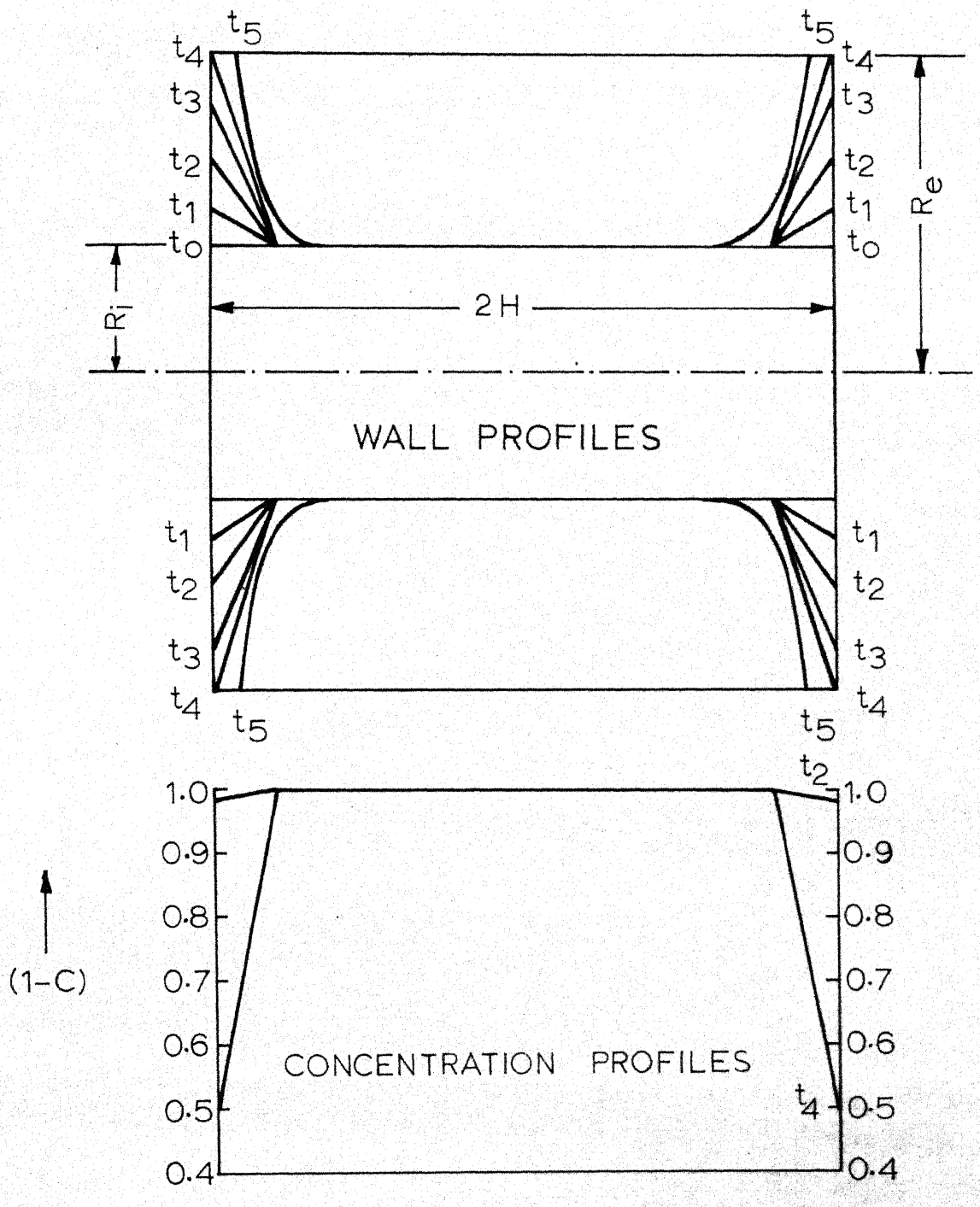

FIGURE 5-11

algebraic equations in Rose's scheme was not persued because of the prohibitively long time of computation and probably no added advantage in accuracy. Taking into consideration the above factors computations were done on IBM 7044 and IBM-360 using the Explicit Forward Difference scheme for all temperatures of reaction with $\Delta x = 0.2$ and $b = 0.4$. The concentration and wall profile data thus obtained are graphically represented on pages 153 - 158.

It is clear from the plots on pages 153-158 that the numerical data for axial concentration distributions and pore wall profiles are too diverse for quantitative comprehension. The length of computation time is the most crucial factor which puts serious limitations on the accuracy and vastness of the data, or for that matter, on the general scope for qualitative or quantitative betterment of the data. With a view to reduce the computation time, several alternatives in Fortran language were tried. Accuracy, being very important in the initial stages of computation, the variable C (of the order of 1) was replaced by a new variable $f = 1-C$ (of the order of zero) so that the same 16 significant decimal places retained by the computer gave greater accuracy. Besides attempting various difference schemes the distance and time grids were also increased to their maximum permissible values. In this connection, it may be noted that the five percent error introduced by the increased time increment Δt is always on the negative side i.e. the poremouth radius at higher Δt is

always less than that at lower Δt. Although this error affects the quantitative results, the nature of the qualitative conclusions remains unchanged. Thus, unto the time an analytical solution or a quickly converging finite difference scheme for the system of quasilinear parabolic differential equations describing the unsteady state chemical reaction in a pore are made available, the conclusions drawn from single pore studies may at best be considered qualitative comprehension.

Before going into the details of conclusions, some observations may be made regarding the experimental anomalies and computational procedures. Graphs on pages 81 and 82 indicate that higher temperatures fail to give increased rate constants. In fact, if experimental accuracy is taken for granted, k at 870°C actually is less than that at 746°C. This may apparently look absurd, but if Knudsen diffusivity is operative, the results become well explainable and the levelling off of weight loss curves is quite a common phenomenon under the diffusion controlled regime. Secondly, on page 153, the profile data indicates that the experimentally observed pore mouth radius is less than that predicted by computations. A similar trend is noticed at other temperatures, too. This general deviation may be due to a number of reasons.

For beginning calculations in the Modified Richardson Difference Scheme, independent values were chosen from results of

explicit forward difference scheme and Milton Lees Extrapolated Scheme. Even in other schemes, to doubly ensure stability, values obtained from one difference scheme were fed as the starting data for another scheme, and the error trend was observed to be unchanged. In most of the cases, computations were stopped when the poremouth radius became equal to the outer radius because by then the quasisteady state gets well established. In cases where calculations are continued beyond this stage, there is no solid material left for reaction at the pore mouth. Therefore equation 4-122 is replaced by the corresponding diffusion equation.

$$f(n,m+1) - f(n,m) = \frac{D\,\Delta t}{H^2\,\Delta x^2}\left\{f(n+1,m)-2f(n,m)+f(n-1,m)\right\} \quad \ldots 5\text{-}6$$

and $$R(n,m+1) = R(n,m) \quad \ldots 5\text{-}7$$

Thus forward march is continued by using a suitable combination of equations 5-6, 5-7 and the respective difference forms for 4-122 and 4-123. Mesh sizes in eqn. 5-6 are kept unaltered in order to retain the same magnitude of error. This is one more requirement which dictates the choice of mesh sizes. Difference schemes mentioned so far give the radius only at grid points 1,2,3,4 etc.(see figure 5-2). There is no provision to calculate the rate at which point A travels towards point D at grid number 2. It is difficult to calculate this without increasing the number

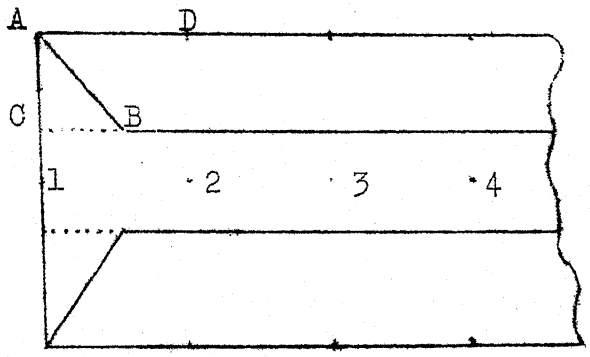

FIGURE 5-2

of grids at the pore mouth and hence without affecting the stability and accuracy in the course of calculations. To avoid this, the average rate at which A travels towards D is taken as the rate at which C travels towards B. Thus the rate at which the interface travels is determined.

As has already been pointed out in the introductory remarks, the use of the parameter 'temperature' in improving the yield of a heterogeneous gas solid reaction is generally overstressed. To bring to surface the fact that temperature can not only be an unimportant factor, but even a negative factor in improving the yield of a chemical reaction of a porous solid, a combination of physically realizable k, D and C_{Ao} and their variation with temperature is presented in Table 5-3.

TABLE 5-3

Temperature	k $\frac{cm}{sec}$	D $\frac{cm^2}{sec}$	C_{Ao} $\frac{gm.mol}{cc}$	Wt. loss of a standard cylinder after $\frac{1}{2}$ hour reaction.
T_1	5	1.50	0.23×10^{-5}	13 mg
T_2	50	1.75	0.19×10^{-5}	22 mg
T_3	100	2.00	0.14×10^{-5}	18 mg

Let $k = k_o e^{-E/RT}$ ...5-8

$D \propto T^{\alpha}$ ...5-9

$C_{Ao} \propto T^{-\beta}$ ...5-10

where k_o is the pre-exponential factor and E is the activation energy, R the ideal gas constant, and α and β are positive

constants. Now, if the reaction is diffusion controlled, and further, if the quasisteady state has already been attained, the rate of chemical reaction (R') is essentially governed by the term $-D(\frac{dC_A}{dz})$ or $-DC_{Ao}\frac{dC}{dz}$, where the factor $\frac{dC}{dz}$ (predominently dependent on pore geometry) remains constant with temperature. Therefore

$$R' \propto DC_{Ao}$$
$$\propto T^{\alpha} T^{-\beta}$$
$$\propto T^{\alpha-\beta} \qquad \ldots 5\text{-}11$$

Under quasisteady state conditions, the rate of diffusion controlled chemical reaction in a pore

(a) increases marginally with temperature if $\alpha > \beta$

(b) does not change with temperature if $\alpha = \beta$

(c) decreases marginally with temperature if $\alpha < \beta$.

For most of the systems at moderate pressures, $\beta \simeq 1$ and $0.4 < \alpha < 2.2$. If Knudsen diffusion is operative, $\alpha = 0.5$ and it can be seen that the reaction rate actually decreases with increasing temperature even though k increases. Maahs [100] identifies a similar phenomenon by referring to the deviation of k from normal Arrhenius plot for the oxidation of pyrolytic graphite at high temperatures, and keeps the discussion inconclusive by making a casual reference to the possible shortcomings of Scala's theory [101, 102] of diffusion controlled chemical reactions. An accurate estimate of the index α for the variation of effective diffusivity with temperature may give a clue for the deviation of k, especially when the material is almost nonporous or the average pore radius is small.

Normally, for a diffusion controlled reaction the chemical reaction rate constant is sufficiently large and the molal concentration of the fluid reactant on the pore surface is nearly zero. Therefore the rate should be governed essentially by the mass transfer rate at the pore mouth. Experimental weight loss curves for most of the porous solids indicate a varying rate of reaction in the initial stage and a constant rate in the final stage. This phenomenon is easily explained on the basis of a "shrinking pore model". Figure 5-3 illustrates a typical diffusion controlled fluid-solid reaction. The natural pore system indicated in 5-3A is modelled by a parallel pore system shown in 5-3B. Now, during the course of reaction the solid undergoes a surface transformation from5-3B to 5-3C, and this results in a change in the porewall profile and the concentration gradient at the pore mouth. This naturally causes a variation in the effective mass transfer coefficient at the interface. As the poremouth radii of two adjacent pores increase to their maximum, as shown in Figure 5-3C, the quasisteady state sets in and the interface recedes at a uniform velocity giving rise to a linear weight loss curve. The graph on page 81 clearly indicates a varying $\frac{dW}{dt}$ followed by an almost constant dW/dt. This behaviour may be more pronounced when the pore-mouth concentration gradient is held constant by allowing the flow right across the pore mouth. In an actual porous solid, even though the pore geometry is very different from that modelled in Fig. 5-3B, weight loss

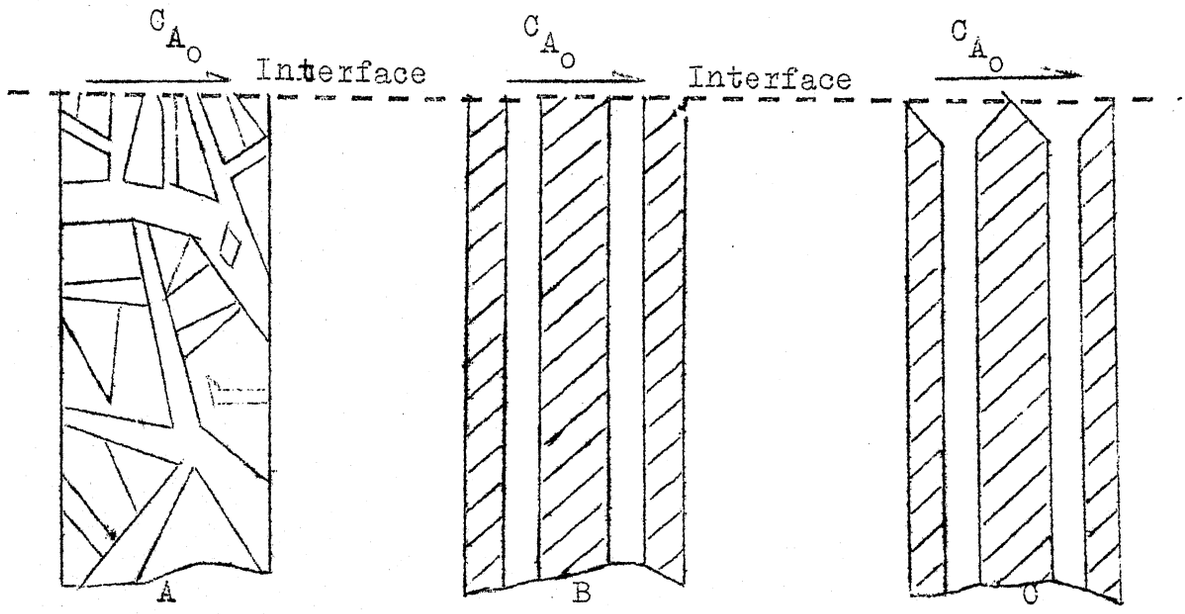

FIGURE 5-3

curves follow the above unsteadystate - quasi-steady state pattern with surprising accuracy. A large number of pores which statistically average out the deviations arising out of the modelled pore structure, may well explain this resemblance of behaviour between the actual and the modelled pore structures. However, this qualitative resembelence cannot and should not induce an underestimation of the difficulties involved in the quantitative matching of theory and practice. At this stage, it may be worth noting that the so called diffusion controlled regime actually refers to the quasisteady state portion of the general diffusion controlled reaction. The unsteady state portion is generally omitted from the discussions or is mistaken for a chemical reaction controlled regime. This may be one of the reasons for the existing contraversies regarding transition

zone between the chemical reaction controlled regime and the diffusion controlled regime.

In the light of the above discussions, it may be interesting to explore the common belief that high density and low temperatures are desirable parameters for the use of graphite as a material of construction in rocket nozzles. It is clear that slightly porous material with fine pore distribution corrodes at a rate slower than high density material (nonporous solid). It has also been seen that when Knudsen diffusion is operative, reaction rate decreases at high temperatures. Thus, at least from the point of view of chemical corrosion, highly nonporous material and low temperature of operation are not always necessarily desirable.

Coming to the use of single pore data to calculate the effectiveness factor, it may be noticed that the poremouth concentration cannot always be used as the basis for the definition, because the pore mouth itself changes its position during the course of reaction. The mouth concentration is thus affected by the external diffusion process. Therefore, to avoid confusion and unnecessary mixing up of initial pore dimensions with the effectiveness factor, the effectiveness factor may be defined only for the period during which the inner radius increases and becomes equal to the outer radius at the poremouth, and only for that axial distance over which the inner radius actually varies. Variation of internal surface area with time becomes an added factor complicating the rate

expression over the entire surface. In view of these difficulties and shortage, of computation time, only an approximate picture of variation of effectiveness factor with time is indicated in Figure 5-4. It is to note that these plots based on single pore data have a remarkable similarity to those defined for entire porous solids [3, 6].

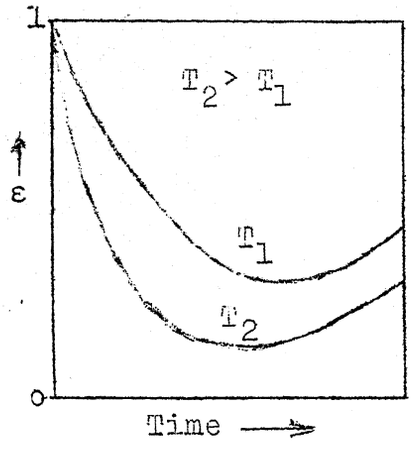

FIGURE 5-4

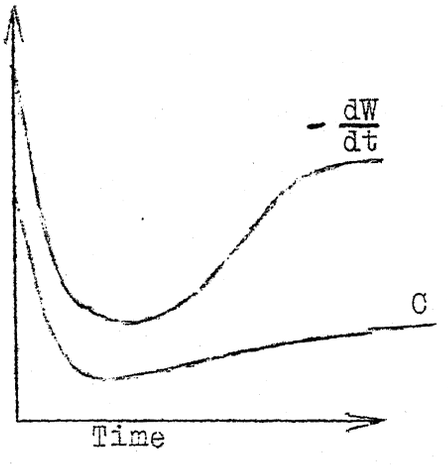

FIGURE 5-5

Similarly in Figure 5-5, the variation of concentration and the rate of weight loss are qualitatively indicated. Initially the rate of weight loss decreases and then it gradually increases as the quasisteady state approaches. In a typically diffusion controlled reaction the percentage conversion during the first half hour is nearly half of that during the subsequent half hour. This fact will have an important effect on the adjustment of the residence time of a pellet in the reactor. It may be profitable to maintain the reactor at less costly conditions in the initial stages and more costly conditions during later stages to attain maximum conversion at minimum cost.

More quantitative data and detailed investigations are called for to impliment such schemes in practice.

From the concentration profiles plotted on pages 155,156, 157,it is clear that in many cases a major portion of the interior of the pore has a fluid concentration which is almost zero. Thus an effective utilization of huge pore surface area would be possible only when high diffusivities are attained. An obvious method would be to introduce pressure diffusion. While empirical data regarding the effect of pressure on the rate of production in blast furnaces, coke ovens, and limekilns etc are available, satisfactory mathematical models have not been proposed. The reasons for the same may be the occurrence of the bulk flow term in the material balance equations, the varying order of reaction and the dependence of diffusivity on concentration at high pressures.

Since it is the first time an attempt is made to develop a "shrinking pore model" with an objective of defining precisely the quantitative effects of the physical factors on the chemical reactivity of porous solids, and of deciding the optimal conditions for carrying out heterogeneous reactions, many difficulties are likely to be experienced in modifying or sophisticating the present model on the following lines:

(a) Introducing radial diffusivity term in the model.

(b) Defining the first order rate constant on the volumetric basis, and introducing it as a function of inner radius.

(c) Considering the axial diffusion in gas phase and radial diffusion in solid phase, to set up two different partial differential equations and solving them simultaneously.

(d) Express k, D, and C_{Ao} as functions of temperature in the present model and try to obtain an expression for the optimum temperature for the heterogeneous gas solid reaction on the basis of "shrinking pore model."

(e) Use the present numerical data to get an analytical expression for the pore radius in terms of time and axial distance, and introduce this R(x,t) in the differential equation 4-122, and solve it again to get a better approximation $R_1(x,t)$, and continue the iteration until accurate analytical expressions for R(x,t) and C(x,t) are available.

(f) Express k as a functionof time varying pore structure and incorporate it into the main equation 4-122.

(g) Use the model for different orders of reactions or for series and parallel reactions under non-isothermal conditions.

(h) When there is a change in the number of moles of the gaseous reactant during the course of reaction, introduce a term for bulk flow due to pressure or express D as a function of concentration and solve the resulting nonlinearity.

(i) Introduce a separate term for pressure diffusion.

A large number of such modifications are possible, but the key factor for the success of any such modification is the availability of a suitable difference scheme which yields satisfactory results by using a reasonably short time of computation. A number of new difference forms [112] are being reported and it is hoped that the whole range off design data for a heterogeneous system - which till now are inadequate to cope up with the complex problems encountered even in relatively simple processes - would soon be available.

REFERENCES

[1] FRANK-KAMENTSKII D.A., Diffusion and Heat Exchange in Chemical Kinetics, Princeton University Press, 1955.

[2] WALKER P.L., Advances in Catalysis, Vol.11,pp.133-221. Academic Press, 1960.

[3] WEN C.Y., Ind. Engng Chem. 1968 60 34.

[4] ARIS R., Ind. Engng Chem. Fundls 1965 4 227.

[5] CALVELO A., Ind. Quim. 1968 26(1), 33-7.

[6] ISHIDA M. and WEN C.Y., Chem. Engng Sci. 1968 23 125.

[7] WHEELER A., Advances in Catalysis, Vol.3, pp 260-327. Academic Press 1950.

[8] WAKAO N. and SMITH J.M., Ind. Engng Chem. Fundls 1964 3 123.

[9] HUGHES E.E.G., Ph.D. Thesis, University of Wales 1963.

[10] WALKER P.L. Jr., in Ref.60a, p.330.

[11] WALKER P.L. Jr.and THOMAS J.M., Chem. Engng Prog. Symp.Ser. 1967 63 73.

[12] ARIS R., Ind Engng Chem. Fundls 1967 6 315.

[13] BEVRIDGE G.S.G. and GOLDIE P.J., Chem. Engng Sci. 1968 23 913.

[14] BISCHOFF K.B., Chem. Engng Sci. 1965 20 783.

[15] DENBIGH K.G., Trans. Instn Chem. Engrs 1962 40 23.

[16] FIENMAN J. and DREXTER T.D., A.I.Ch.E. Jl 1961 7 584.

[17] SHEN J. and SMITH J.M., Ind. Engng Chem. Fundls 1965 4 293.

[18] SZEKELY J. and EVANS J.W., Chem. Engng Sci. 1970 25 1091.

[19] WESTENBERG A.A. and WALKER R.E., ASME Symposium at Purdue University, McGraw-Hill 1959.

[20] MILTON L. and PHILIP W., Electrochem. Soc. J. 1964 111 1088.

[21] GRIFFITHS D.W.L. and THOMAS W.J., Carbon 1964 1 513.

[22] BOND R.L., Porous Carbon Solids pp. 47-59 Academic Press 1967.

[23] UBBELOHDE A.R. and LEWIS F.A., Graphite and its Crystal Compounds, pp. 153-174. Clarendon Press 1960.

[24] NICHOLS R., Ph.D. Thesis, The Pennsylvania State University 1961.

[25] WICKE E. and KALLENBACH R., Kolloid Z. 1941 97 135.

[26] MATELL C.L., Carbon and Graphite Hand Book, Interscience Publishers 1968.

[27] DOWDEN F.P. and YOUNG J.E., Proc. R. Soc. 1951 A208 444.

[28] MABERRY J.L., AIAA j. 1968 6(11) 2222.

[29] THOMAS W.J., Carbon 1966 3 435.

[30] TINGEY G.L. etal, Chem. Engng Prog. Symp. Ser. 1970 66 73.

[31] HOUGEN O.A. and WATSON K.M., Chemical Process Principles, Part III, Wiley 1950.

[32] SQUIRE A.M., Trans. Instn chem. Engrs 1961 39 10.

[33] WEN C.Y. etal, Advan. Chem. Ser. 1967 69 253.

[34] WEN C.Y. and HUEBLER J., Ind. Engng Chem. Proc. Des. Dev. 1965 4 142.

[35] YAGI S. and KONII D., Proc. 5th Int. Symp. on Combustion, p. 231 1955.

[36] LEVENSPIEL O., Chemical Reaction Engineering. John Wiley 1962.

[37] NARSIMHAN G., Chem. Engng Sci. 1961 16 7.

[38] SATTERFIELD C.N. and FEAKES F., A.I.Ch.E. Jl 1959 5 115.

[39] GOKARAN A.N. and DORAISWAMY L.K., Chem. Engng Sci. 1971 26 1521.

[40] CUNNINGHAM R.E. and CALVELO A., Ind. Engng Chem. Fundls 1970 9 505.

[41] CALVELO A. and CUNNINGHAM R.E., J. Catal 1970 17 1,143.

[42] CANNON K.J. and DENBIGH K.G., Chem. Engng Sci. 1957 6 145.

[43] MEHTA B.N. and ARIS R., Chem. Engng Sci. 1971 26 1699.

[44] LEWIS W.E. and PAYNTER J.D. Chem. Engng Sci. 1971 26 1357.

[45] THIELE E.W., Ind. Engng Chem. 1939 31 916.

[46] PETERSEN E.E., A.I.Ch.E. Jl 1957 3 443.

[47] WEISZ P.B. and PRATER C.D., Adv. Catal. 1954 6 167.

[48] PETERSEN E.E., Chem. Engng Sci. 1965 20 587.

[49] PETERSEN E.E., Chemical Reaction Analysis. Prentice Hall 1965.

[50] BISCHOFF K.B., Chem. Engng Sci. 1967 22 525.

[51] SCHWEITZER G.C. and SINGER R.M., Proceedings of the 5th Conference on Carbon, pp. 215-240. Pergamon Press 1962.

[52] HAWTIN P. and HUBER R.A., Carbon 1968 6 887, 901.

[53] GULBRANSEN E.A. and ANDREW K.F., Ind. Engng Chem. 1952 44 1034, 1039, 1048.

[54] BOND R.L. and PINCHIN F.J., Nature 1958 182 129.

[55] HAWTIN P. and GIBSON J.A., Carbon 1966 4 489.

[56] HENNIG G.R., 1st and 2nd Conference on Carbon, p.103. University of Buffalo 1956.

[57] FRANKLIN R.E., J. Chem. Phys. 1953 50 c26.

[58] THOMAS J.M. and WALKER P.L., 1st Symp. on Carbon Tokyo 1964.

[59] HEINTZ E.A. and PARKER W.E., Carbon 1966 4 104.

[60a] WALKER P.L., (Ed.), Chemistry and Physics of Carbon, Vol.1, pp. 71-352. Marcel Dekker Inc. New York 1960.

[60b] Ibid.,Vol.2, pp. 29-39.

[60c] Ibid.,Vol.3, pp. 122-138.

[60d] Ibid.,Vol.4, 1964.

[60e] Ibid.,Vol.5, 1965.

[61] ARIS R., Introduction to the Analysis of Chemical Reactors p. 13. Prentice Hall 1965.

[62] Tables of Selected Values of Thermodynamic Properties NBS Washington D.C. 1949.

[63] BLACKMAN L.C.F., Modern Aspects of Graphite Technology.AP 1970.

[64] DeBOER J.H., (Ed.), Industrial Carbon and Graphite. pp 302-326. Soc. Chem. Ind. London 1958.

[65] HILL T.L. etal, J. Am. Chem. Soc. 1951 73 5102, 5833.

[66] BULL H.I. etal, J. Am. Chem. Soc. 1931 53 837.

[67] NELSON R. and SMITH, Qurtl. Rev. 1959 13 287.

[68] FELDMAN M.H., GOEDDEL W.V., DIENES G.J. and GOSSEN W., J. appl. Phys. 1952 23 1200.

[69] KANTER M.A., Phys. Rev. 1957 107 655.

[70] WATT J.D. and FRANKLIN R.E., Nature 1957 180 1190.

[71] KOSIBA W.L., Advances in Catalysis, Vol.9, p.398 AP 1956.

[72] DEITZ V.R. and PROSEN E.J., Nature 1958 181 109.

[73] HARTECK P. and DONDES S., J. chem. Phys. 1957 27 1419.

[74] STRICKLAND CONSTABLE R.F. Trans. Faraday Soc. 1944 40 333.

[75] RAO P.V.N.R. and PETERSEN E.E., Ind. Engng Chem. 1958 50 331.

[76] FREY H.M., Proc. R. Soc. 1955 A228 510.

[77] BLYHOLDER G., BINFORD J.S. and EYRING H., J.phys. Chem. 1958 62 263.

[78] DAY R.J. Ph.D. Thesis, The Pennsylvania State University 1949.

[79] LEWIS W.K., GILLILAND E.R. and PAXTON R.R., Ind. Engng Chem. 1954 46 1327.

[80] ARMINGTON A.F., Ph.D. Thesis, The Pennsylvania St. Univ 1960.

[81] CHEN M.C., CHRISTENSEN C.J. and EYRING H.J., J. phys. Chem. 1955 59 1146.

[82] CURLVER R.V. and WATTS H., Rev. Pure Appl. Chem. 1960 10 95.

[83] VOLKOV G.M. and KOTOVA T.V., Konstr. Mater. Osn. Graphita 1969 4 80.

[84] LEWIS J.C., FLOYD I.J. and COWALARD F.C., paper presented at the 8th Biennial Conference on Carbon, Buffalo N.Y. 1967.

[85] BLYHOLDER G. and EYRING H.J., J. phys. Chem. 1957 61 682.

[86] HEINDLE R.A., J. Am.Ceramic Soc., 1955 38 89.

[87] ROSSBERG M., Z. Elektrochemie 1956 60 952.

[88] LONG F.J. and SYKES K.W., Proc. R. Soc. 1948 A193 377.

[89] BONNER E. and TURKEVICH J., J. Am. Chem. Soc. 1951 73 561.

[90] LETORT M. etal, J. Chim. Phys. 1950 47 548.

[91] HARKER H. etal, J. Nucl. Mat. 1970 37(3) 331.

[92] HARKER H. etal, Carbon 1966 4 401.

[93] ARIS R., Chem. Engng Sci. 1957 6 262.

[94] PARKER A.S. and HOTTEL H.C., Ind.Engng Chem. 1936 28 1334.

[95] MAYERS M.A., Trans Am. Inst. Mining Met.Engrs 1938 130 408.

[96] CHUKHANOV Z.F. and KARZAVINA N.A., Fuel 1941 20 73.

[97] KUCHTA J.M. and KANT A., Ind. Engng Chem. 1952 44 1559.

[98] TU C.M., DAVIS H. and HOTTEL H.C., Ind. Engng Chem. 1934 26 749.

[99] SCHWEITZER D.G., Nucl. Sci. Engng 1962 3 3.

[100] MAAHS H.G. and HOWARD G., NASA TN D-7005 p.33, 1970.

[101] SCALA S.M., R 62, S.D.72 Missile and Space Division Gen. Elect. 1962.

[102] SCALA S.M. and GILBERT L.M., AIAA J. 1965 3 No.9 61965).

[103] RALPH NORMANN, Ph.D. Thesis, North Carolina State University, Raeigh 1969.

[104] ASTM Standards, 1969 Book, Part 19, D1857-68. 1969.

[105] PERRY J.H., Chemical Engineers Handbook. McGraw-Hill 1963.

[106] BIRD R.B., STEWART W.E. and LIGHTFOOT E.N., Transport Phenomena Wiley 1960.

[107] BISCHOFF K.B., Ind. Engng Chem. Fundls 1966 5 285.

[108] MILTON LEES, Nonlinear Partial Differential Equations (Ed. W.F. Ames) p. 193. Academic Press 1967.

[109] KELLER H.B., Numerical Solutions of Partial Differential Equations II SYNSPADE 1970 (Ed. Bert Hubbard) p.327. Academic Press 1971.

[110] MILTON LEES, J. Soc. Appl. Math. 1959 7 2.

[111] DOUGLAS J. and JONES B.F., J. Soc. Indst. Appl. Math. 1963 11 195.

[112] DOUGLAS J., Advances in Computer Vol. II, pp. 1-54. Academic Press 1961.

[113] MANNING W.A., A. Fortron IV Problem Solver. McGraw-Hill 1970.

[114] FORSYTHE G.E. and WASOW W.R., Finite Difference Methods for Partial Differential Equations, pp.107-131. Wiley 1960.

[115] COLLATZ L., Numerical Treatment of Partial Differential Equations. Academic Press 1965.

[116] DuFORT E.C. and FRANKEL S.P. Math. Tables Aids Comput. 1953 7 135.

[117] HILSENRATH J., Tables of Thermodynamic and Transport Properties Pergamon Press 1960.

[118] FLÜGGE-LOTZ, Numerical Solutions of Partial Differential Equations (Ed. W.F. AMES) p.165. Academic Press 1966.

[119] MILNE W.E., Numerical Solutions of Differential Equations p.120 Wiley 1960.

[120] HAWTIN P. and MURDOCH R., Chem. Engng Sci. 1964 19 819.

...

APPENDIX - A

One of the common methods of linearizing the equation 4-3 for the determination of k from the experimental weight loss curves is to make an approximation of the following type

$$e^{x^2}\{1-\text{erf}\ (x)\} = [\ ax + b\ ]^{-1} \qquad \ldots A\text{-}1$$

where a and b are numerical constants and $x = k\sqrt{t/D} = y\sqrt{t}$. The approximate relation A-1 can be made accurate at two values of x by choosing suitable numerical values of a and b. Assuming maximum and minimum limits for x as 2.0 and 0.05, the equation A-1 may be rewritten as

$$e^{x^2}\{1-\text{erf}\ (x)\} = [\ 1.772x + 0.736\ ]^{-1} \qquad \ldots A\text{-}2$$

Thus, equation 4-30 becomes

$$-\frac{1}{S}\frac{dW}{dt} = k\,C_{A_o}\,[\ 1.772y\sqrt{t} + 0.736\ ]^{-1} \qquad \ldots A\text{-}3$$

$$\therefore \frac{0.736}{S}\left(\frac{dW}{dt}\right) = \frac{-1.772y}{S}\left(\sqrt{t}\,\frac{dW}{dt}\right) - k\,C_{A_o} \qquad \ldots A\text{-}4$$

Thus a plot of $\frac{dW}{dt}$ versus $\sqrt{t}\,\frac{dW}{dt}$ should result in a straight line, the intercept of which gives $k\,C_{A_o}$ and hence the value of k. It may be noted that the maximum error obtained by differentiating the function $e^{x^2}\{1 - \text{erf}(x)\} - [1.772x + 0.736\ ]^{-1}$ with respect to x is of the order of 4%. Thus simplifications of the type A-2 become useful in the estimation of the first order rate constant.

...